The 13th International Congress on Rock Mechanics
ISRM CONGRESS 2015
Palais des congrès de Montréal, Québec, Canada May 10 to 13, 2015

DDA in Rock Mechanics Practice

Yossef H. Hatzor

Sam and Edna Lemkin Professor of Rock Mechanics

Co-Chair, ISRM DDA Commission

Dept. of Geological and Environmental Sciences

Ben-Gurion University of the Negev, Israel

Organized by:

CIM ICM Canadian Institute of Mining, Metallurgy and Petroleum

In collaboration with:

ISRM CARMA ARMA McGill University of Toronto Queen's

Talk Outline

- Brief review of DDA theory
- Major improvements since DDA was first published
- Benchmark tests: verifications and validations
- Two selected rock mechanics applications
  - ❑ Rock Slope Stability
    - ❖ Thermal vs. seismic effects on block stability
  - ❑ Deep Underground Excavations
    - ❖ Rock bursts in discontinuous rock masses

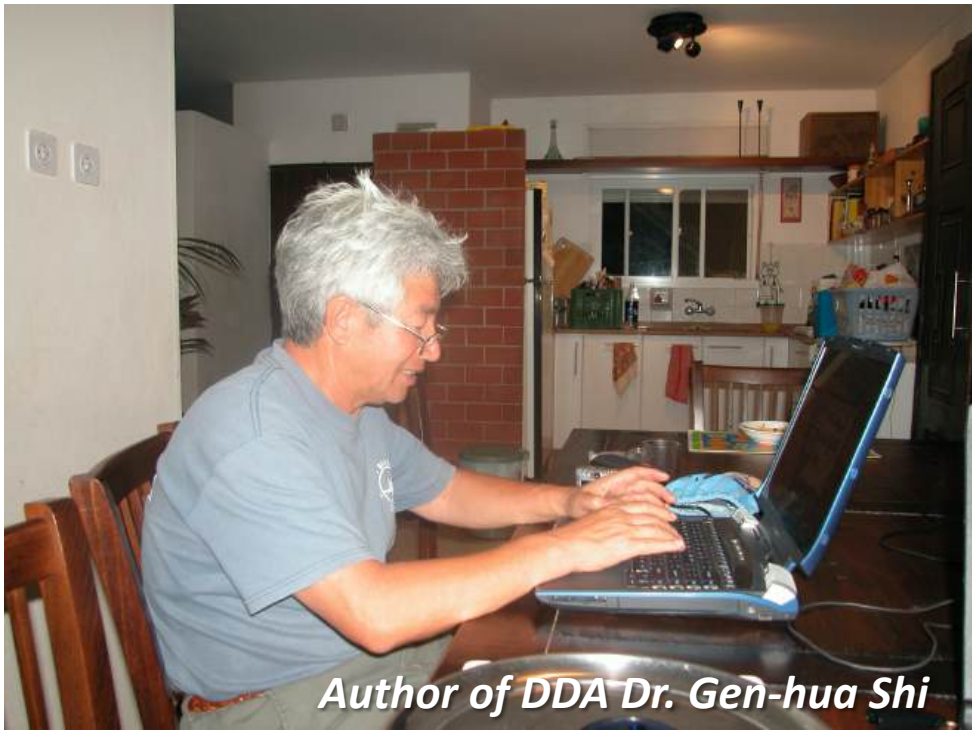

Brief review of DDA theory

Main Features of DDA

Dr. Shi (1988) lists the following attributes of DDA:

- Complete kinematic theory and its numerical realization
- Perfect first order displacement approximation
- Strict postulate of equilibrium
- Correct energy consumption
- Large deformation

There are some restrictions however….

- The first order approximation limits accuracy, particularly in case of large rotations
- Simply deformable blocks assumption limits the accuracy when solving a block systems consisting of few or very large blocks
- The penalty method used in DDA contact algorithm is very sensitive to the choice of the penalty value
- Correct choice of numerical control parameters requires experience

Basic DDA Theory

- **Potential Energy Minimization**

$$\frac{\partial \Pi_P}{\partial D}+\frac{\partial \Pi_V}{\partial D}+\frac{\partial \Pi_I}{\partial D}+\frac{\partial \Pi_E}{\partial D}+\frac{\partial \Pi_\sigma}{\partial D}+\frac{\partial \Pi_C}{\partial D}=0$$

Point Load | Body Force | Inertia Force | Elastic Force | Initial Stress | Contact Force

Π = potential energy
D = block displacement at gravity center

- **First Order Approximation**

Since displacements in every time step are very small, for most engineering purposes a 1st order approximation for block displacement is sufficient:

$$\begin{pmatrix} u \\ v \end{pmatrix} = \begin{pmatrix} 1 & 0 & -(y-y_0) & (x-x_0) & 0 & (y-y_0)/2 \\ 0 & 1 & (x-x_0) & 0 & (y-y_0) & (x-x_0)/2 \end{pmatrix} \begin{pmatrix} u_0 \\ v_0 \\ r_0 \\ \varepsilon_x \\ \varepsilon_y \\ \gamma_{xy} \end{pmatrix} = [T_i][D_i]$$

where: (u, v) are displacements of an arbitrary point (x, y) in X and Y directions; (x_o, y_o) co-ordinates of the block centroid; (u_o, v_o) rigid body translations of block i; r_o= rigid body rotation angle (in radians) of Block i with a rotation center at $(x_o\ y_o)$; $(\varepsilon_x,\ \varepsilon_y,\ \gamma_{xy})$ normal and shear strain components of Block i, $[Ti]$ is the first order displacement function and $[Di]$ is the vector displacement variables of Block i.

Basic DDA Theory

- **Penalty Method**

$$\Pi_C = \frac{1}{2} K d^2$$

Π_c = Potential energy by contact force
d = penetration
K = contact spring stiffness

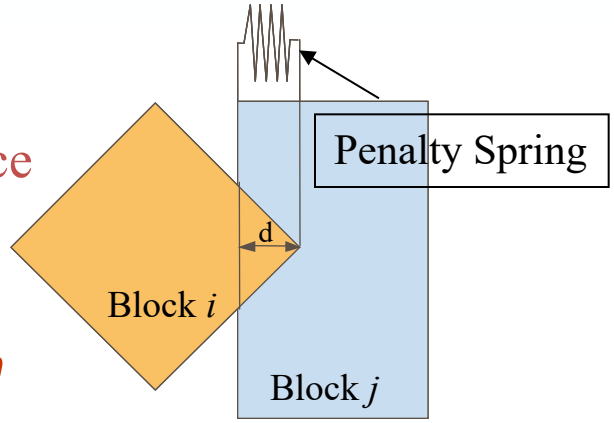

"open-close" iterations to satisfy *no tension* - *no penetration* constraint in all contacts

After Ohnishi, 2005

- **The Kinematic Equation of Motion:**

Applying Hamilton's principle of least action and expanding resulting terms (complicated math…):

$$M\ddot{u} + C\dot{u} + Ku = F$$

M = Mass matrix, C = Viscosity matrix, K = Stiffness matrix, F = external force vector

The components of these matrices are extensively discussed by Shi.

The equation of motion is solved using two more equations provided by Newmark's β and γ method with parameters β = 0.5 and γ = 1.0, and the algebraic equation for the increase in displacement is solved for each time increment by collecting the terms on both sides.

Basic DDA Theory

Newmark's (1959) equations for direct time integration:

$$u_t = u_{t-\Delta t} + \Delta t \dot{u}_{t-\Delta t} + \left(\frac{1}{2} - \beta\right)\Delta t^2 \ddot{u}_{t-\Delta t} + \beta \Delta t^2 \ddot{u}_t$$

$$\dot{u}_t = \dot{u}_{t-\Delta t} + (1-\gamma)\Delta t \ddot{u}_{t-\Delta t} + \gamma \Delta t \ddot{u}_t$$

In DDA $\beta = ½$ and $\gamma = 1.0$:

$$u_t = u_{t-\Delta t} + \Delta t \dot{u}_{t-\Delta t} + \frac{\Delta t^2}{2}\ddot{u}_t$$

$$\dot{u}_t = \dot{u}_{t-\Delta t} + \Delta t \ddot{u}_t$$

Let $u_{t-\Delta t} = 0$ and solve for a_t:

$$\ddot{u}_t = \frac{2}{\Delta t^2}\left(u_t - \Delta t \dot{u}_{t-\Delta t}\right)$$

Now solve for v_t:

$$\dot{u}_t = \frac{2}{\Delta t} u_t - \dot{u}_{t-\Delta t}$$

Basic DDA Theory

Substituting the acceleration and velocity terms obtained using Newmark's integration with $\beta = 0.5$ and $\gamma = 1.0$ into the kinematic equation of motion and rearranging:

For complete derivation of the basic kinematic equation of motion for DDA see for example Ohnishi et al., 2005. *ICADD-7*.

$$\frac{2}{\Delta t^2} M\left(u_t - \Delta t \dot{u}_{t-\Delta t}\right) + C\left(\frac{2}{\Delta t} u_t - \dot{u}_{t-\Delta t}\right) + K u_t = F_t$$

$$\left[\frac{2}{\Delta t^2} M + \frac{2}{\Delta t} C + K\right] u_t = F_t + \left[\frac{2}{\Delta t} M + C\right] \dot{u}_t$$

Collecting terms on both sides we get the familiar DDA system of equations:

or in matrix form:

$$\boldsymbol{K} \cdot \Delta \boldsymbol{u} = \boldsymbol{F}$$

$$\begin{pmatrix} K_{11} & K_{12} & K_{13} & \cdots & K_{1n} \\ K_{21} & K_{22} & K_{23} & \cdots & K_{2n} \\ K_{31} & K_{32} & K_{33} & \cdots & K_{3n} \\ \vdots & \vdots & \vdots & \ddots & \vdots \\ K_{n1} & K_{n2} & K_{n3} & \cdots & K_{nn} \end{pmatrix} \begin{pmatrix} D_1 \\ D_2 \\ D_3 \\ \vdots \\ D_n \end{pmatrix} = \begin{pmatrix} F_1 \\ F_2 \\ F_3 \\ \vdots \\ F_n \end{pmatrix}$$

K_{ij} = 6x6 coefficient sub-matrices

D_i = 6x1 deformation matrix of block i

F_i = 6x1 loading matrix of block i

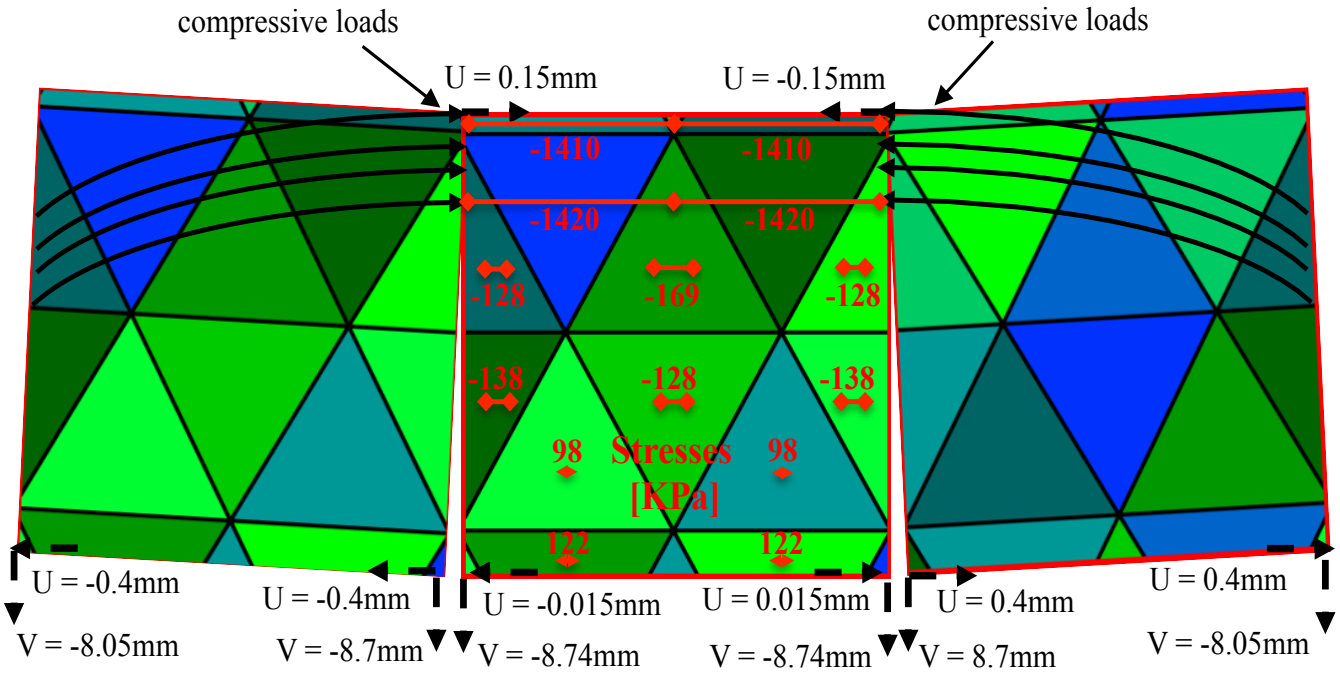

Major improvements since DDA was first published by Shi in 1988

Block discretization and higher order displacement

- To overcome simply deformable blocks assumptions **Block Discretization** was originally proposed by *Ke, 1995* and *Amadei et al., 1996.*
- To enable fracture mechanics type of modeling **Coupling between DDA and FEM** was proposed by many researchers (e.g. *Scheele, 1999; Shyu et al., 1999; . Zhu et al., 2007; Cao et al., 2007; Ma et al., 2007; Grayeli and Mortazavi, 2007; Jiao and Zhang ,2012 ; Zhao et al., 2013*).
- To improve accuracy in problems involving wave propagation and bending deformation **higher order displacement function** was introduced into DDA, both 2nd as well as 3rd order (e.g. *Koo et al., 1995; Grayeli and Mortazavi, 2005; Wang et al., 2007; Huang et al., 2010; Wu et al., 2012*)

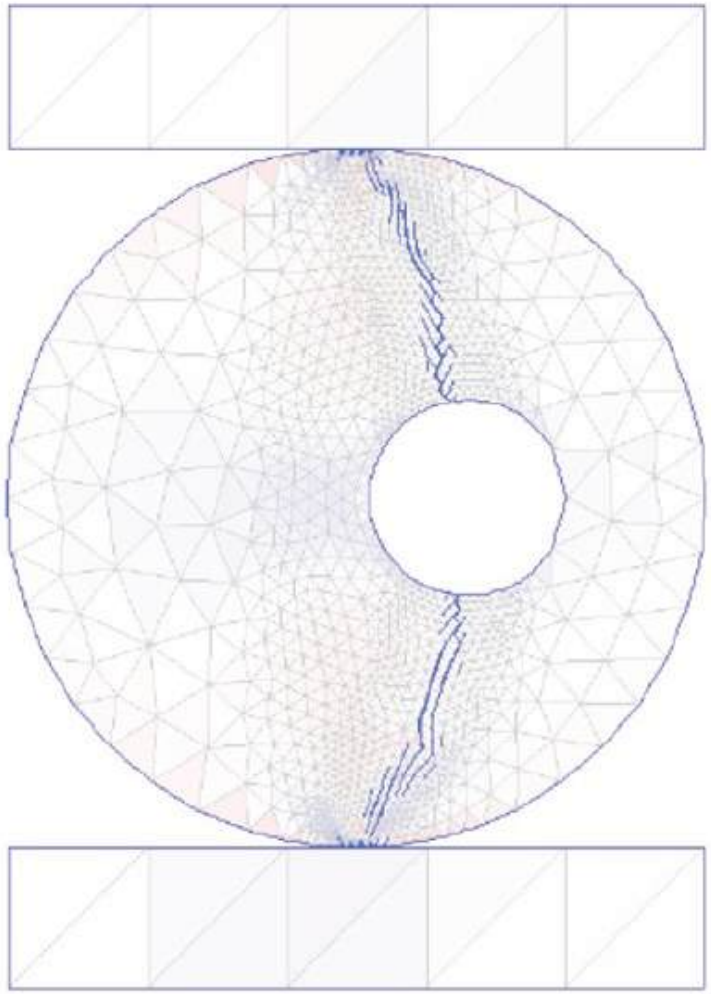

Failure of a Brazilian disc with an initial hole using nodal based DDA (Zhao et al., 2013)

Improved contact algorithm

- In the penalty method **stiff springs are set in normal and/or shear directions** between blocks to transfer the inequality problem of contact constraint into equality problem of computing contact displacements and contact forces.
- The main shortcoming of the penalty method is that it **can only fulfil the contact constraint approximately**, and the contact treatment precision is affected by selected penalty number.
- With relatively large penalty number the penalty method can treat the contact of blocks well, however **if the penalty number is too large the system of equilibrium equations may become ill – conditioned** resulting in un-acceptable errors.
- Amadei et al. (1996) modified the original DDA contact using the **Augmented Lagrangian Method** so as to retain the simplicity of the penalty method and yet to minimize the disadvantages of the penalty method and the classical Lagrange Multiplier Method, the implementation of which would require an increase in the system of the governing equations. This approached was followed and expanded by *Ning et al., 2010* and *Bao et al. 2014,* among others.

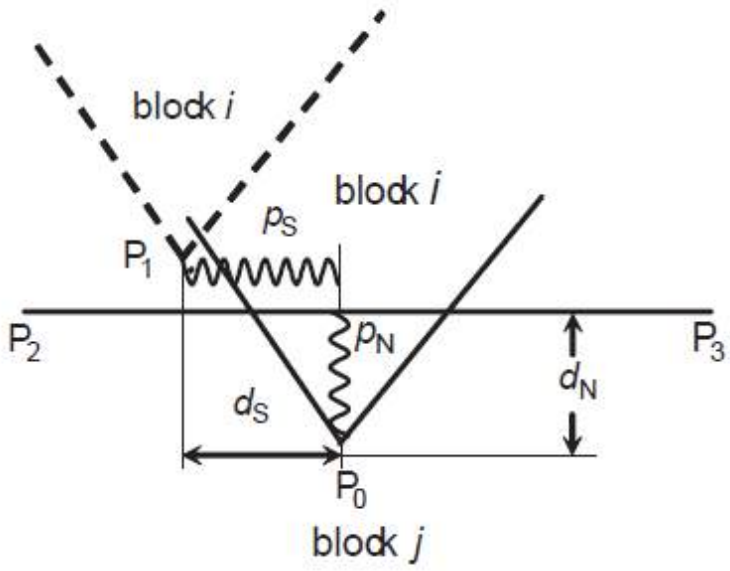

Angle – edge contact in DDA (Ning et al., 2010)

Viscous damping

- In the original DDA implementation of **viscous damping** was ignored because it was not clear how to select the best value of the viscous coefficient.
- When modeling **earthquakes** with DDA began, it became necessary to introduce viscous damping to better represent physical damping processes that are active in natural block systems. This was demonstrated by, among others, *Shinji et al. (1997)*, and *Sasaki et al. (2005)*.

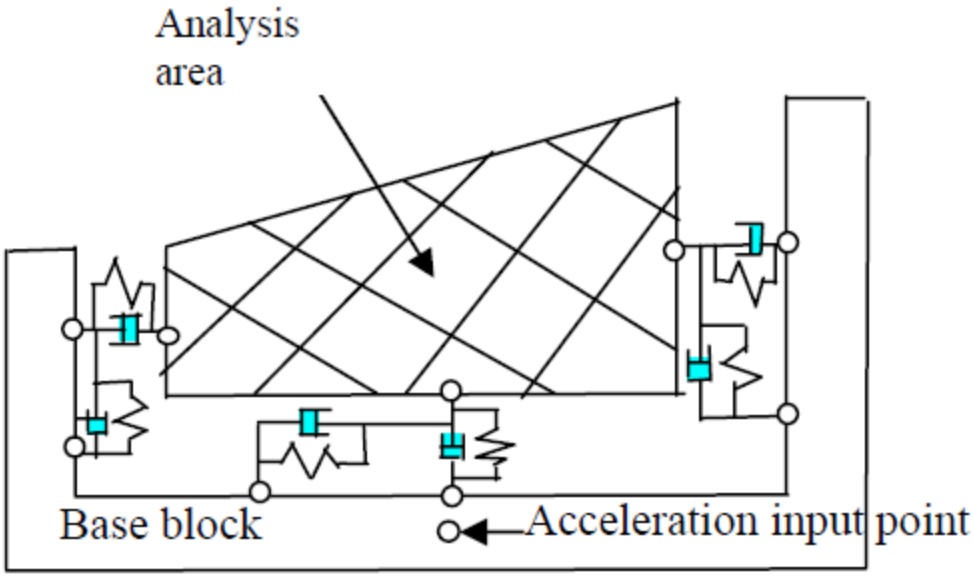

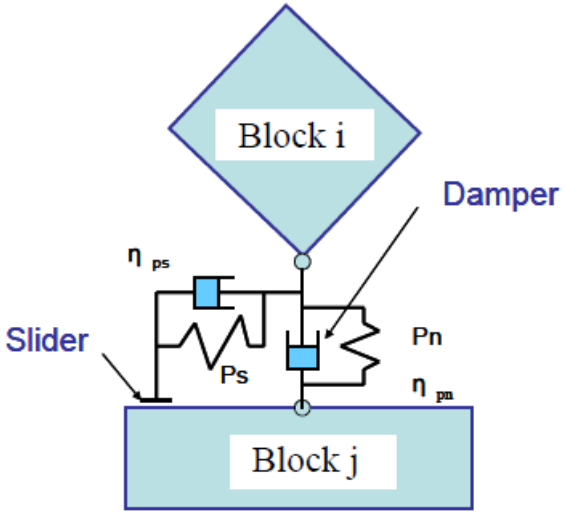

Boundary condition of earthquake response analysis (Left) and Voigt-type viscous damping of friction (Right) implemented in DDA to model earthquake induced rock falls in Niigata prefecture, Japan. (Sasaki et al., 2005).

Non-reflective boundaries

- When modeling **blasting with DDA** reflection of waves from the artificial boundaries of the modeled domain must be diminished to avoid obscuring the studied wave propagation.
- **Non reflective boundaries** for DDA were first proposed by *Jiao et al. (2007)* based on a viscous boundary condition originally proposed by *Lysmer and Kuhlemeyer (1969)* for the FEM method.

- *Bao et al. (2012)* introduced a new viscous boundary submatrix with **high absorbing efficiency** which was developed specifically for DDA, based on the viscous boundary condition originally introduced by *Lysmer and Kuhlemeyer (1969)*.

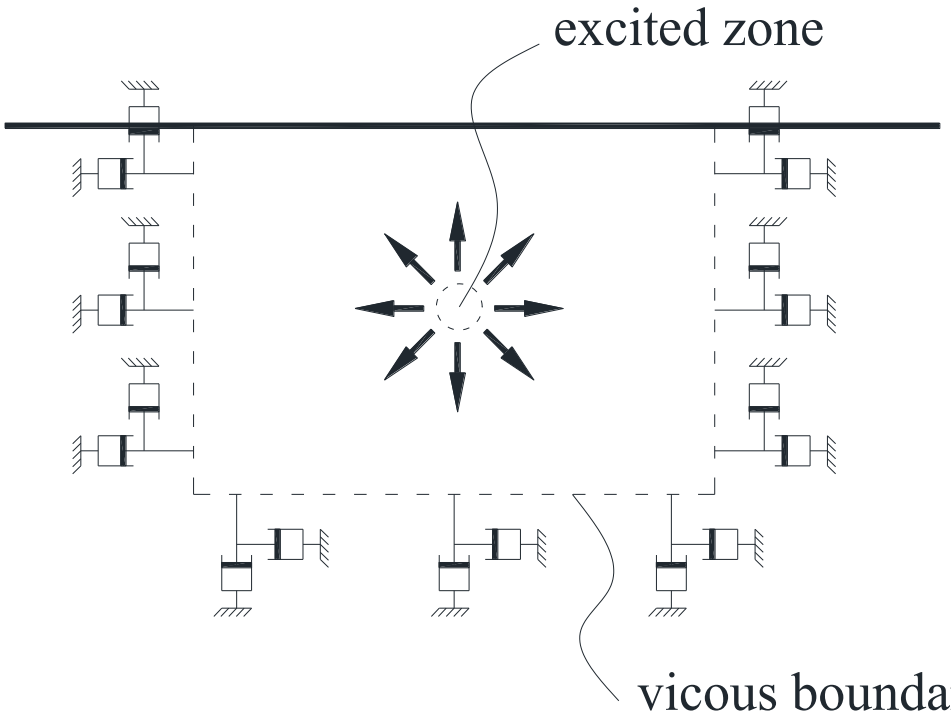

Non-reflective boundaries for blasting simulations (Bao, Hatzor, and Huang 2013)

Granular deformation

- Thanks to the powerful **simplex integration** technique used in DDA and NMM (*Shi, 1996*), blocks in the original DDA can have any shape, concave or convex, with or without holes, but they must still be closed polygons.
- This may cause numerical problems when attempting to model with the original DDA interactions between circular blocks since they would have to be modeled as polygons with many edges.
- The first efforts in developing **circular and elliptical elements** for DDA were presented by Ohnishi and his group (*Ohnishi, 1995; Ohnishi and Miki, 1996*).
- This was followed through by many workers in the **soil mechanics and geotechnical engineering** fields (e.g. *O'Sullivan and Bray, 2001; Thomas et al., 1996*) as well as the **rock mechanics and mining community** (*Balden et al.*, 2001; *Guo and Lin*, 2007; *Lin and Qiu*, 2010)

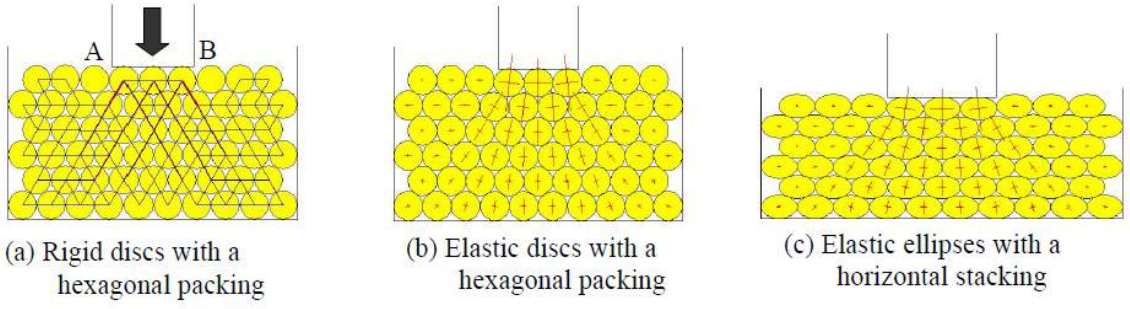

DDA for elastic elliptical elements (Ohnishi et al., 2005)

Pore pressure and fluid flow

- *Jing et al. (2001)* derived, for the first time, **explicit expressions for contributions from fluid pressure** to the global stiffness matrix and load vectors of the discrete block systems for rigid blocks, triangle and quadrilateral elements (used for internal block discretization) by closed form integration.
- **Coupled hydro-mechanical DDA** models were proposed by *Rouainia et al. (2001)* for petroleum applications and by *Ben et al., (2012, 2013)* to model hydraulic fracturing.
- *Chen et al. (2013)* introduced **seepage forces** into DDA to analyze the stability of coastal breakwater structures against tsunami damage.

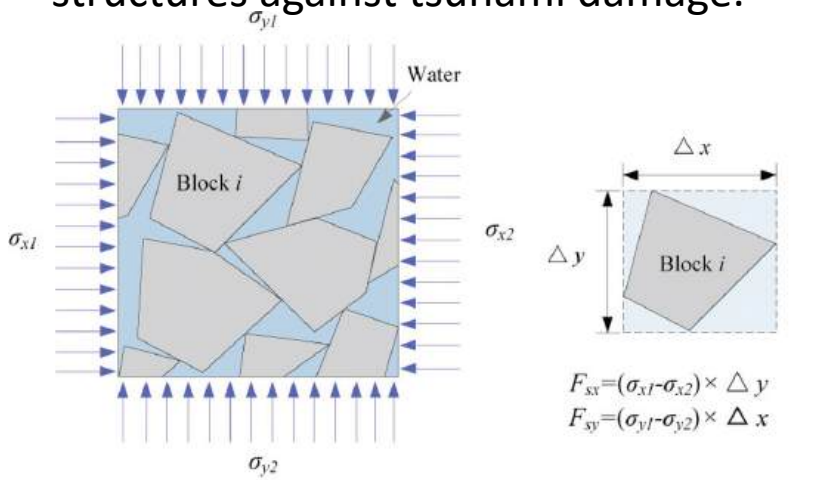

(a) Water pressure in finite element (b) Extent force induced by water pressure in DDA block

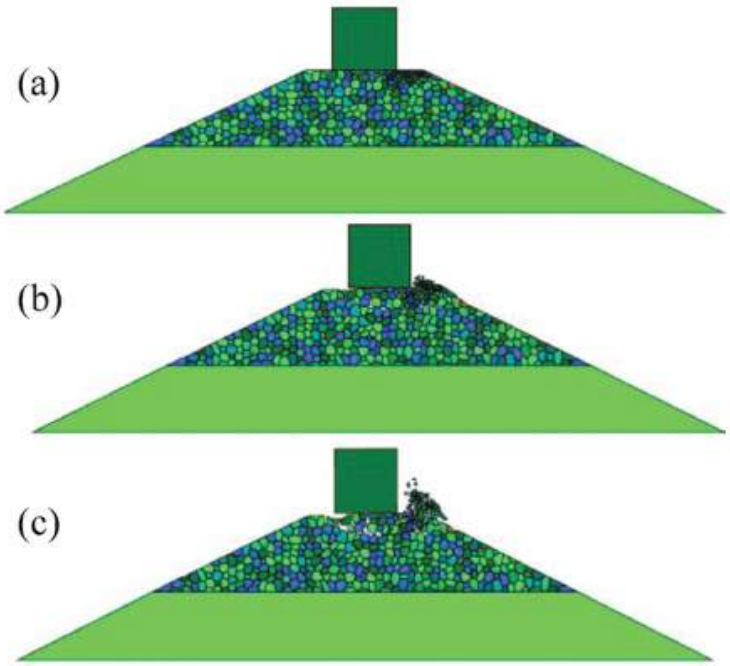

Modeling concept of coupled hydro-mechanical processes in DDA (Left) and application in stability analysis of breakwater structure against tsunami damage in Japan (Chen et al., 2013).

Velocity/displacement dependent friction

- In the original DDA a **constant friction angle is assumed**, regardless of sliding distance or sliding velocity.
- Both field and experimental evidence suggest that **fictional resistance is velocity and/or displacement dependent.**

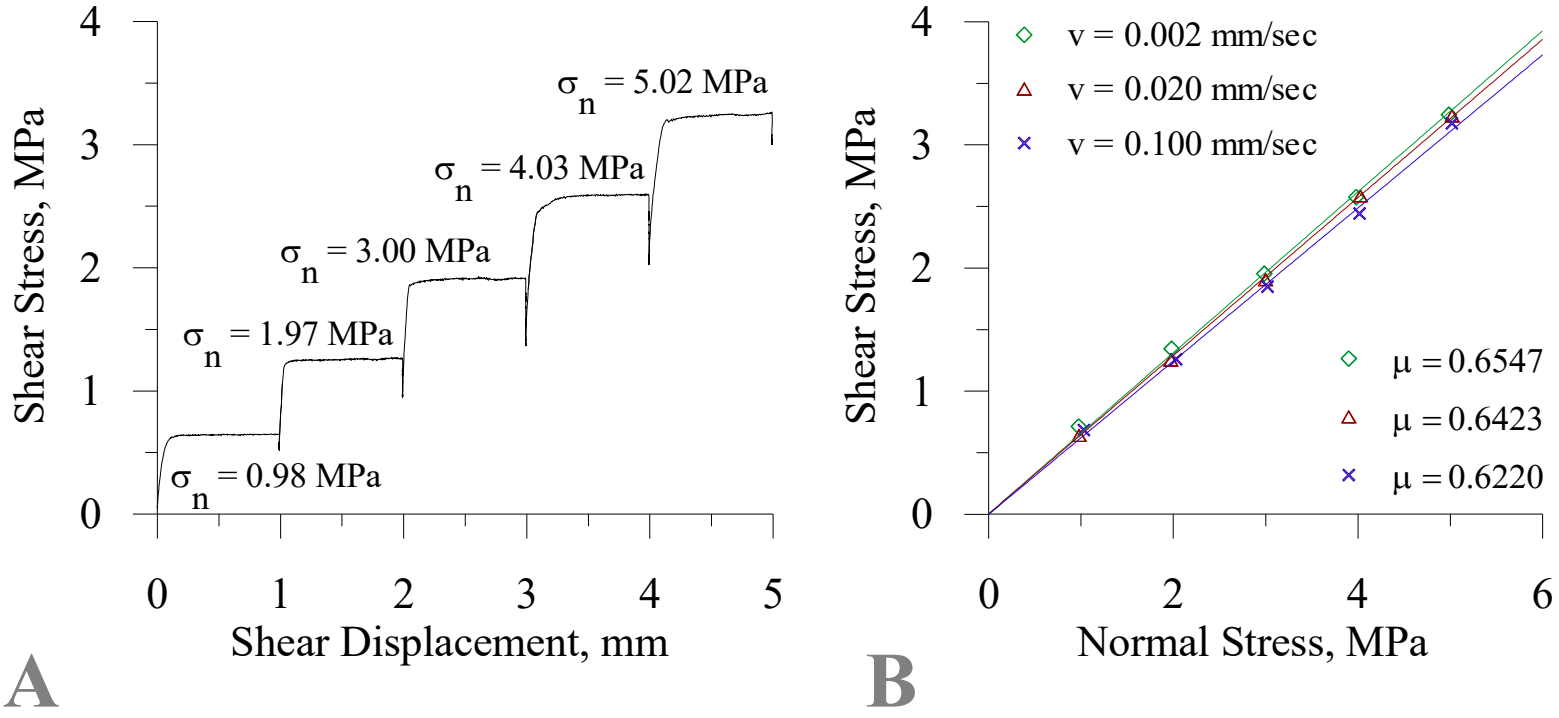

Servo-controlled direct shear tests performed on concrete interfaces at various velocities (Bakun-Mazor, Hatzor, and Glaser, 2012).

Shaking Table Experiments

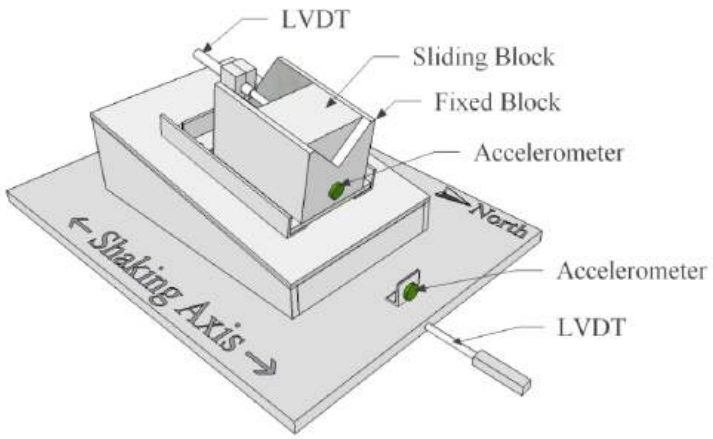

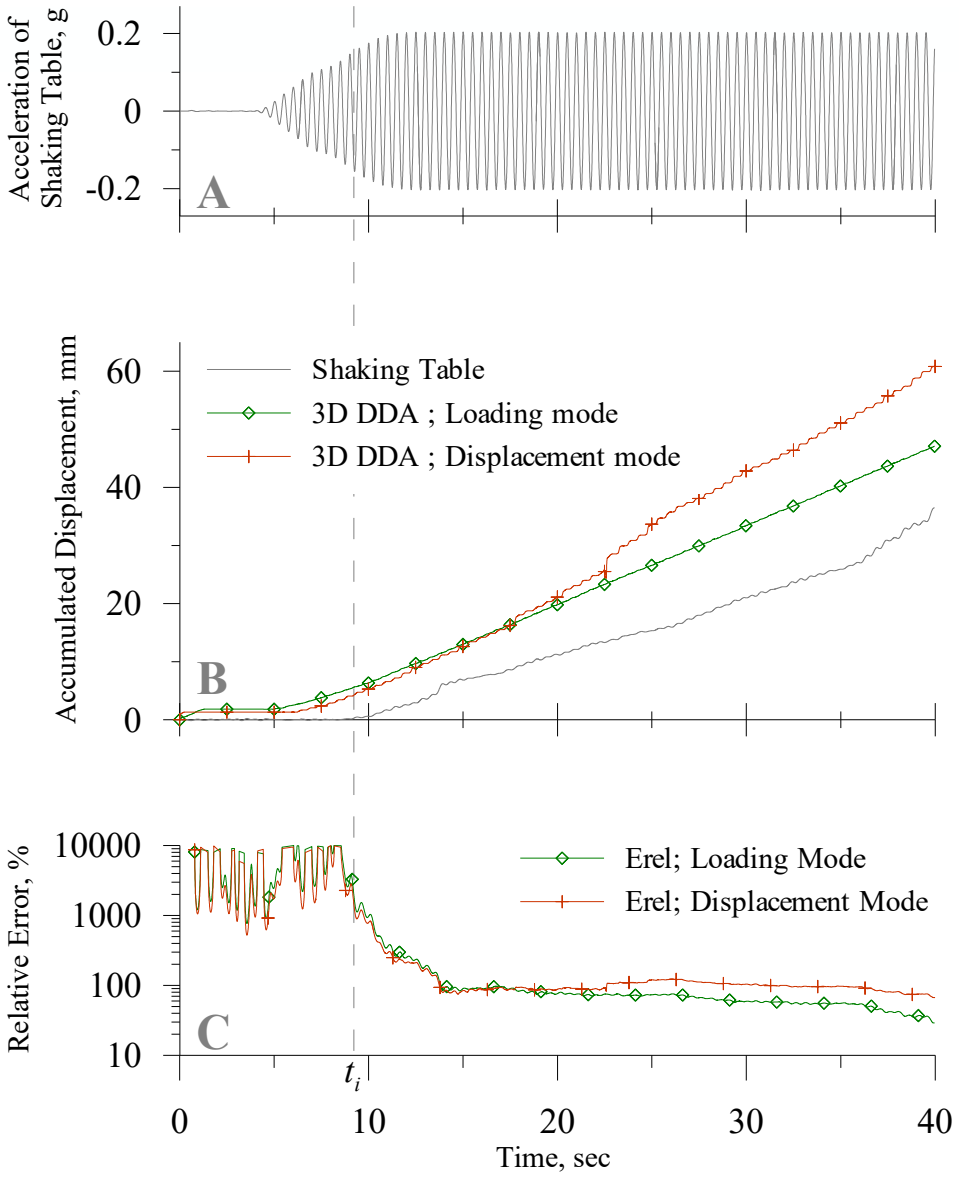

Observed Block "Run-out"

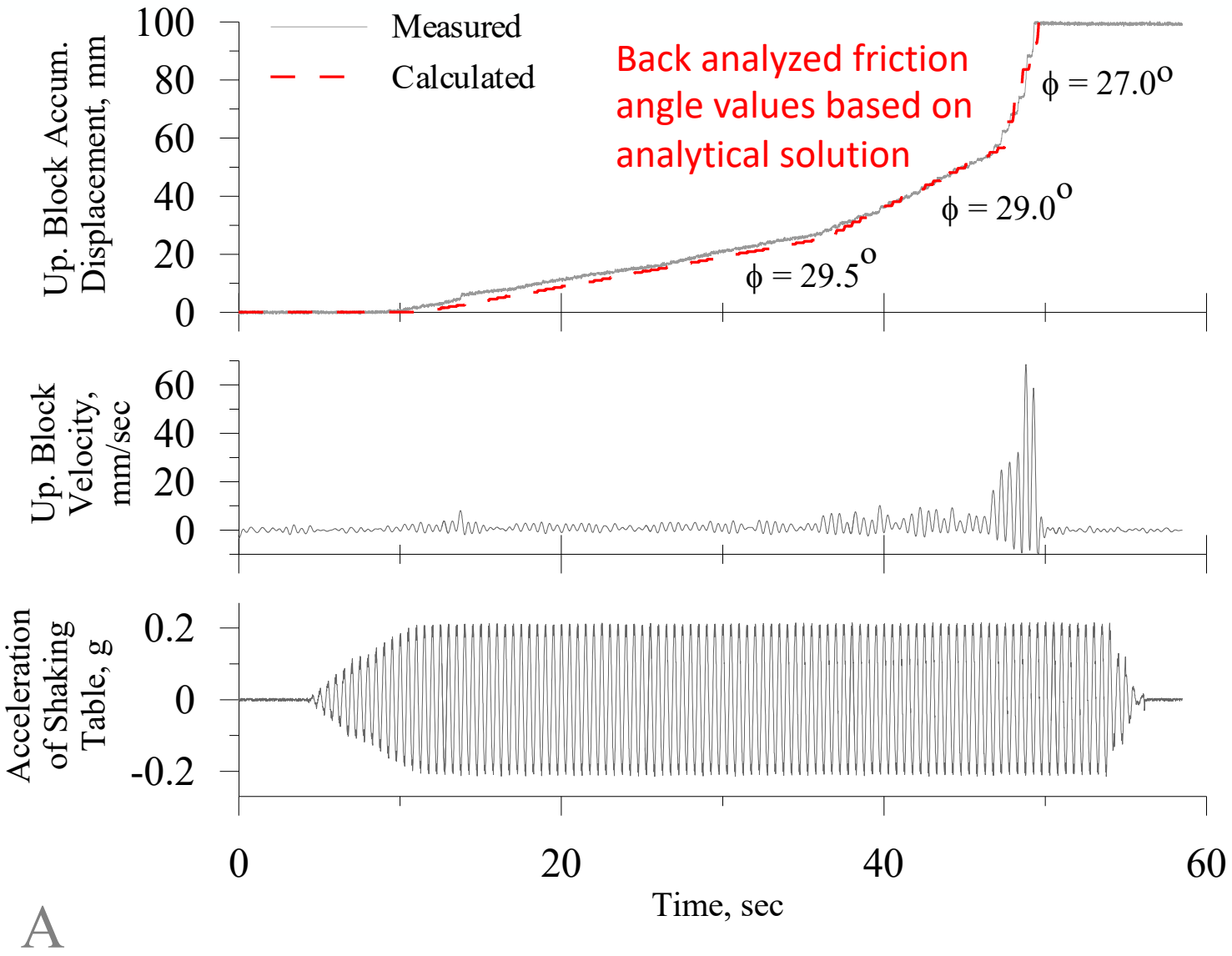

A

Friction Angle Degradation

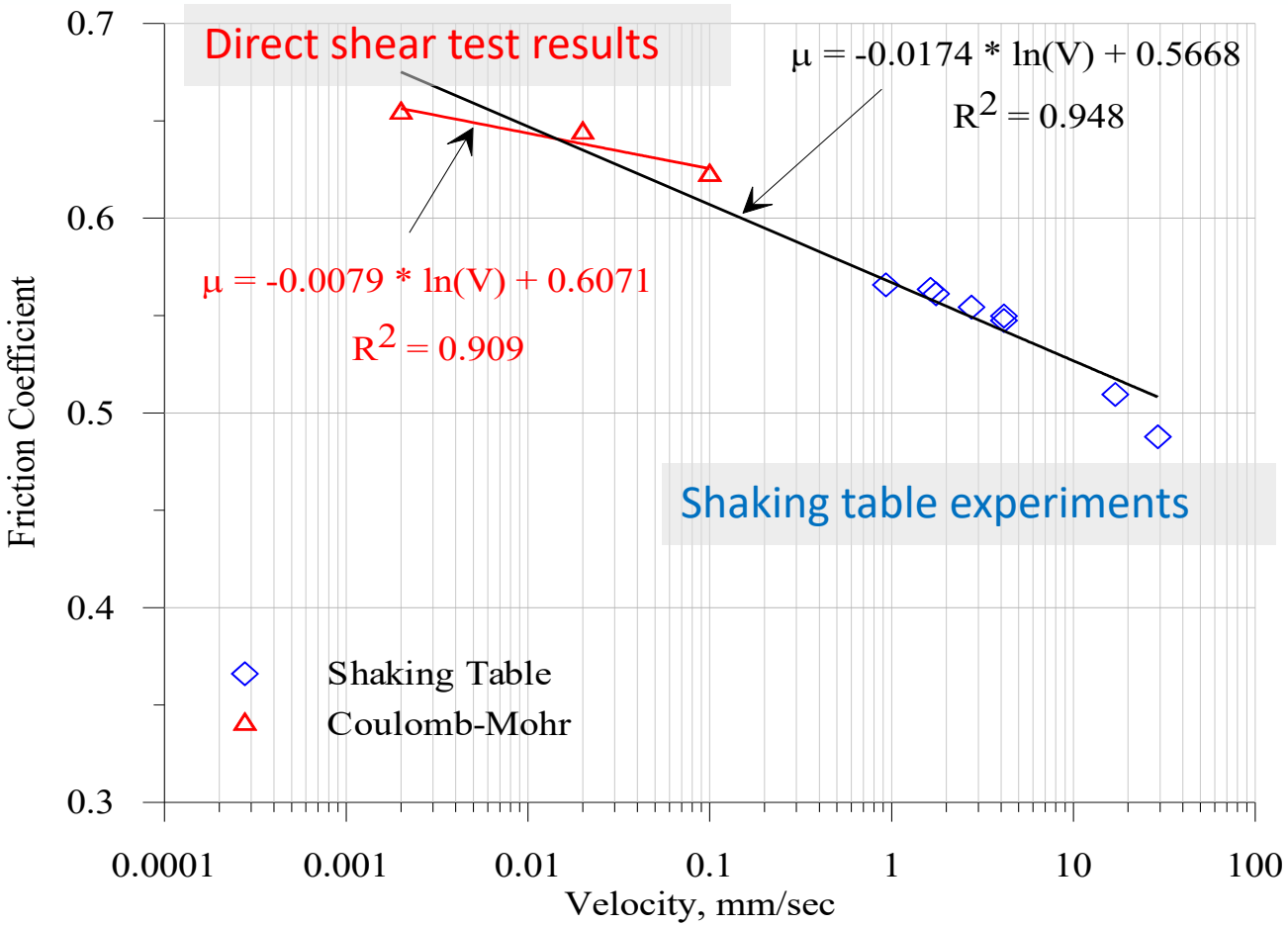

Sitar et al. (2005) have identified the need to introduce **friction degradation** in DDA in his slope stability analyses, the Vajont slide included. *Osada and Tanityama (2005)* incorporated **rate and state friction** in DDA and *Wang et al. (2013)* introduced **displacement dependent friction** into DDA.

So… what have *we* done? ☺

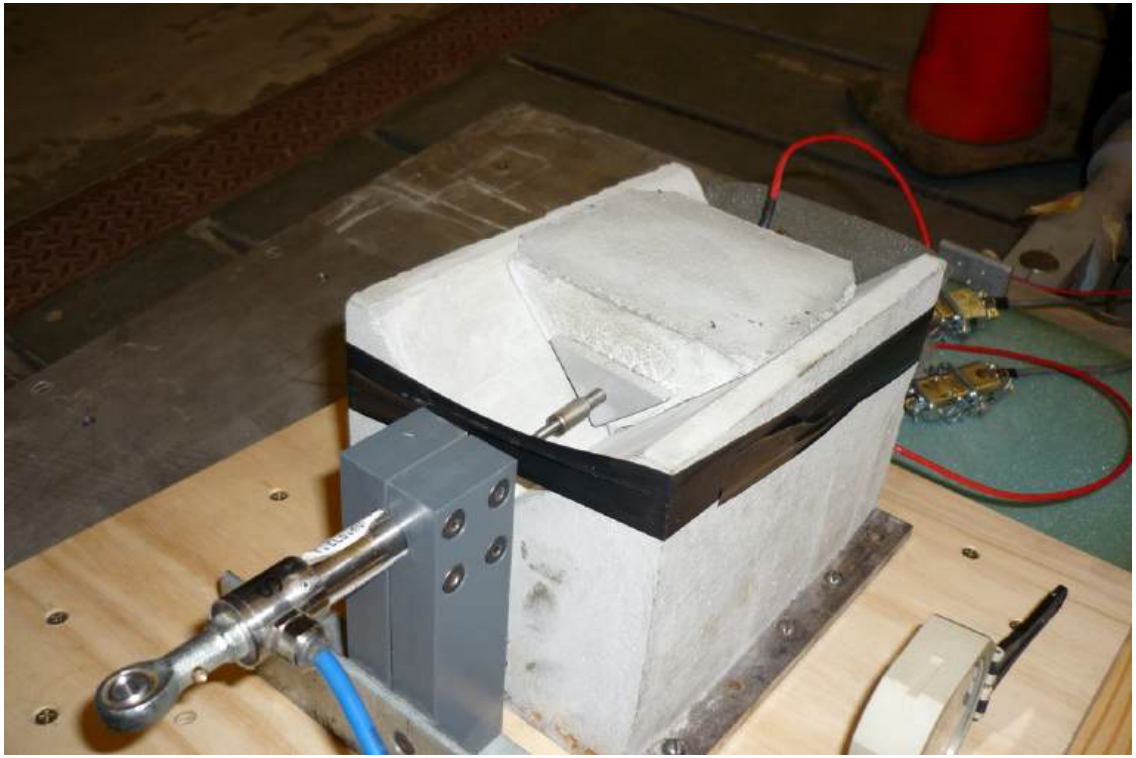

Benchmarking the DDA method: verifications and validations

Single Face Sliding – 2D

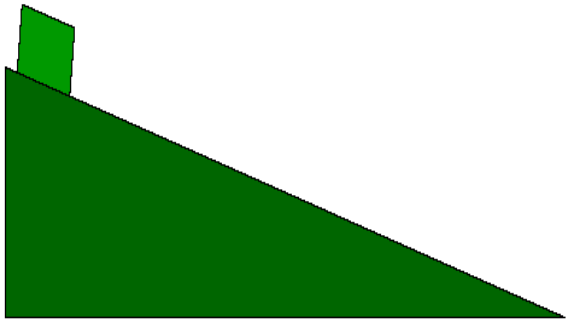

- **Dynamic sliding under gravitational load** only was originally studied by *McLaughlin (1996)*
- **Sinusoidal input** first studied by *Hatzor and Feintuch (2001)*, and later improved by *Kamai and Hatzor (2008)*.
- A **detailed study** of this problem was published by *Ning and Zhao (2012)*.

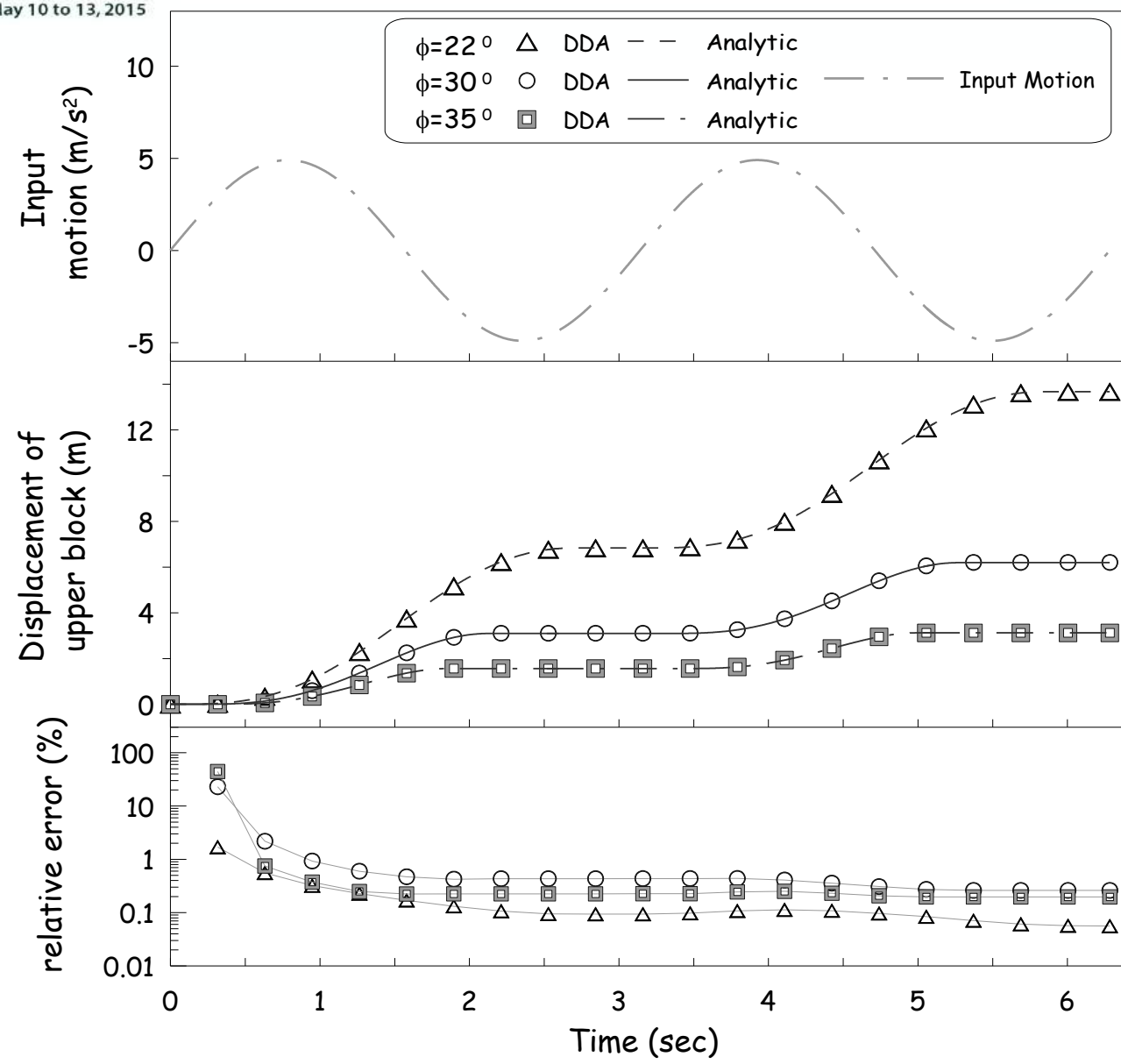

Kamai and Hatzor (2008).

Single Face Sliding – 3D

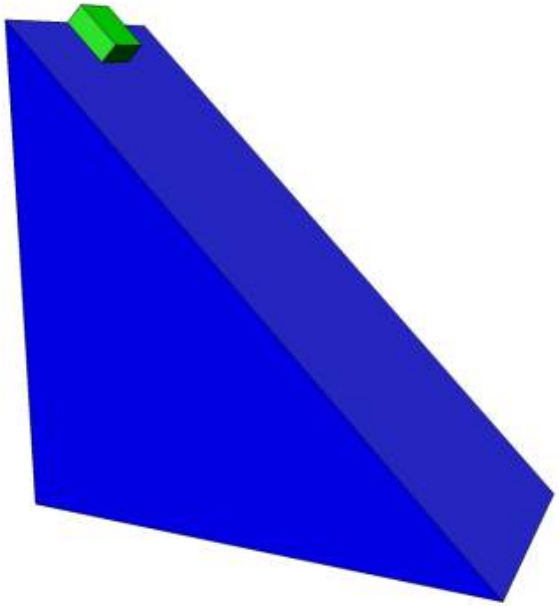

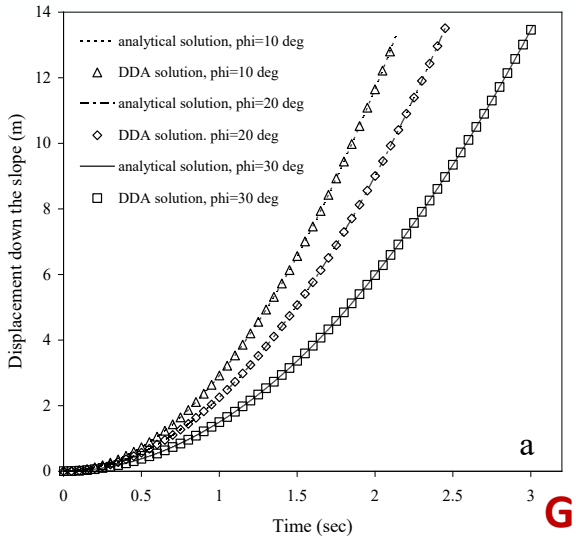

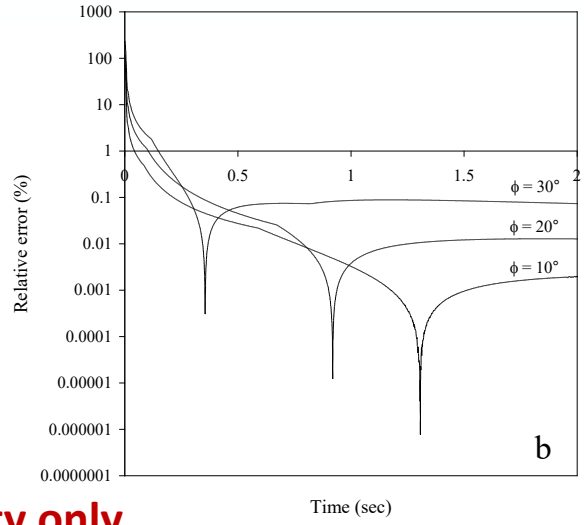

Gravity only

Initial attempts to verify 3D-DDA have been conducted by several research groups. Bench marking of 3D-DDA using the "block on an incline" problem for **static and dynamic loading** is shown in the figure.

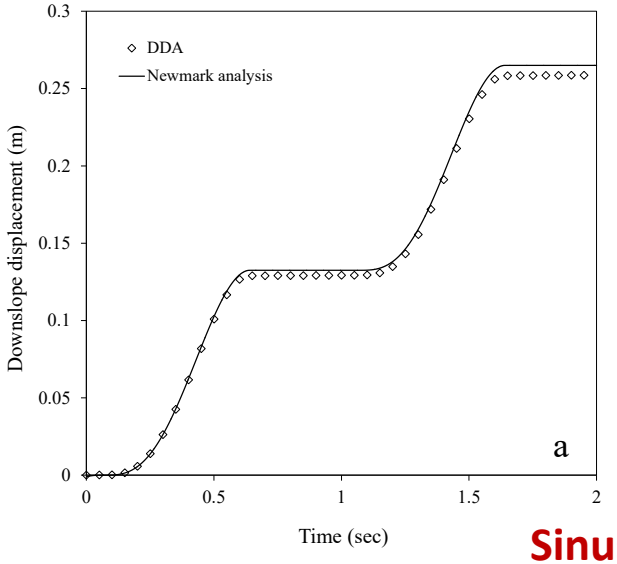

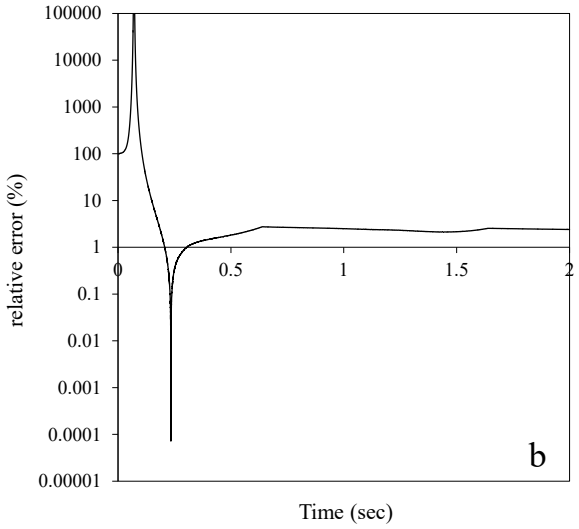

Sinusoidal input

Yagoda-Biran and Hatzor (in prep.).

Double Face Sliding – 3D

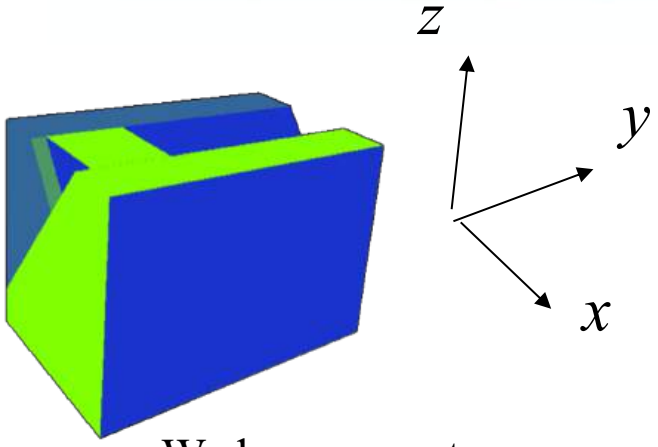

Wedge parameters:

P_1=52/063, P_2=52/296

$\phi_1=\phi_2=30^o$

- Three dimensional DDA is particularly suitable for studying dynamic sliding of rock wedges.
- An analytical solution was developed by *Bakun-Mazor et al. (2012)* to enable benchmarking of 3D-DDA for this case.

Bakun Mazor, Hatzor, and Glaser (2012).

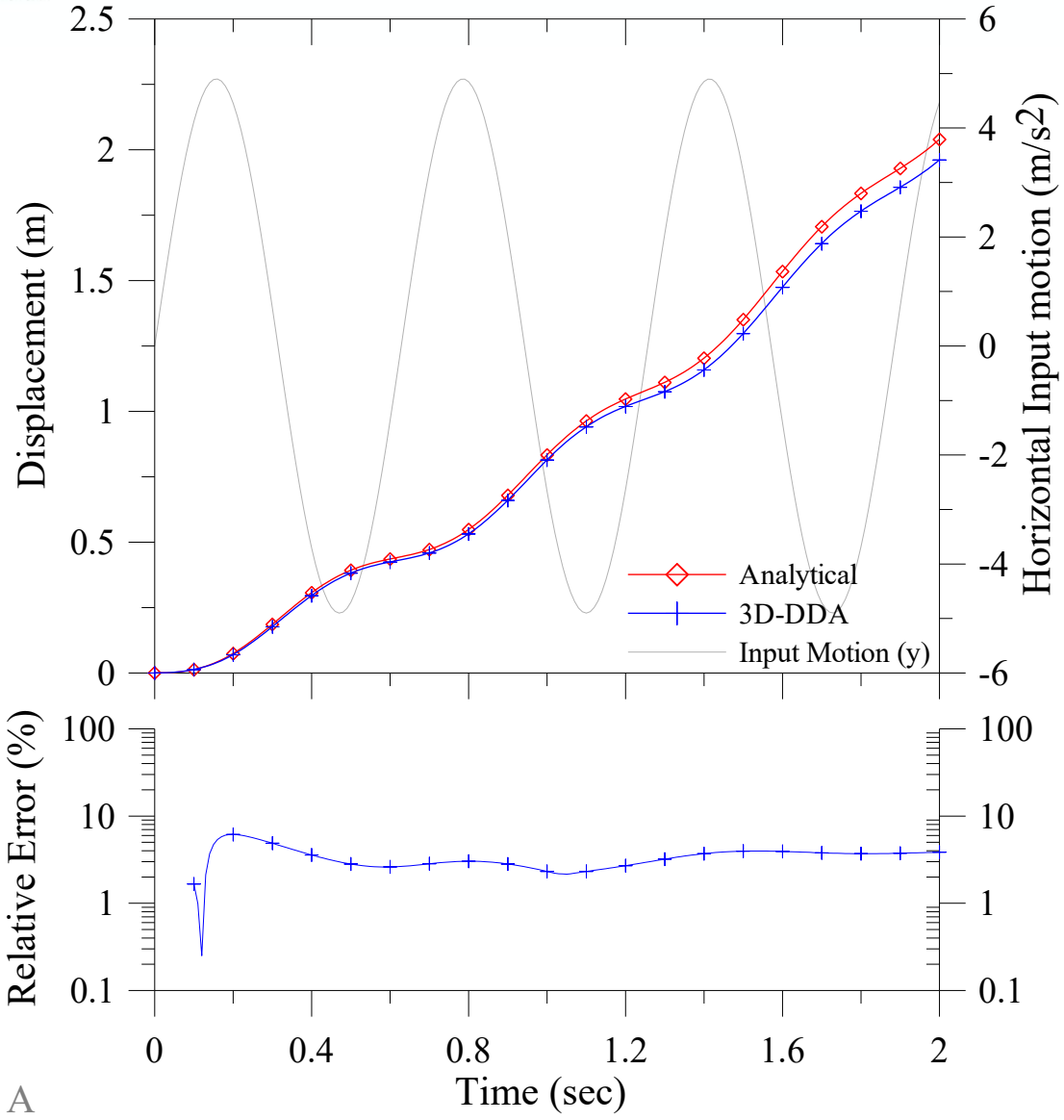

Block response to shaking foundation

Shaking foundation: 2D

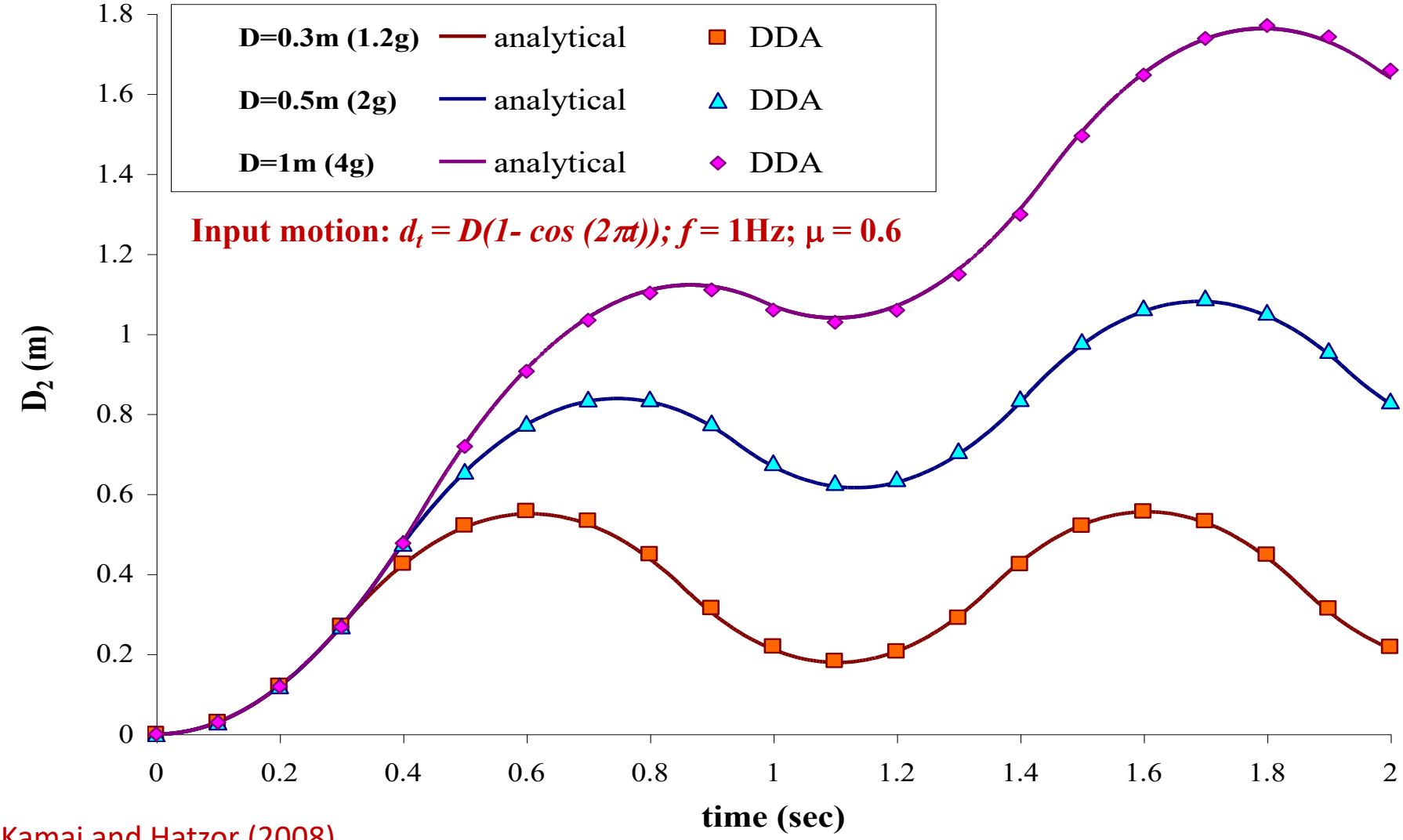

Kamai and Hatzor (2008).

Shaking foundation: 3D

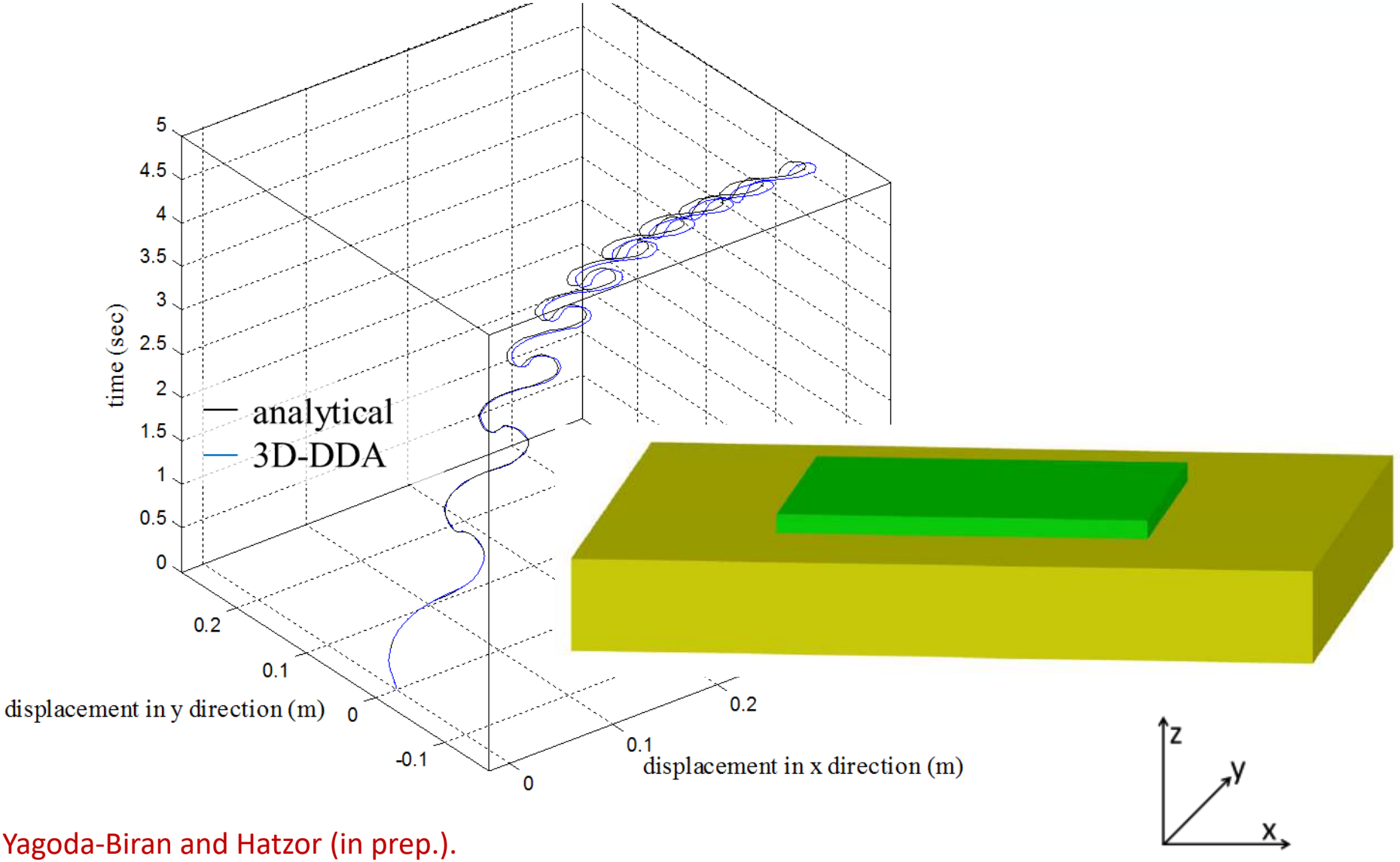

Yagoda-Biran and Hatzor (in prep.).

Rocking block on firm foundation: 2D

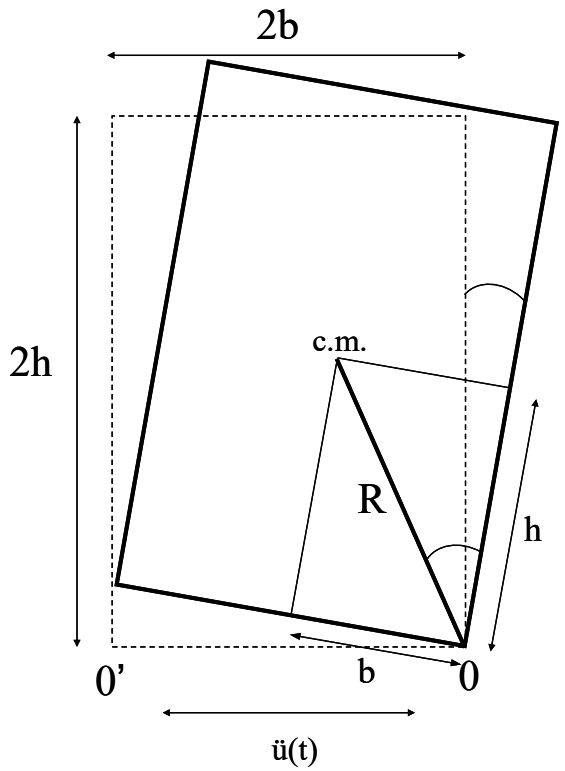

- **Analytical solution proposed by: *Makris and Roussos (2000), Geotechnique*.**
- **DDA verification: *Yagoda-Biran and Hatzor (2010), EESD*.**

a_{peak} slightly lower than *PGA* required for toppling

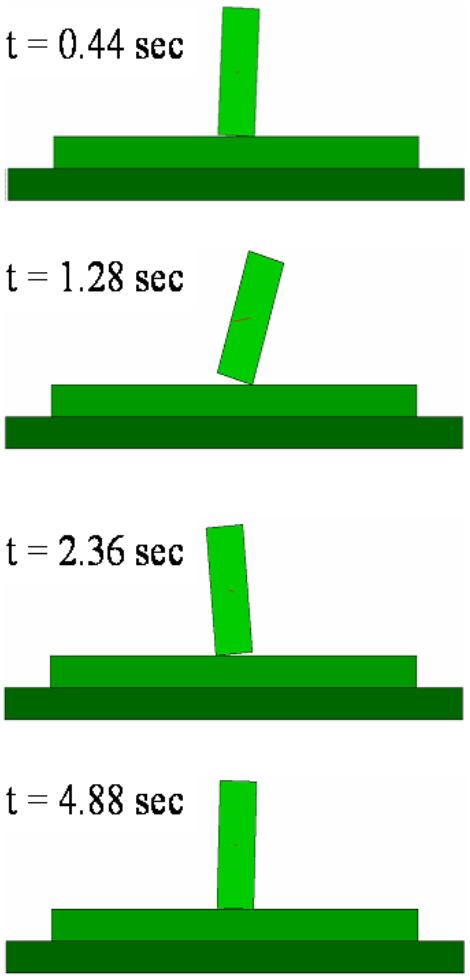

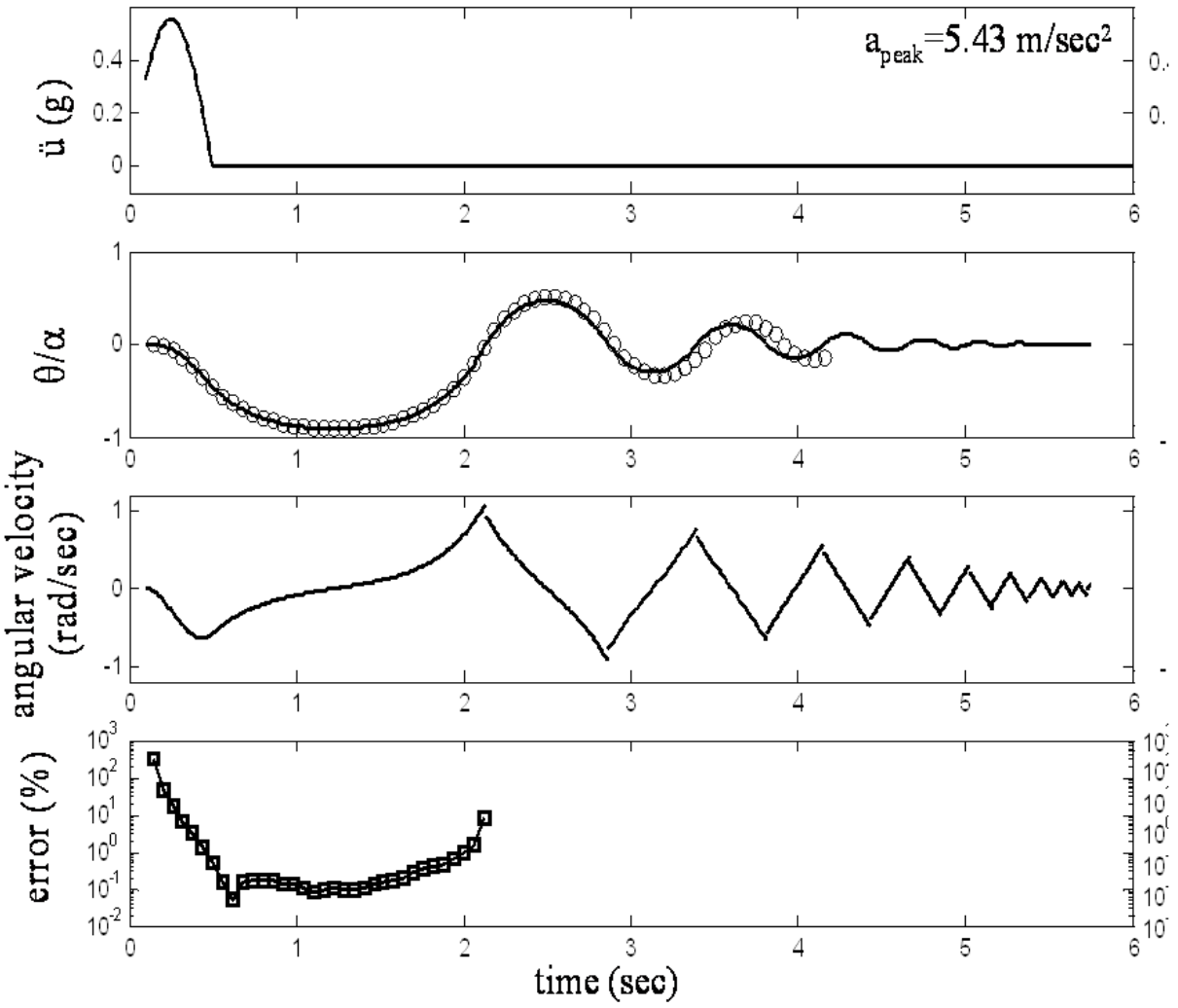

a_{peak} slightly higher than *PGA* required for toppling

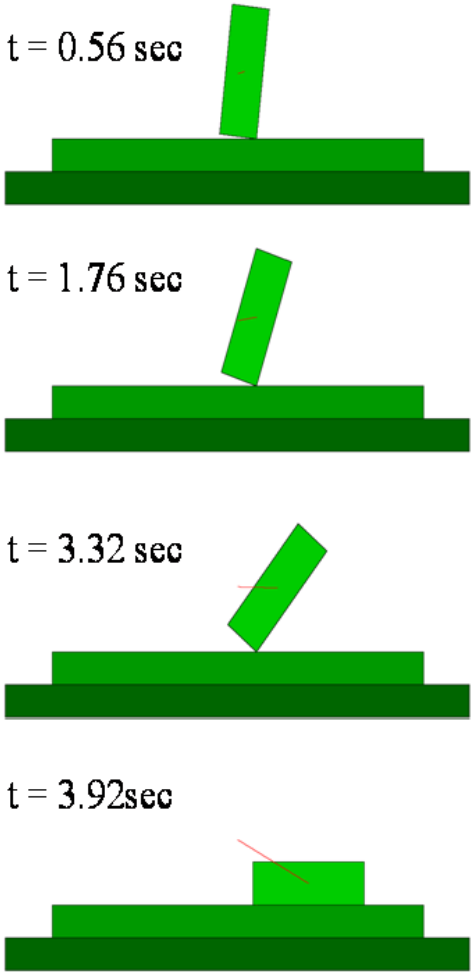

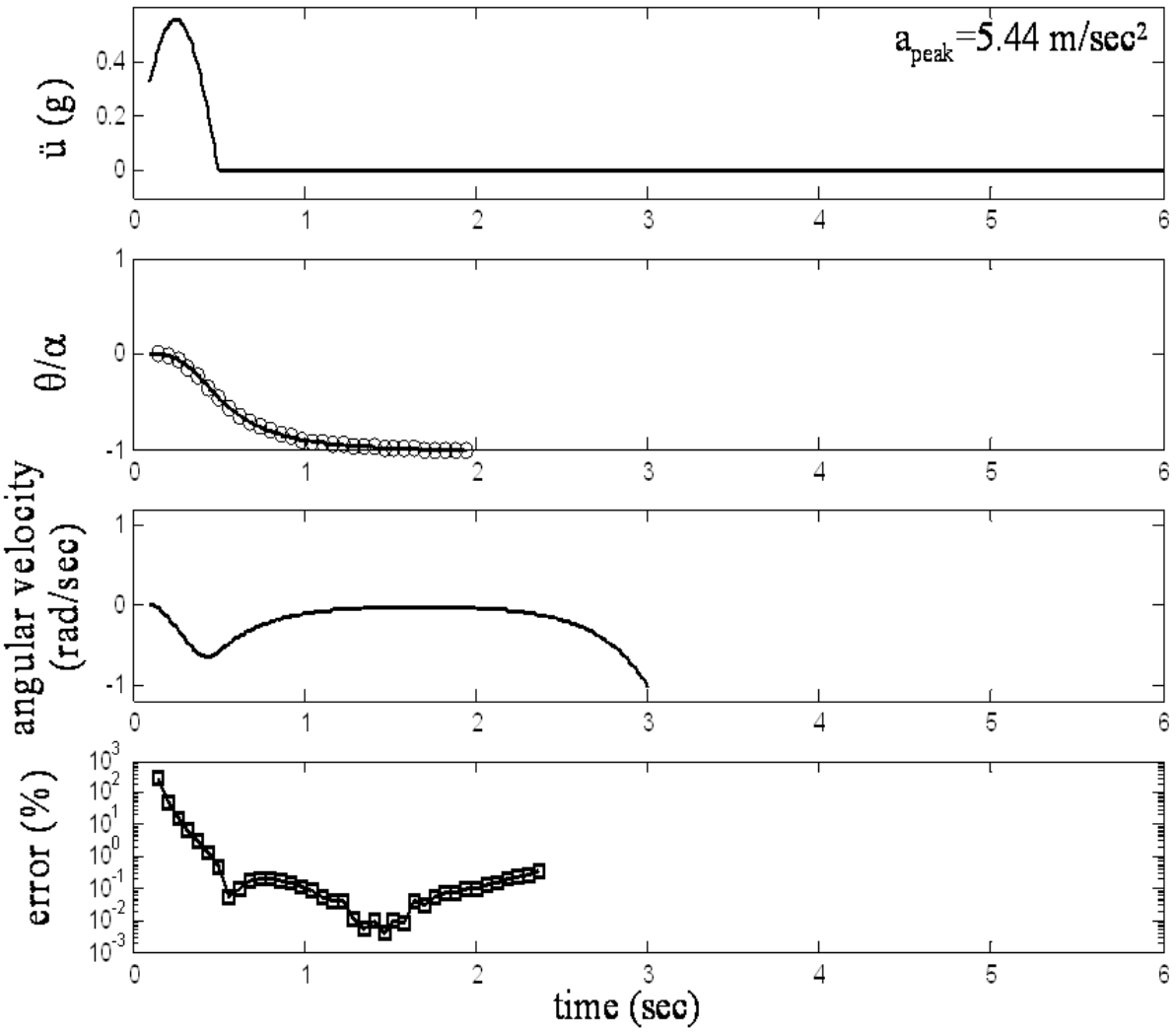

P wave propagation through 1D elastic bar

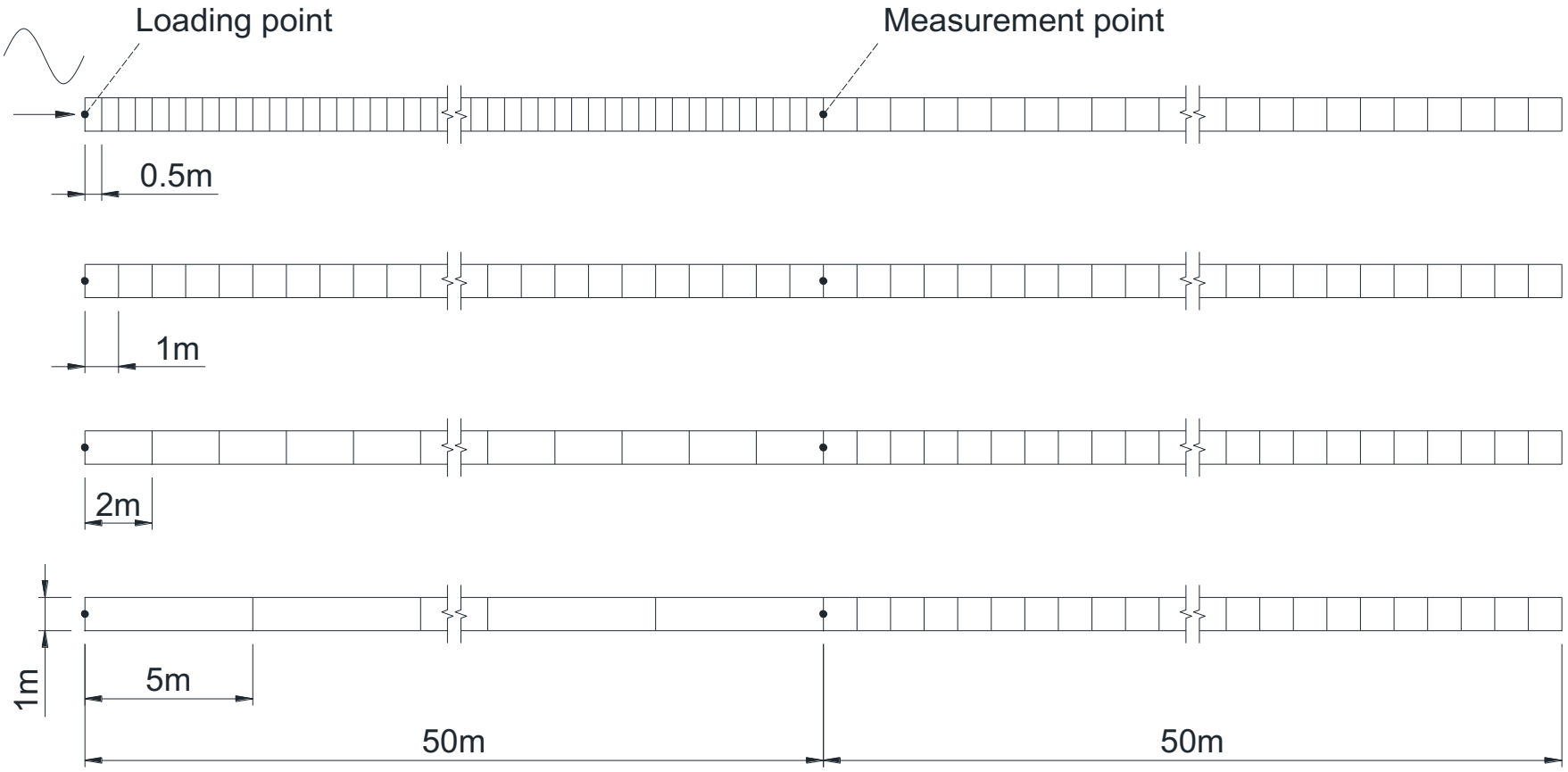

Penalty parameter effect on waveform accuracy

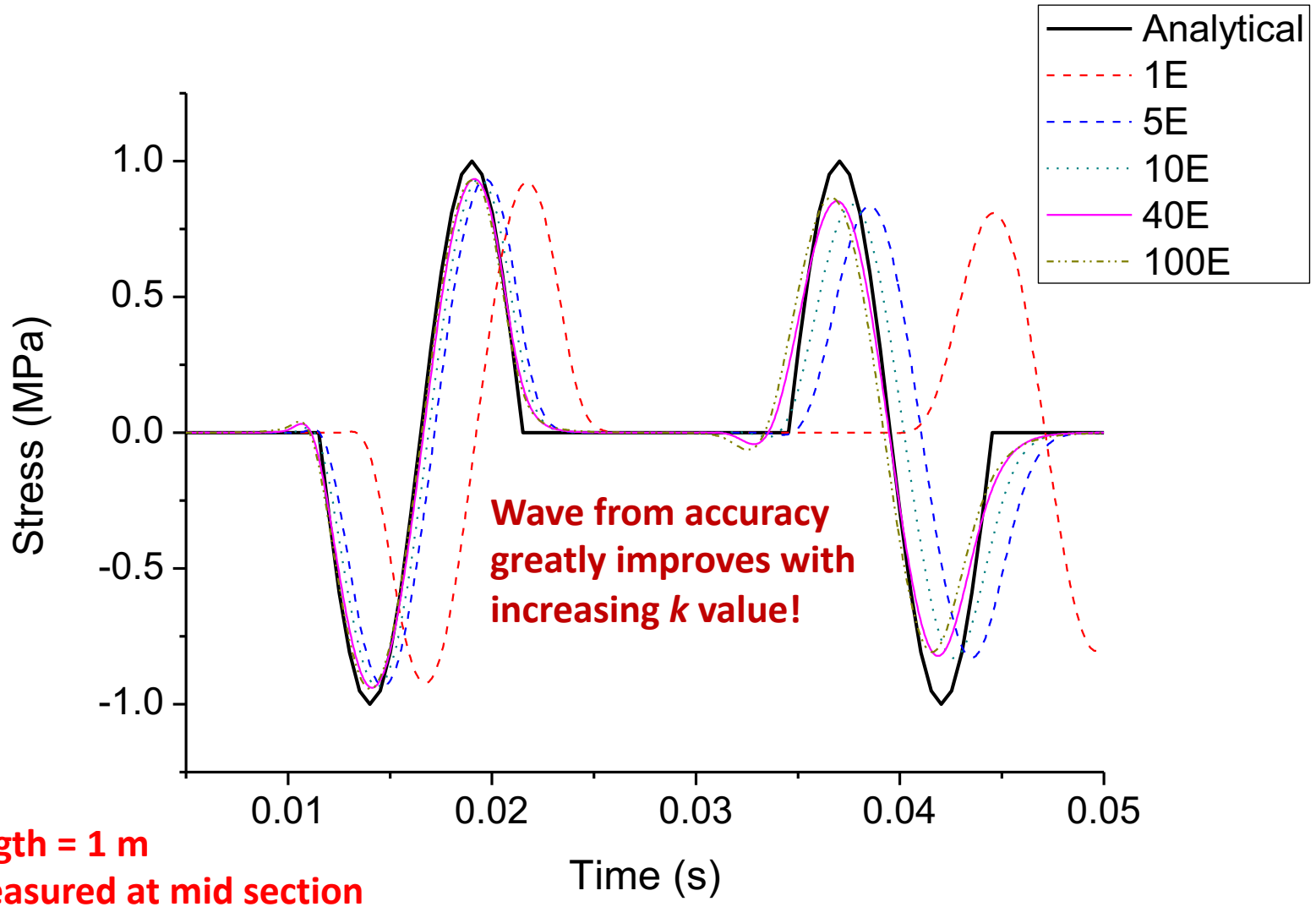

Block length = 1 m
Stress measured at mid section

Time interval effect on waveform accuracy

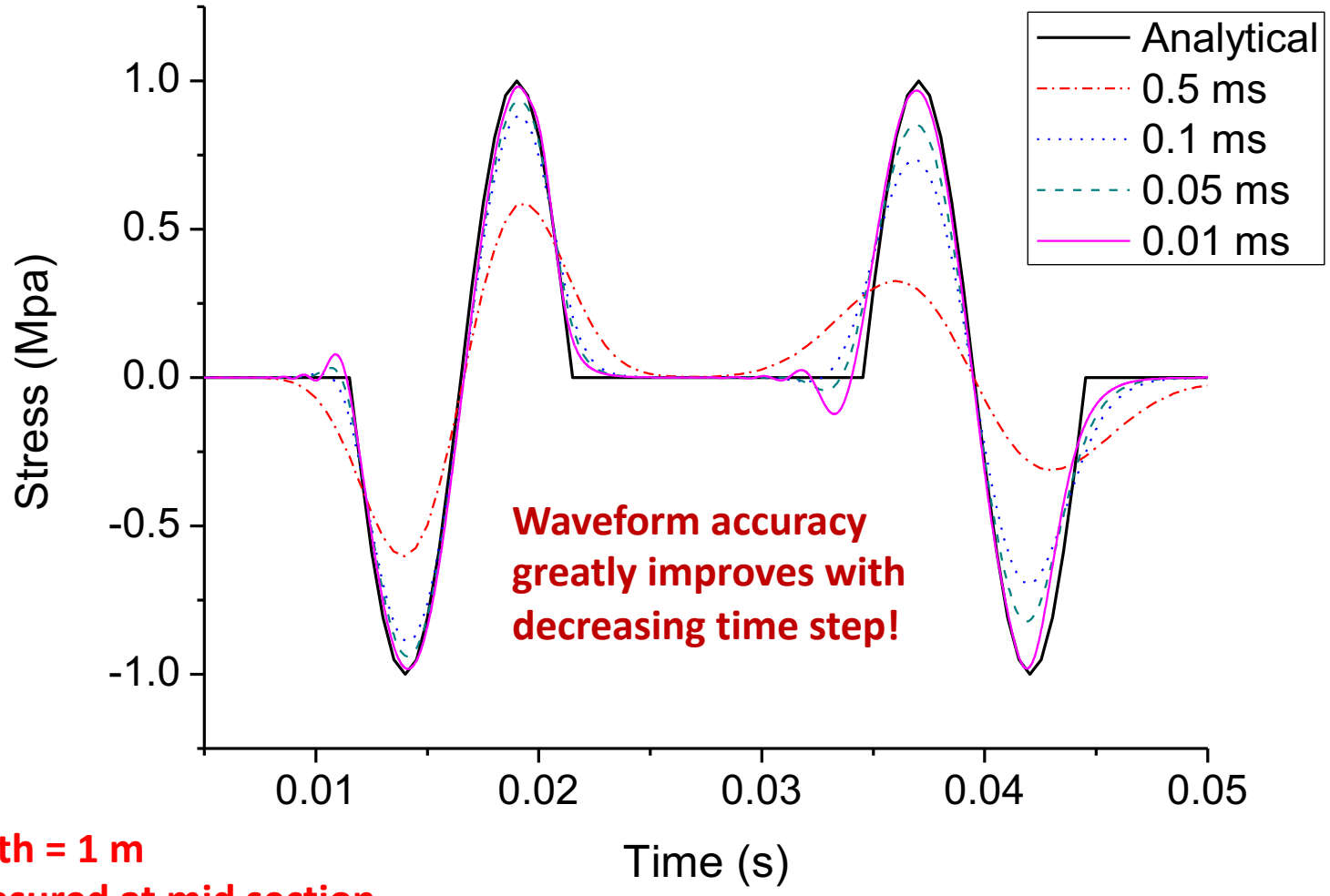

Block length = 1 m
Stress measured at mid section

S wave propagation: DDA vs. SHAKE

DDA Model

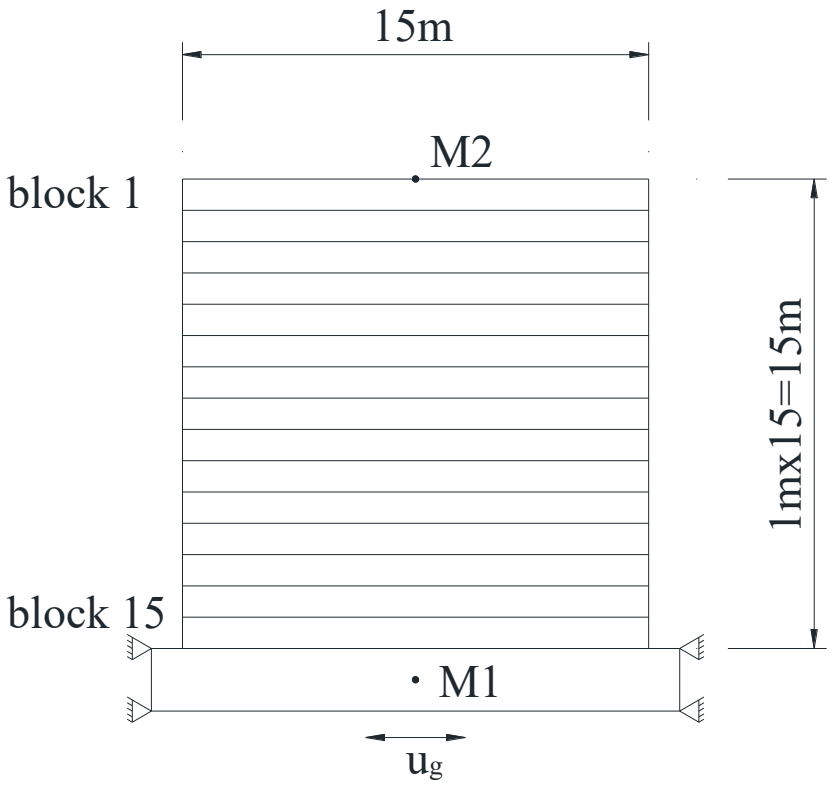

SHAKE model

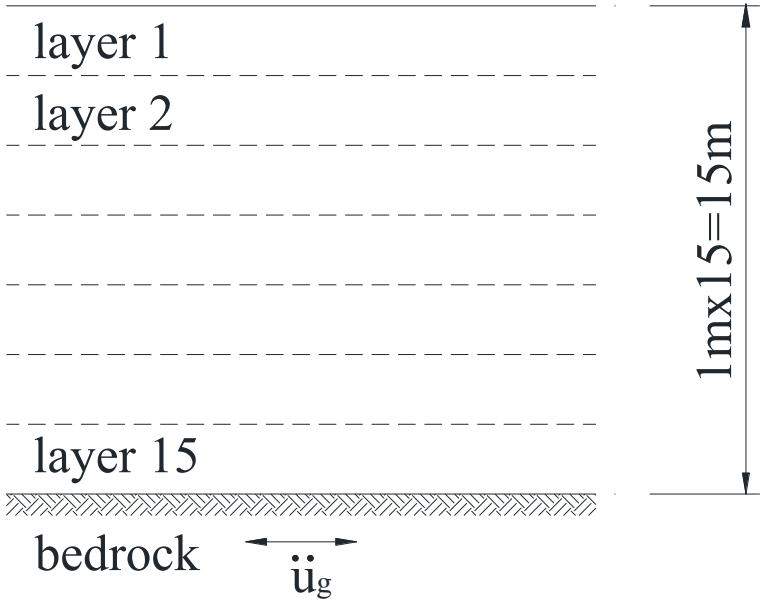

Bao, Yagoda-Biran, and Hatzor (2014) *EESD*.

Input Ground Motions

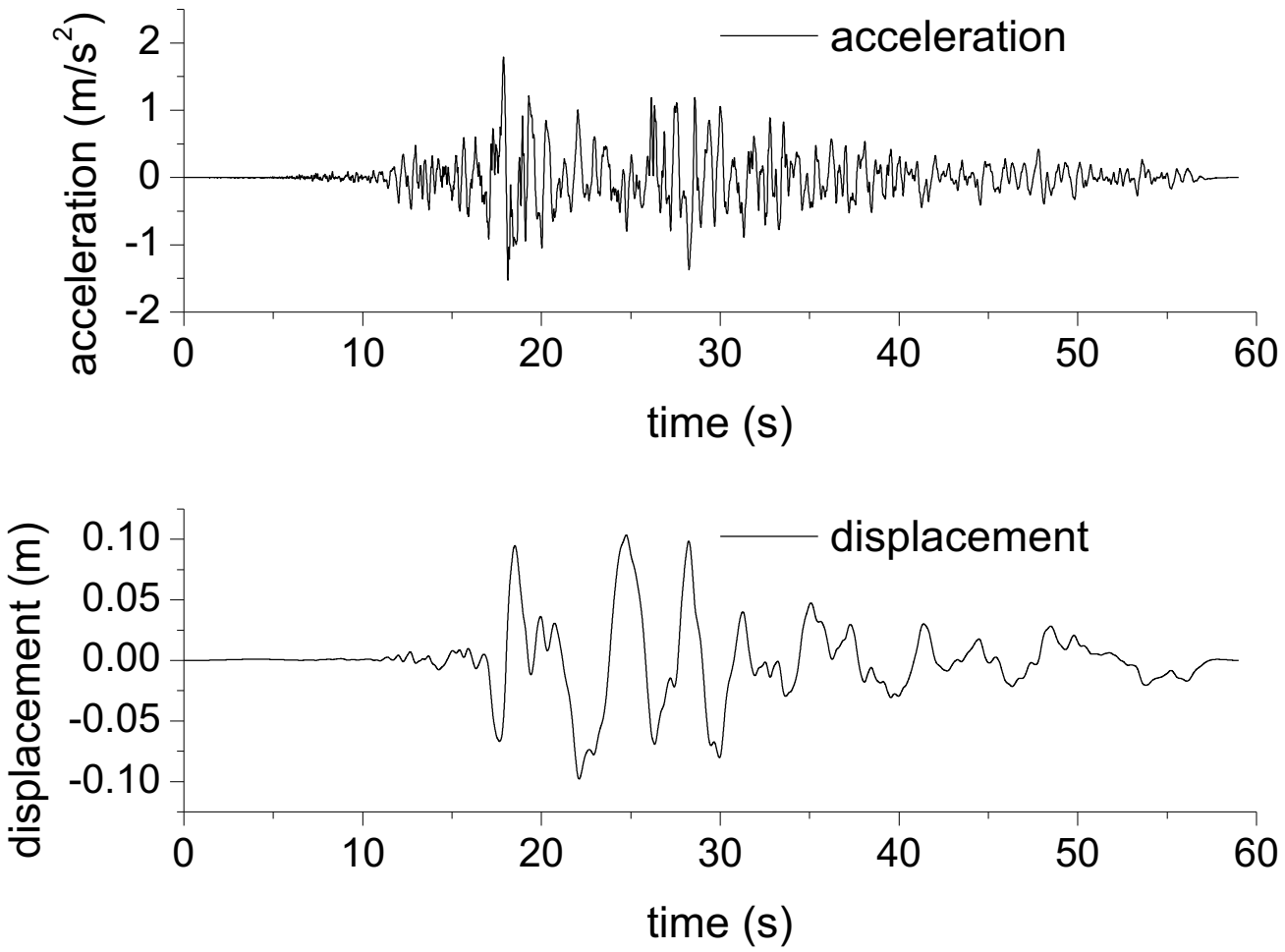

CHI-CHI 09/20/99, ALS, E (CWB): acceleration for SHAKE and displacement for DDA

Spectral Amplification Ratio

DDA numerical control parameters

time step size (s):	**0.001**
Total steps:	**60000**
Spring stiffness (N/m):	**1.50E+12**
Calculated damping ratio:	**2.3%**

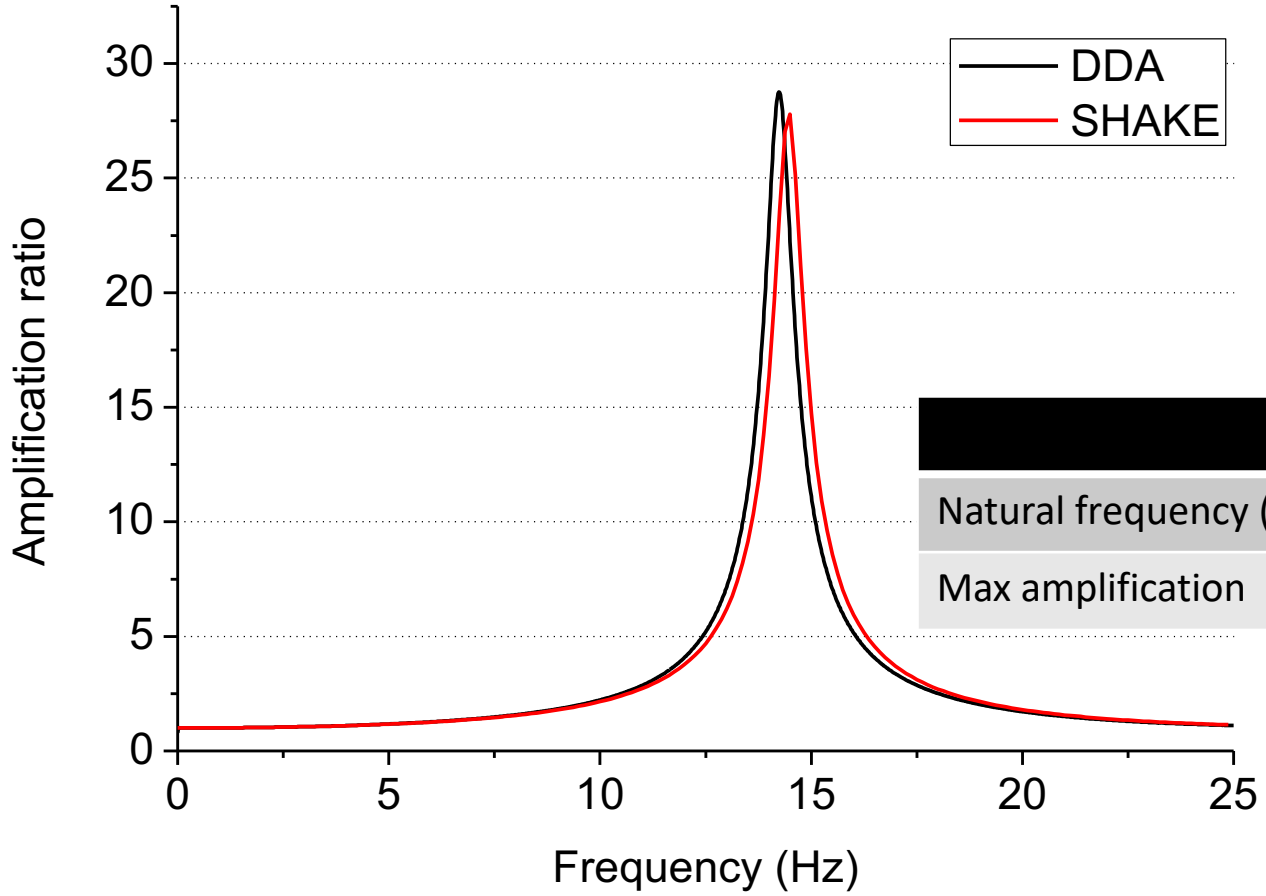

	DDA	SHAKE
Natural frequency (Hz)	14.23	14.50
Max amplification	28.76	27.79

2D Site Response

Bao, Yagoda-Biran, and Hatzor (2014) *EESD*.

"Static" Push and Release at top column

"Dynamic" blow with sledgehammer at column base

Top column response to push

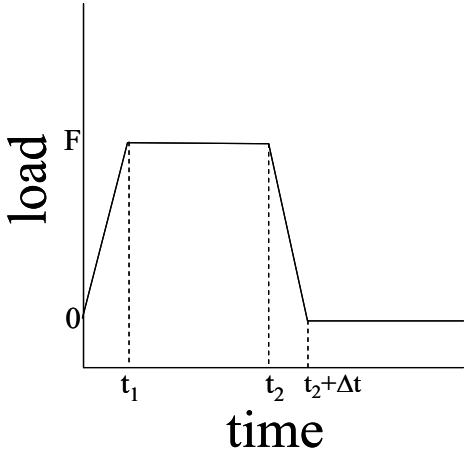

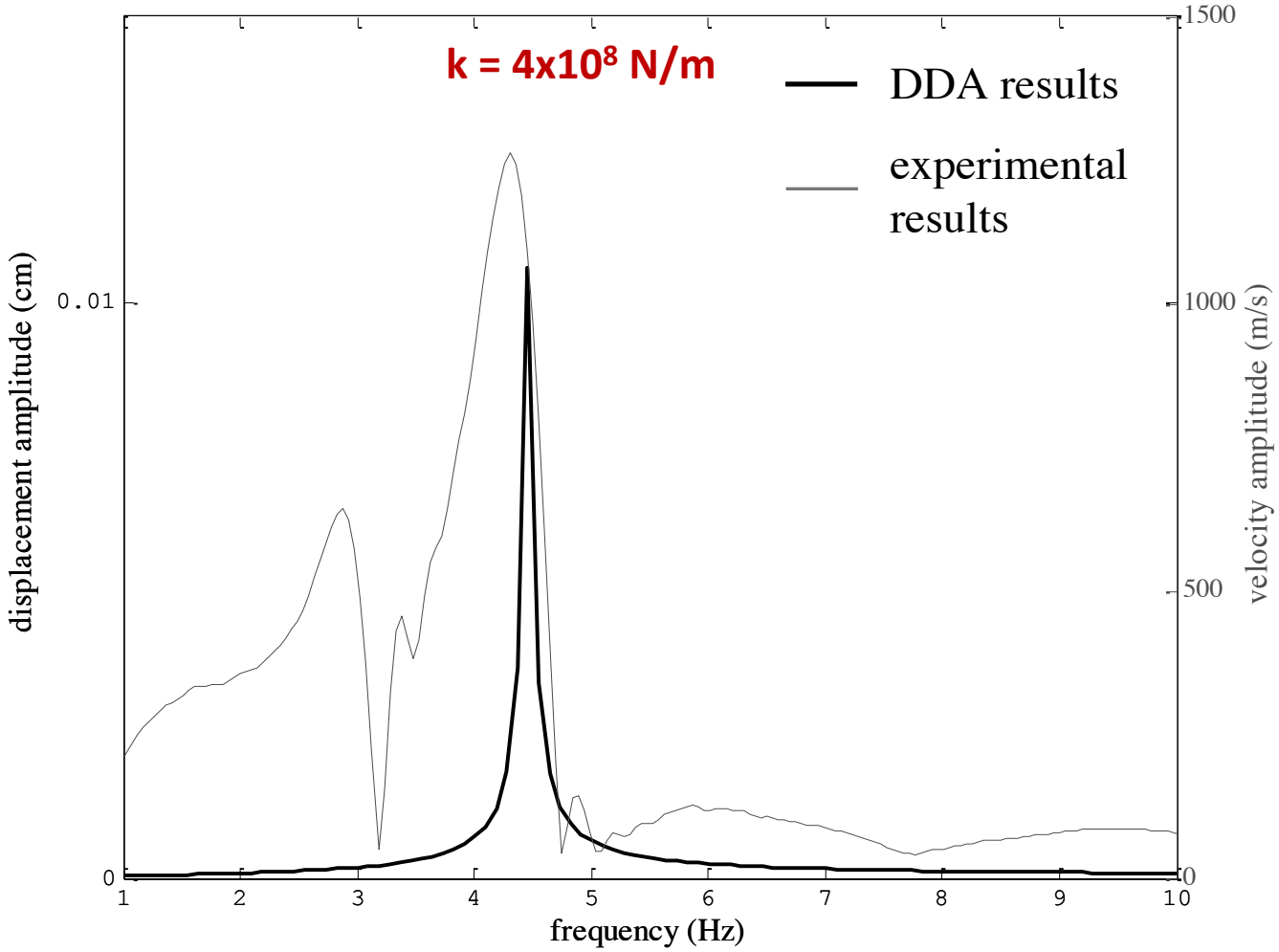

Top column response to blow

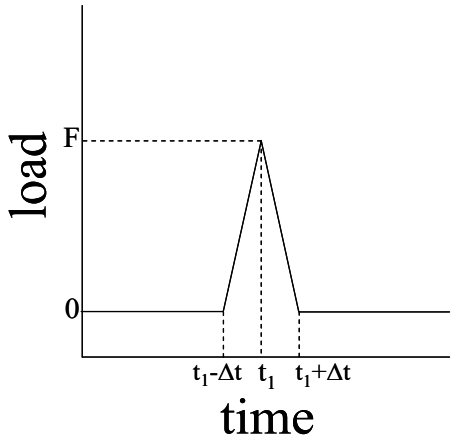

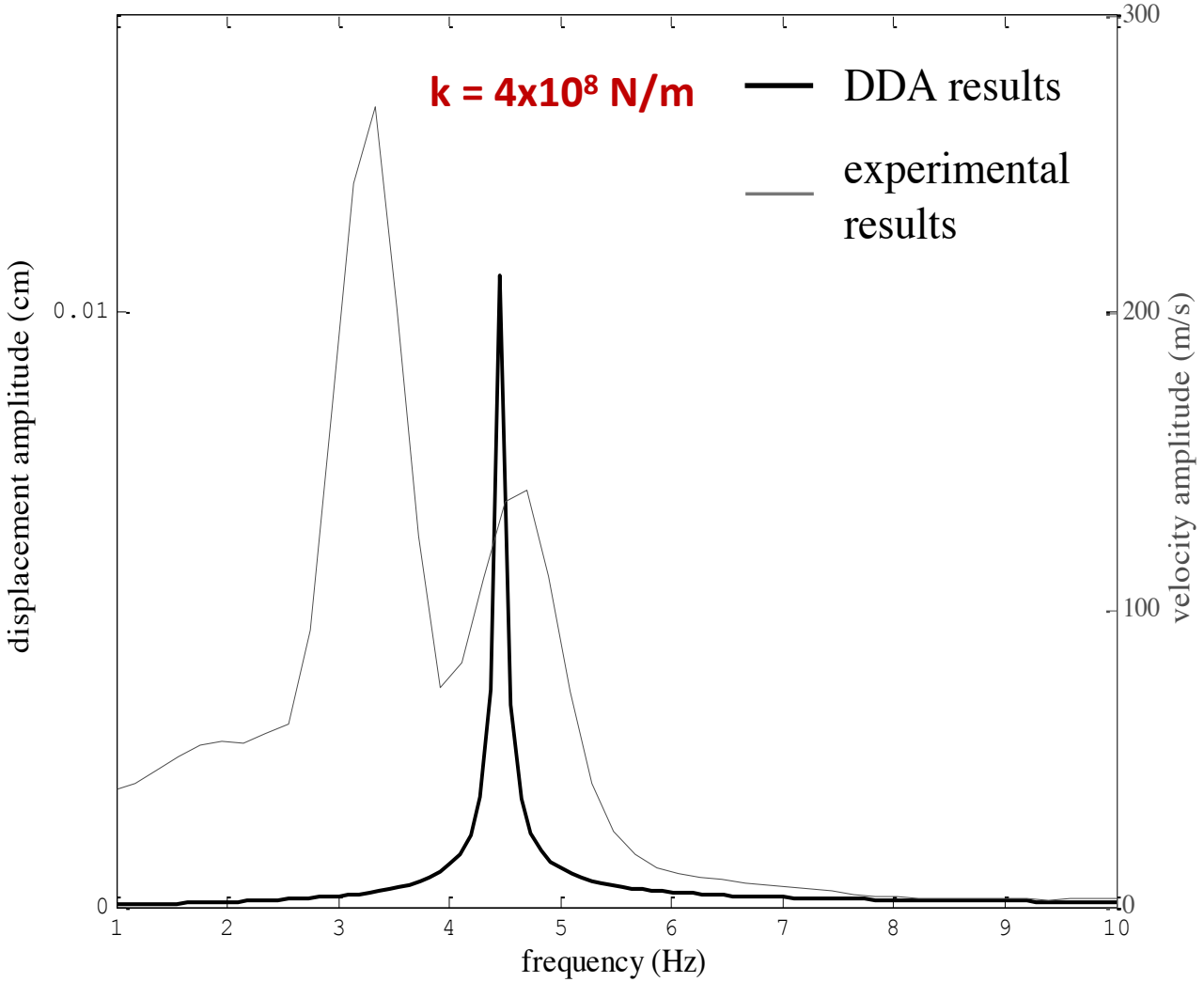

Note sensitivity of resonance frequency to penalty parameter

FFT of uppermost block displacement

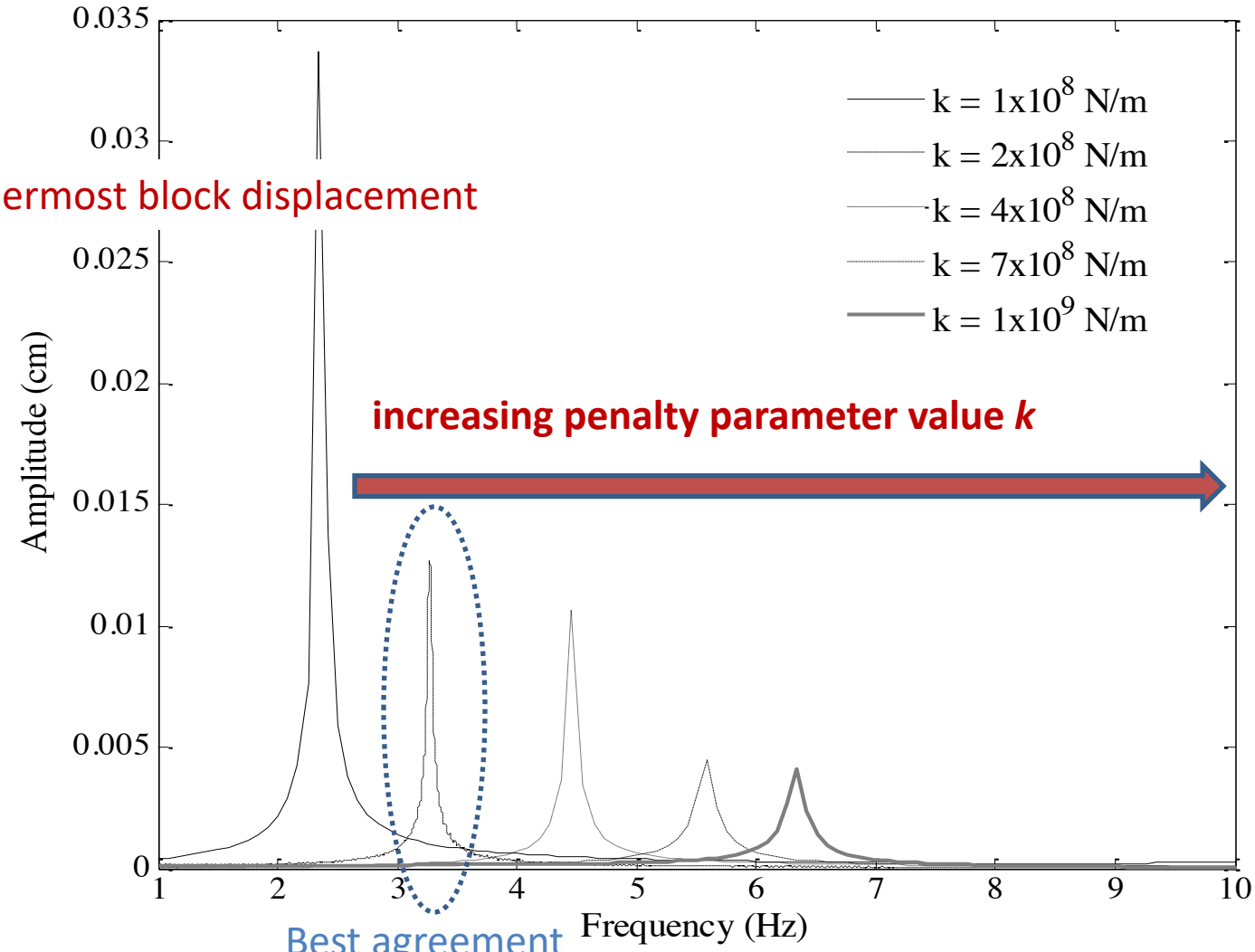

Best agreement with field test

Shock wave propagation

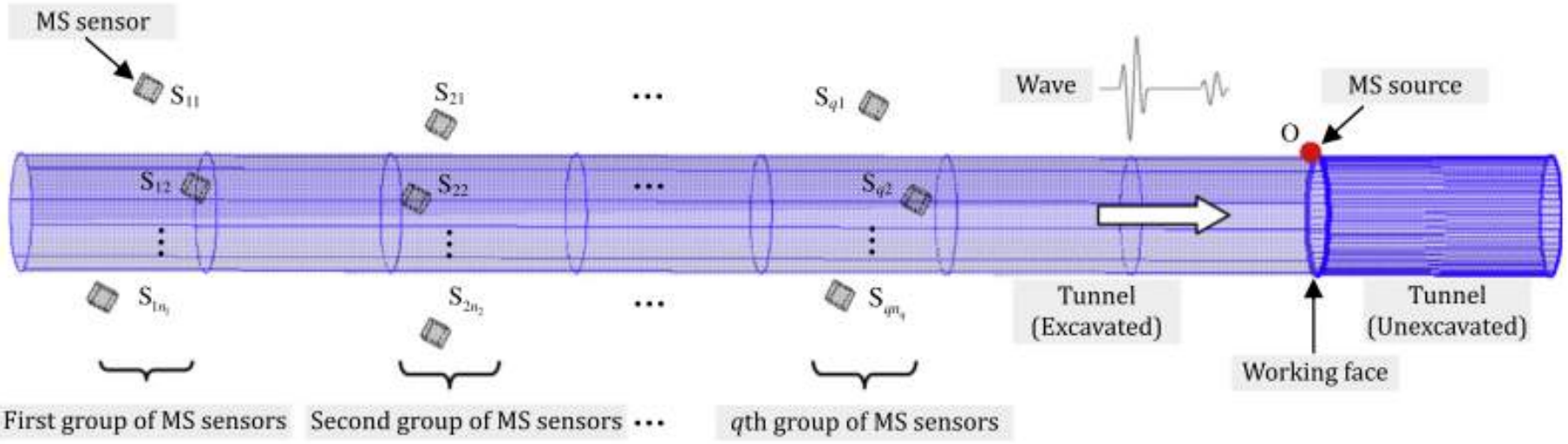

Feng, G.-L., Feng, X.-T., Chen, B.-R., Xiao, Y.-X., Jiang, Q., 2015. Sectional velocity model for microseismic source location in tunnels. *Tunneling and Underground Space Technology* 45, 73-83.

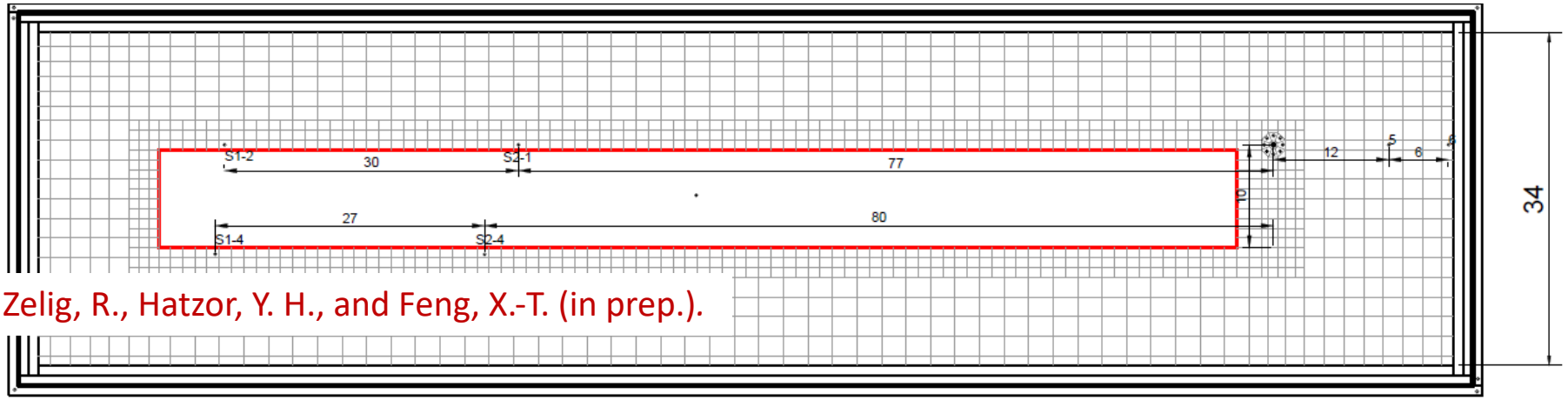

Zelig, R., Hatzor, Y. H., and Feng, X.-T. (in prep.).

Blast element for DDA

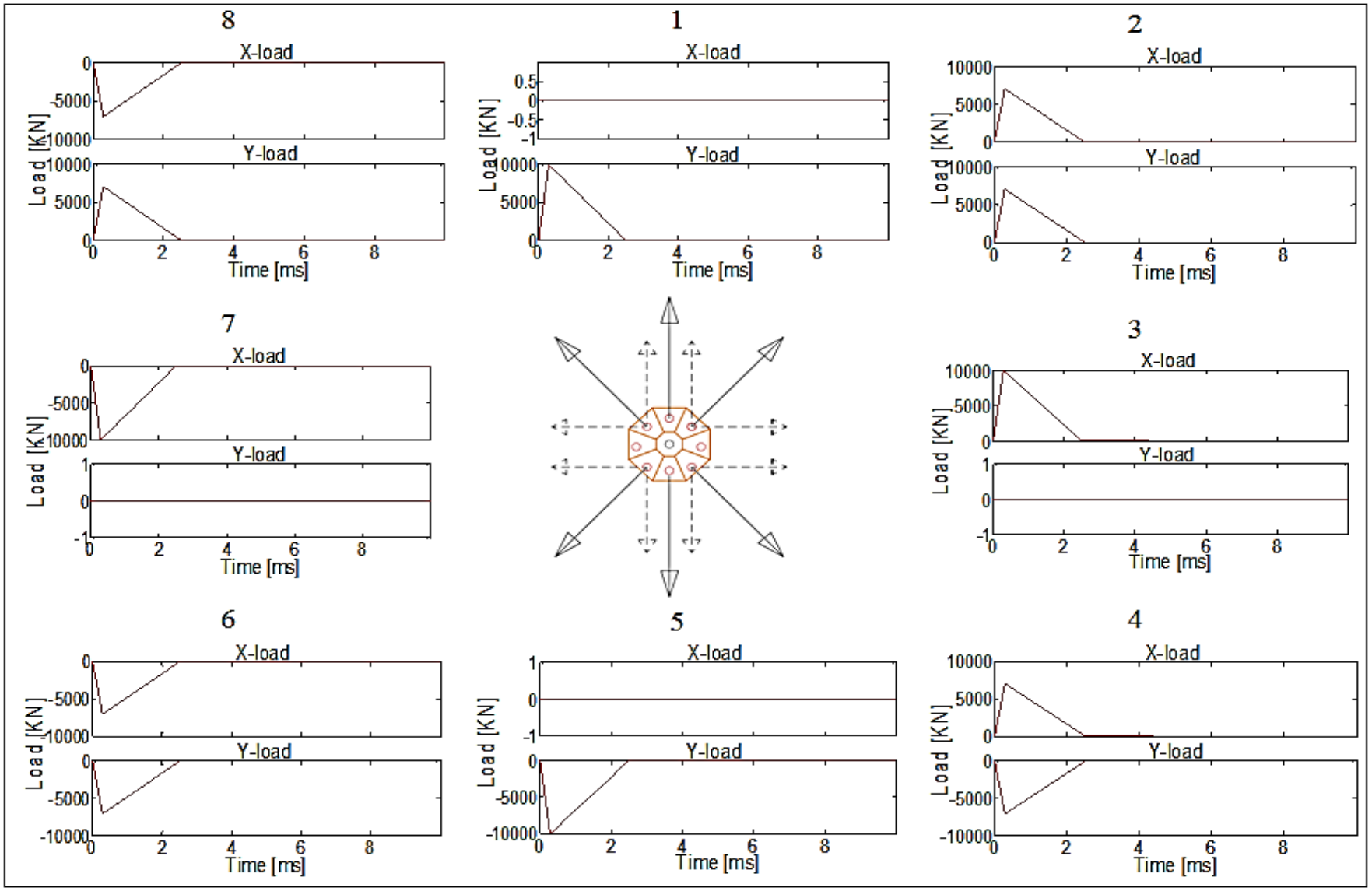

Blast wave arrivals: DDA, analytical solution, and field measurements

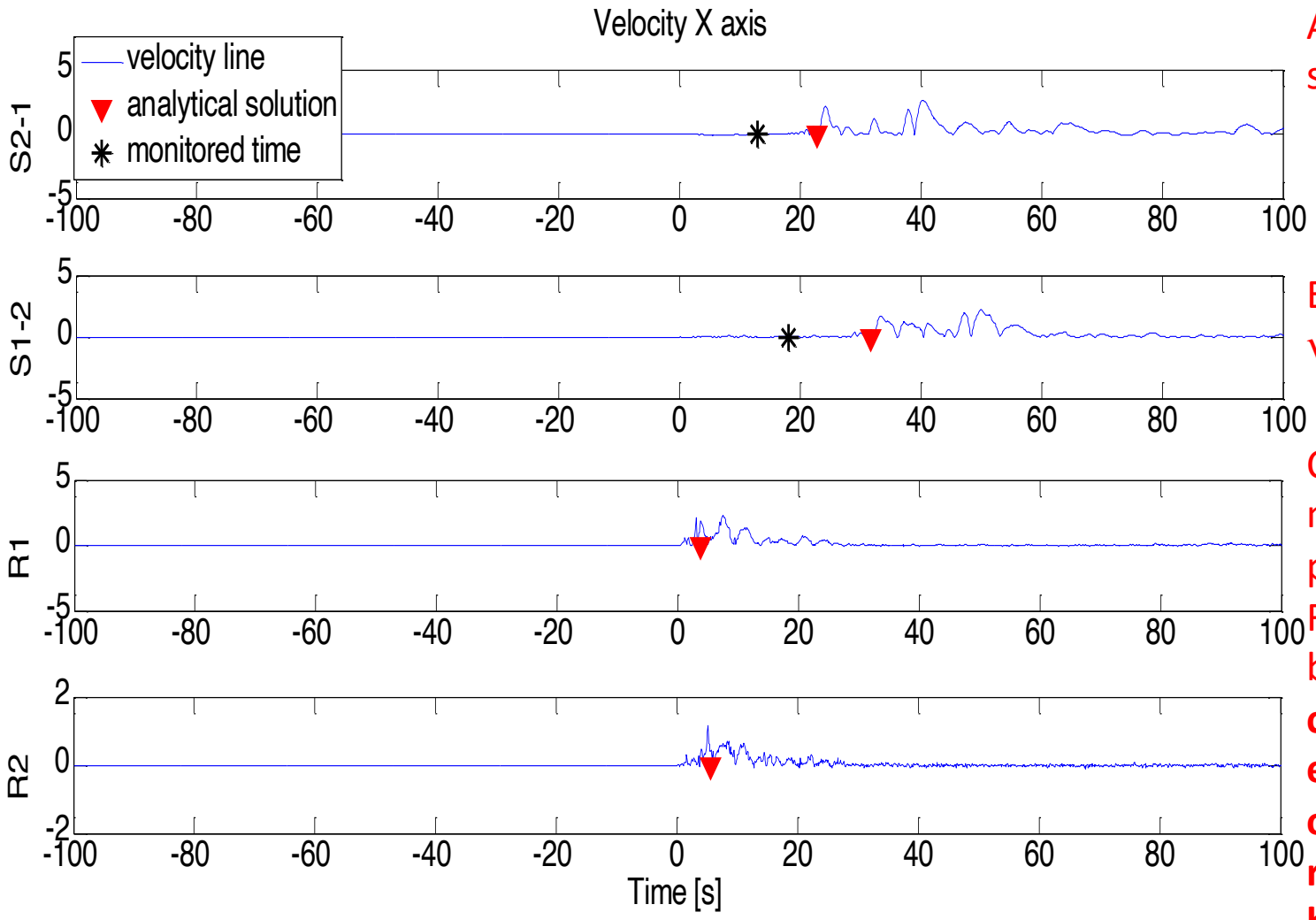

Analytical solution

$$V_p = \sqrt{\frac{\lambda + 2\mu}{\rho}}$$

E = 25.3 GPa

ν = 0.22

Control measurement points (R1, R2) on right boundary **confirming effectiveness of non reflective boundary**

Well, this is all very nice, but can any of this be applied somehow to real rock mechanics ☺ ?

Selected rock slope stability example:

Thermal vs. seismic effects on keyblock stability

A sudden block failure episode in West face of Masada

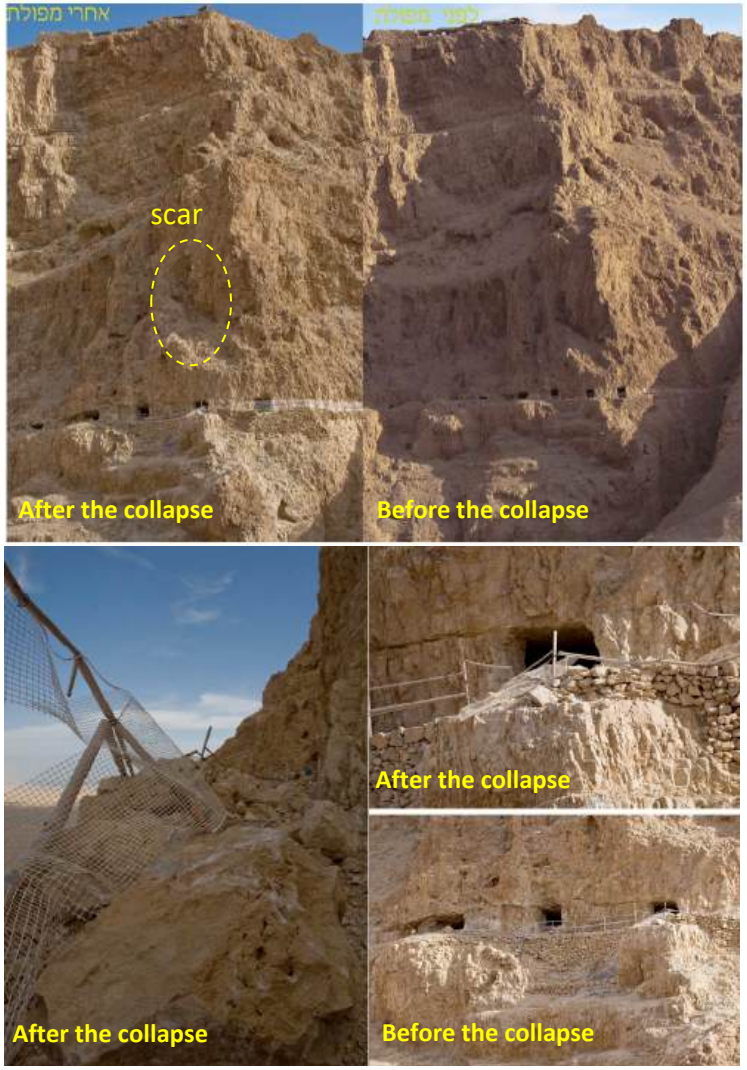

The west slope of Masada before and after the storm of February 10, 2009 .

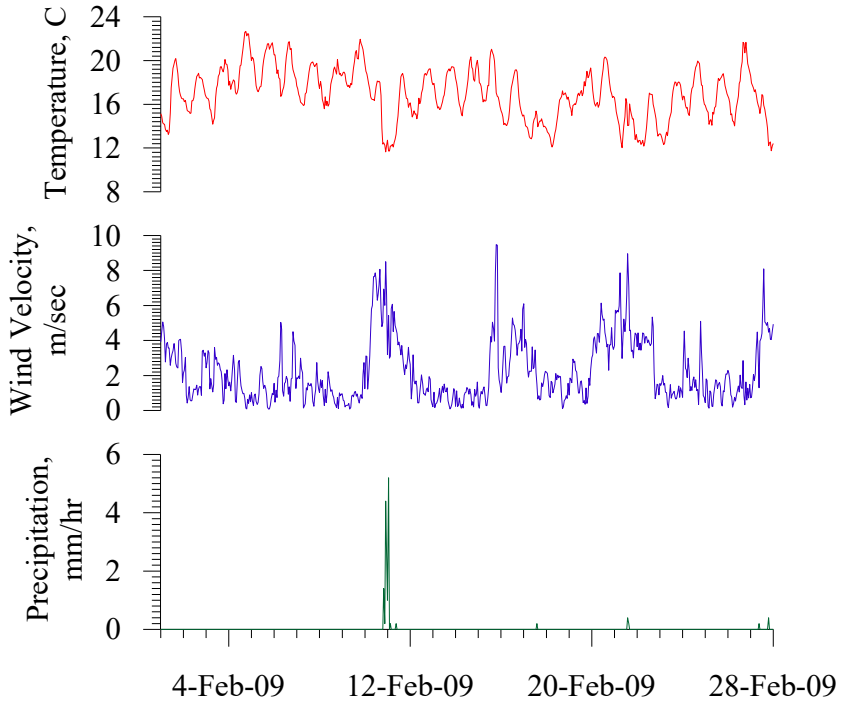

Temperature, wind velocity and precipitation, as recorded in the west slope of Masada, during February 2009.

Joint displacement monitoring in East and West faces of *Masada*

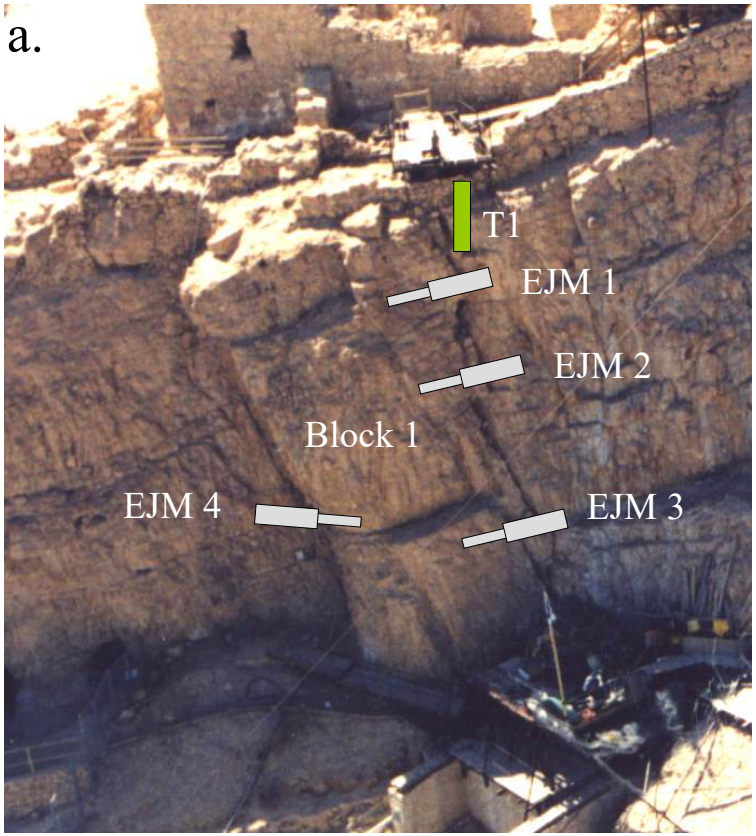

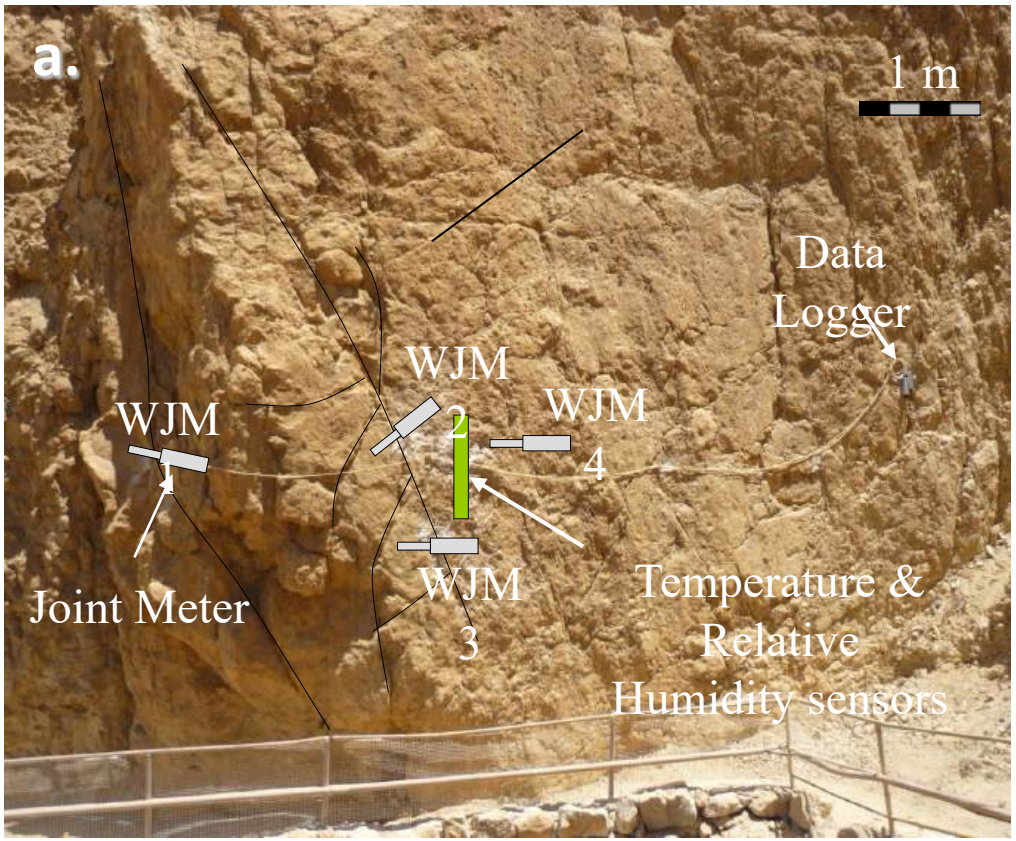

East Slope: 1 – 6/ 1998

Hatzor, Y. H. (2003) *JGGE, ASCE.*

West Slope: 7/09 – 5/11

Bakun-Mazor, Hatzor, Glaser, and Santamarina (2013) *IJRMMS.*

Monitoring output

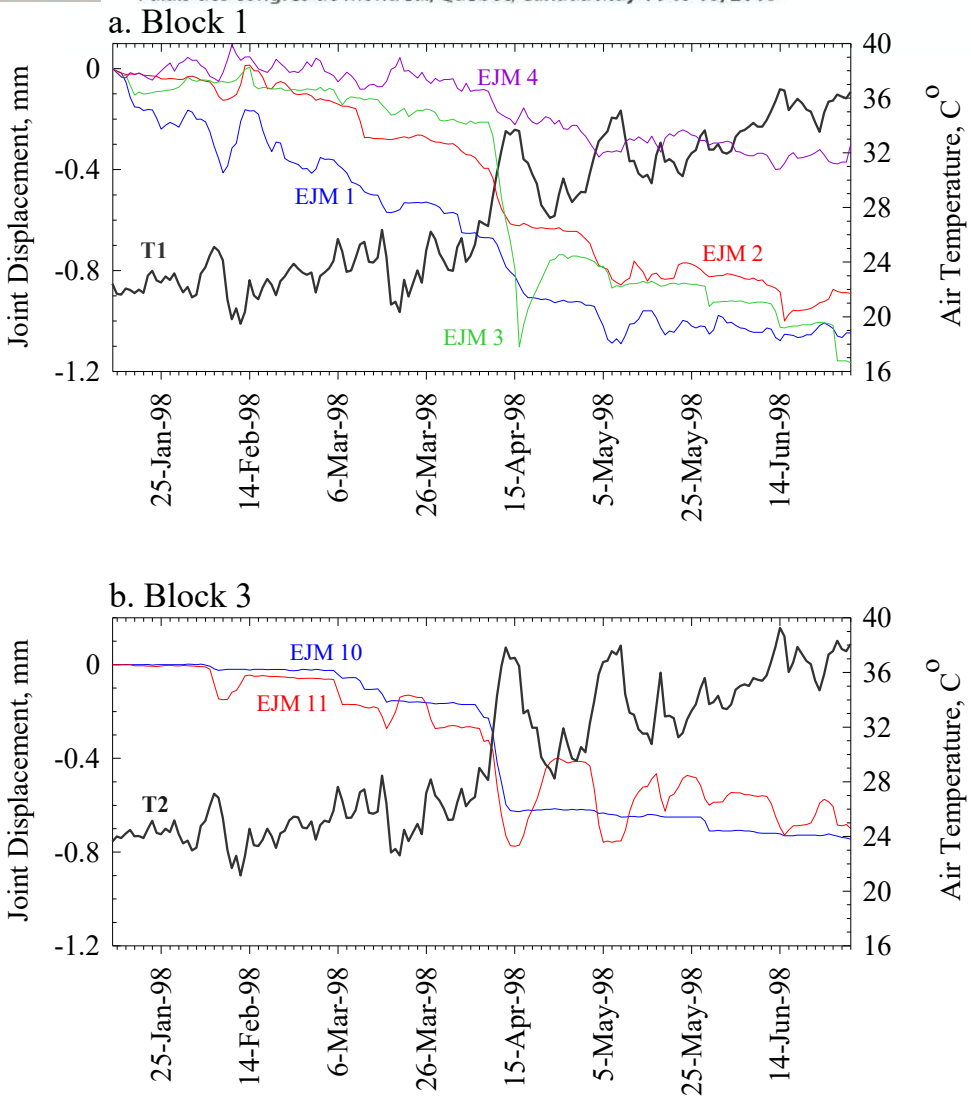

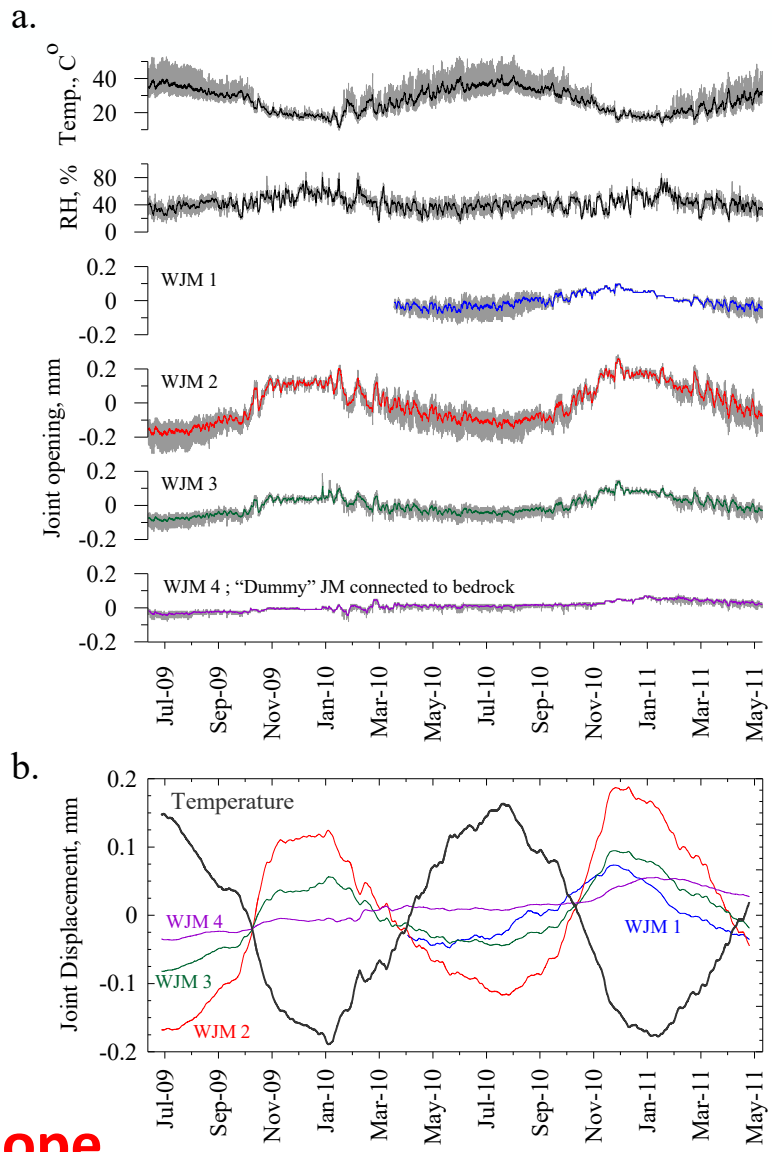

East Slope

West Slope

The 13th International Congress on Rock Mechanics
ISRM CONGRESS 2015
Palais des congrès de Montréal, Québec, Canada May 10 to 13, 2015

Proposed "Wedging – Ratcheting" Mechanism

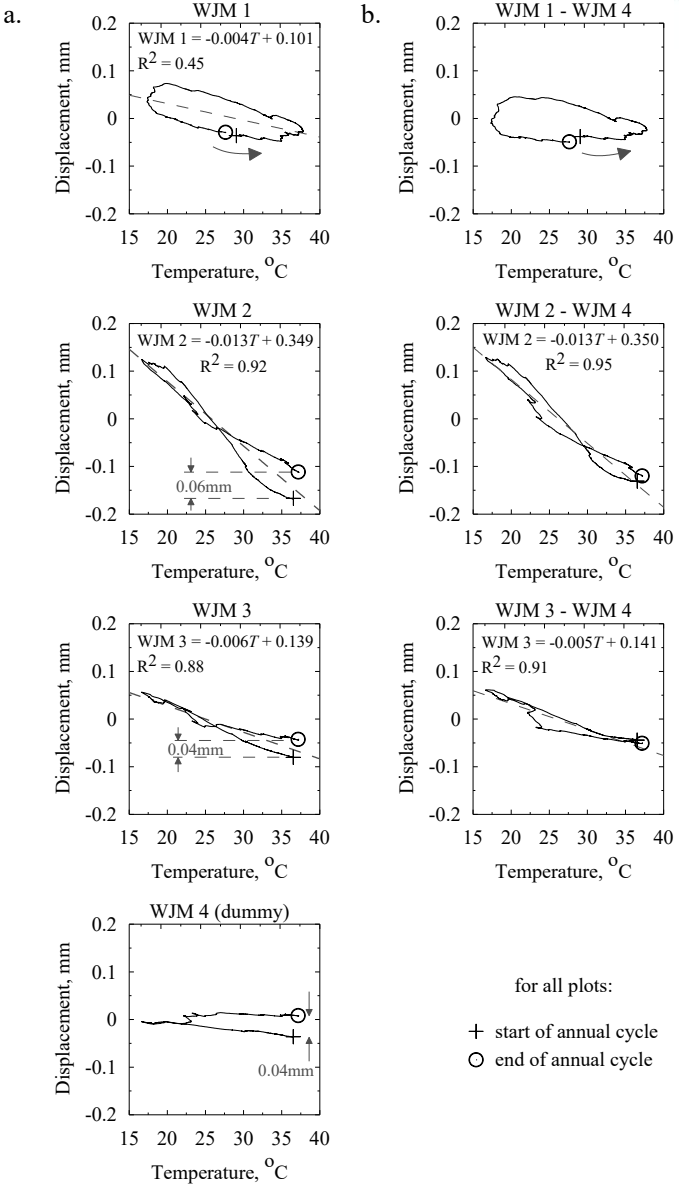

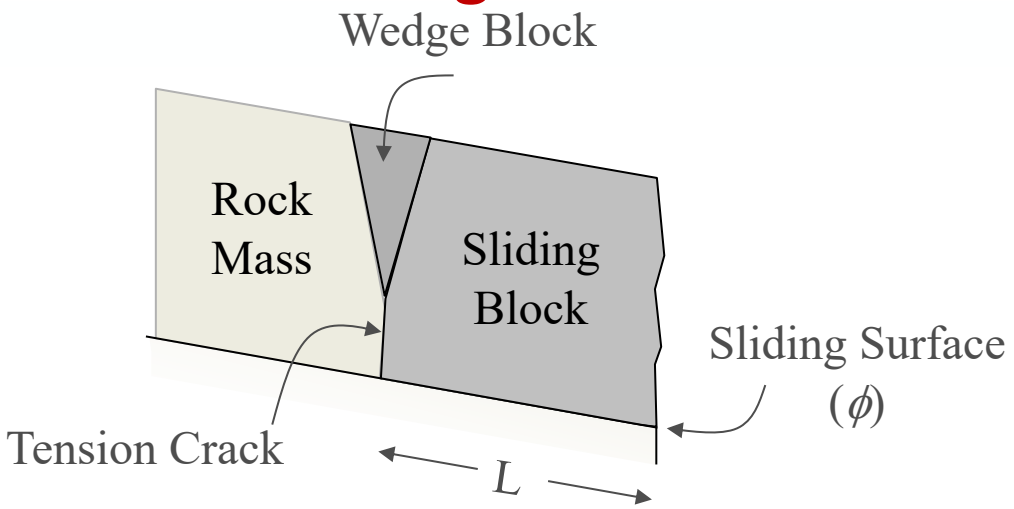

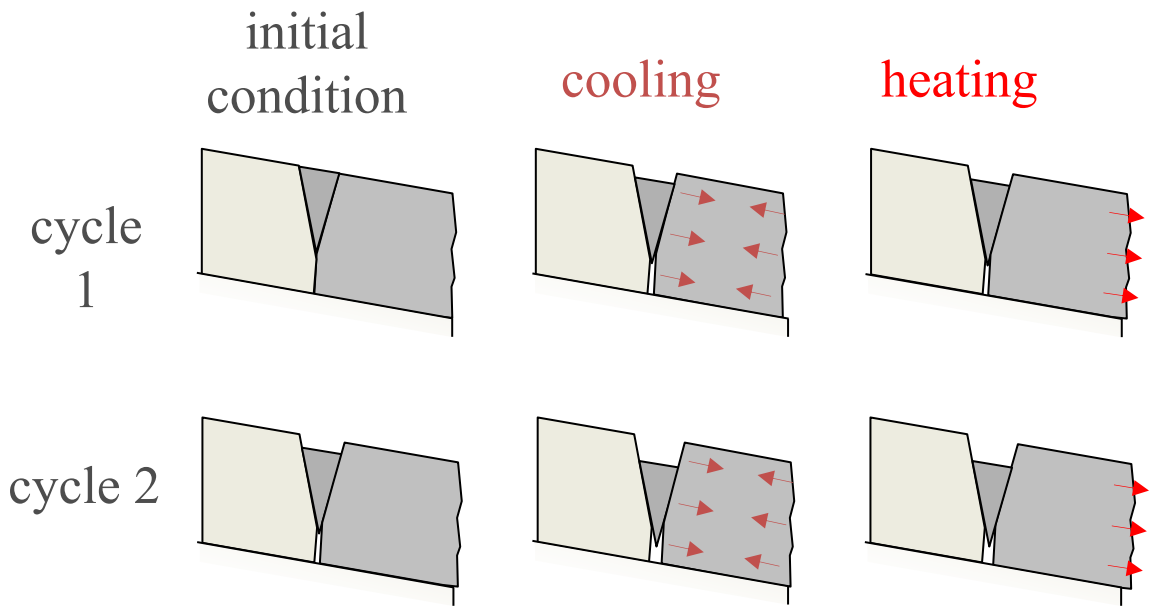

Field evidence and conceptual model for semi-analytical solution

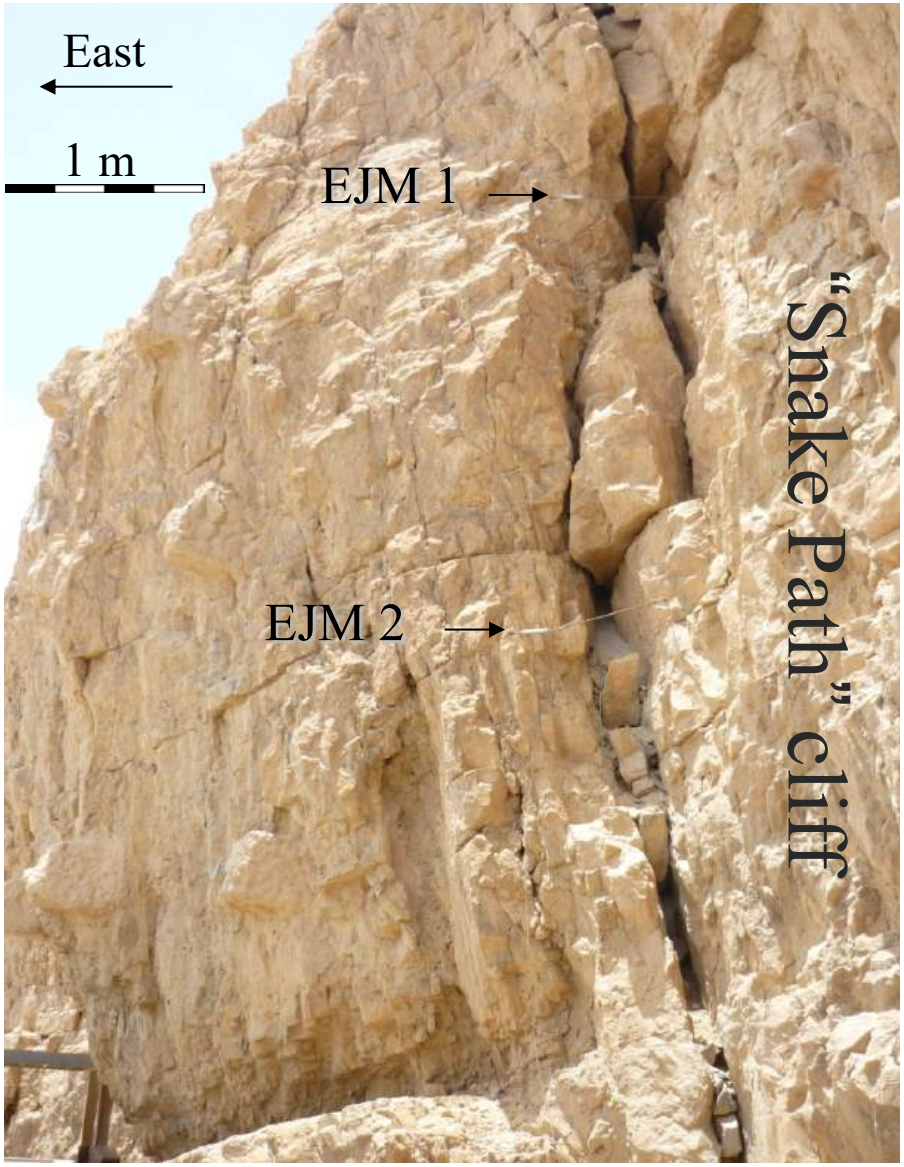

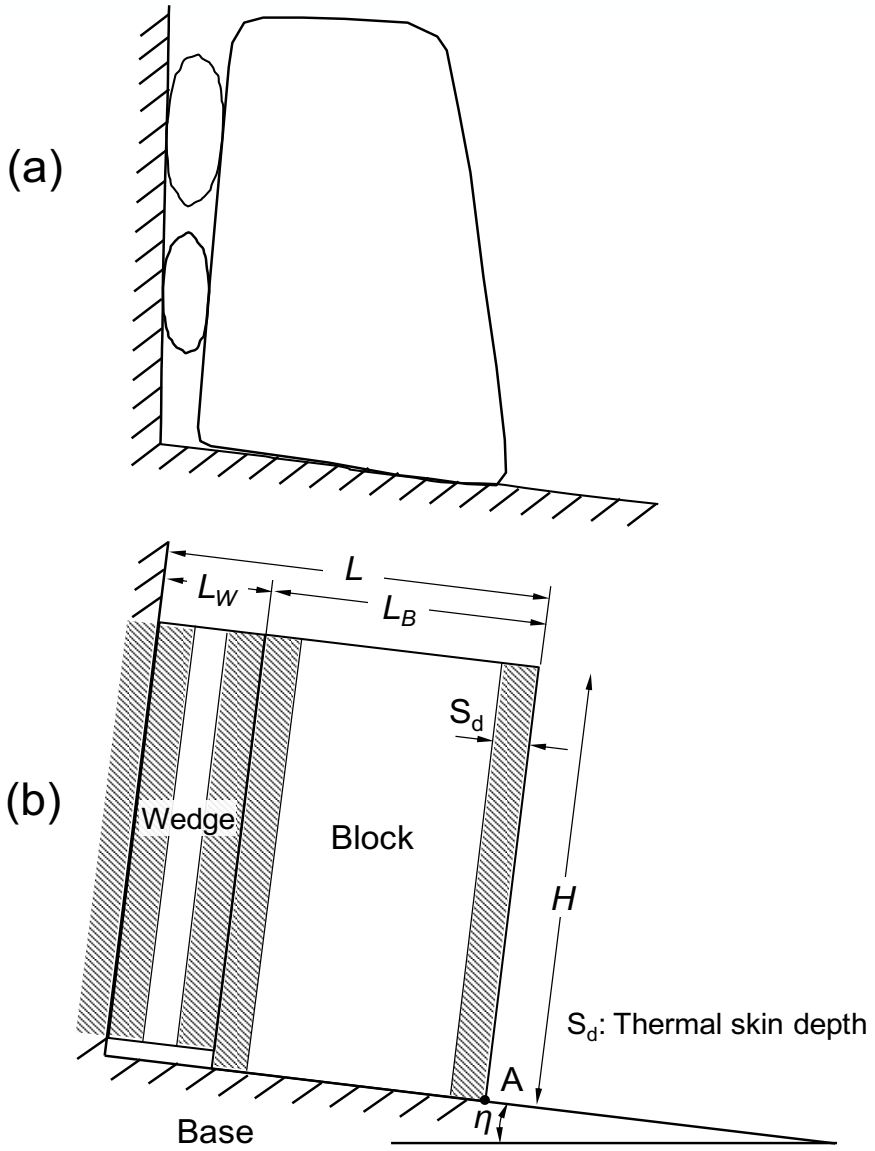

Semi-analytical model prediction for plastic displacement

If the external temperature change ΔT exceeds the maximum temperature for elastic deformation ΔT_{max}, the plastic displacement δ_j^p [m] that the block will experience is may be found by (*Pasten and Santamarina, unpublished report*):

$$\delta_j^p = \delta_T - \delta_\sigma - \delta_j^*$$

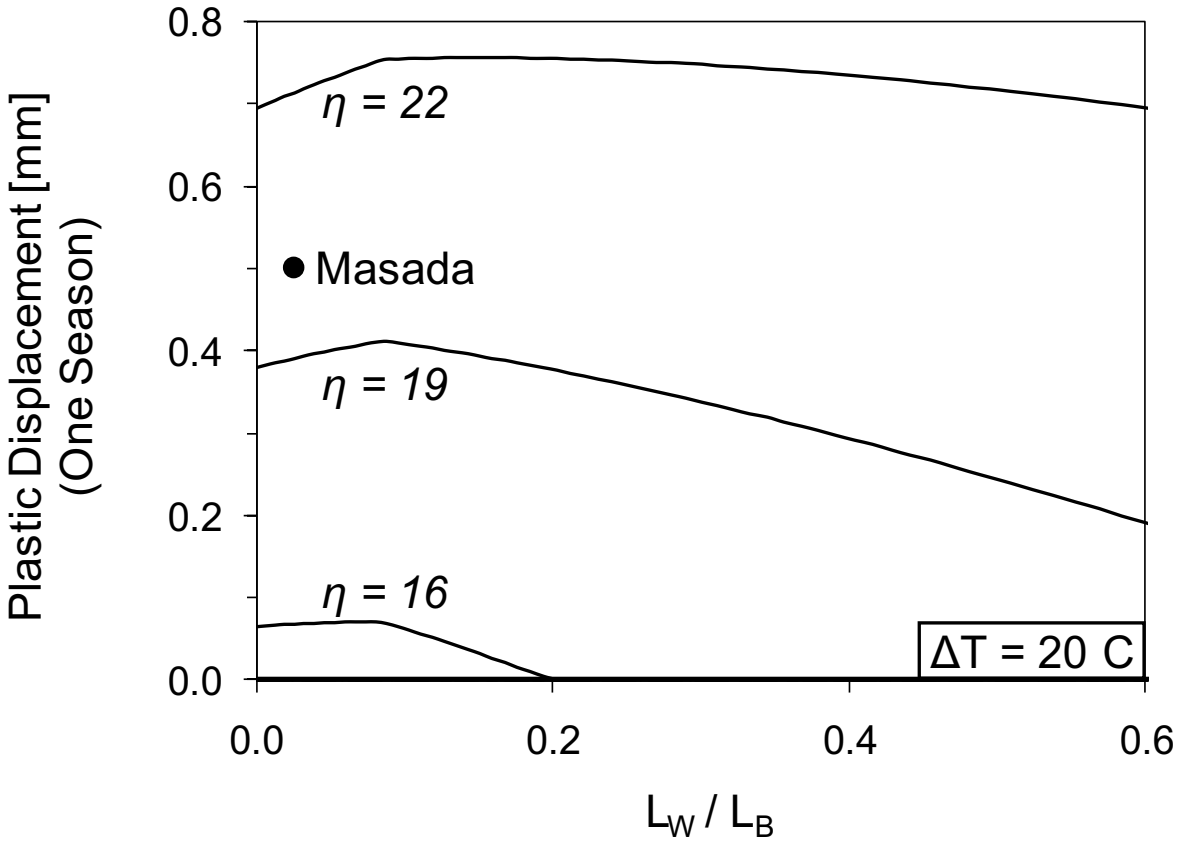

where:

δ_j^p One cycle plastic displacement of joint

δ_T Thermal expansion of wedge

δ_σ Elastic compression of rock material

δ_j^* Elastic compression of sliding interface

One-cycle plastic displacement for several plane inclination angles. Dolomite block-wedge system subjected to a seasonal temperature change ΔT= 20°C. For details see Bakun-Mazor et al., 2013.

To check displacement under seismic excitation we must first optimize the penalty parameter

DDA results vs. analytical solution for the dynamic displacement of Block 1 when subjected to a sinusoidal input function with 0.5g amplitude and the two dominant frequencies for Masada : 1.3 Hz (a) and 3.8 Hz (b).

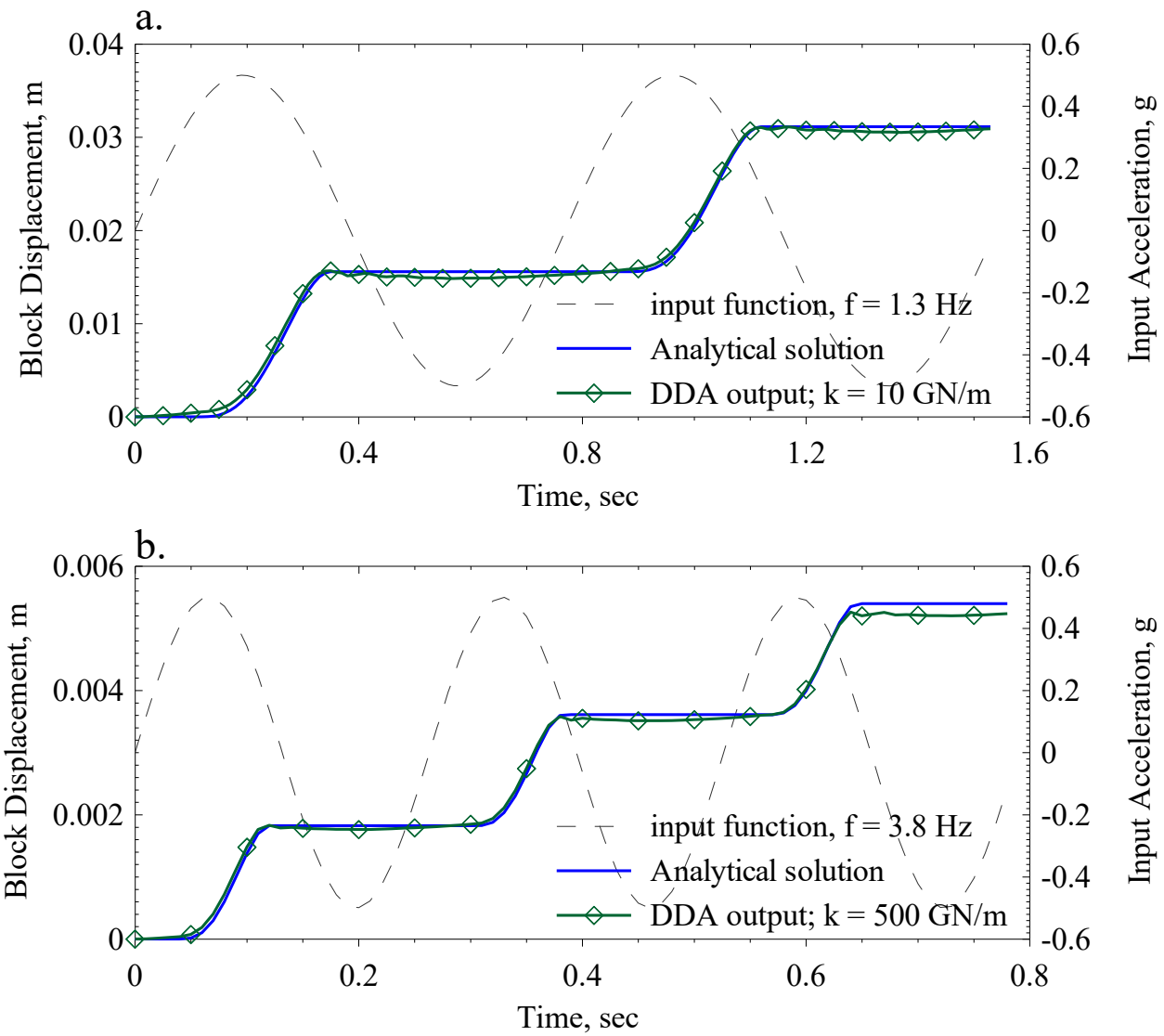

Scaling input motion by earthquake magnitude

a) The Nuweiba earthquake as recorded in Eilat on a soil layer de-convoluted for bedrock response (*Zaslavsky and Shapira, 2000*) and scaled to PGA = 0.275g, corresponding to a Mw= 6.0 earthquake at a distance of 1 km from Masada

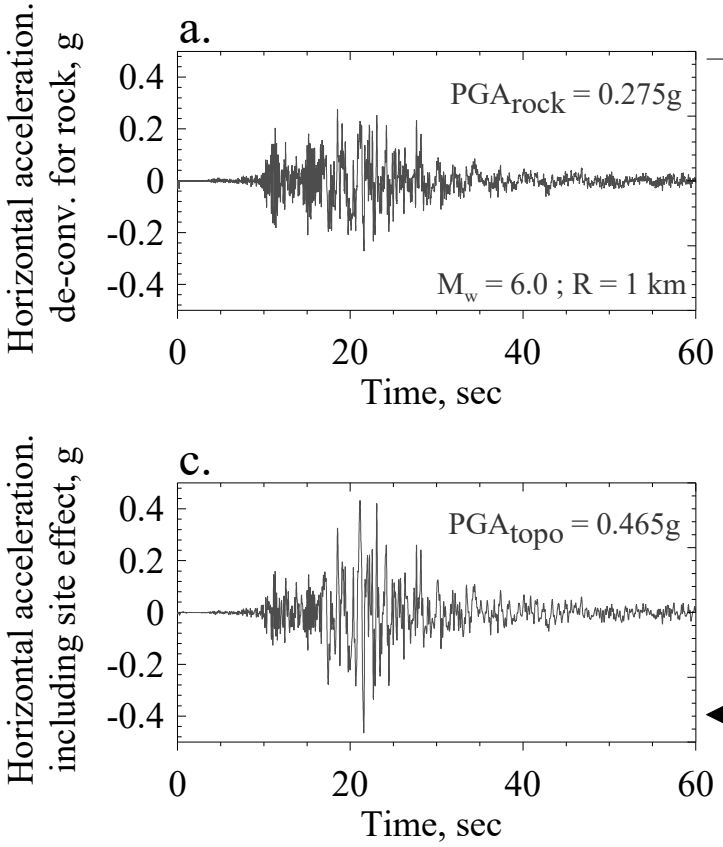

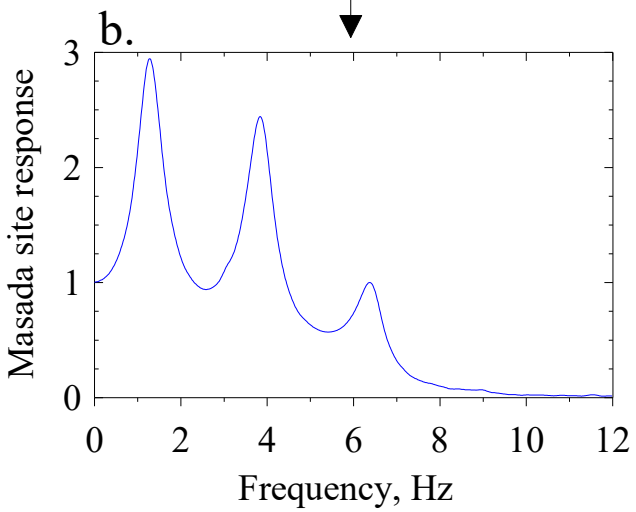

b) an empirical site response function for Masada (after *Zasalavsky et al. 2002*)

c) convoluted time series of the modified Nuweiba record (a) to include the empirical site response function for Masada (b)

Results for Masada Block 1 (East Face)

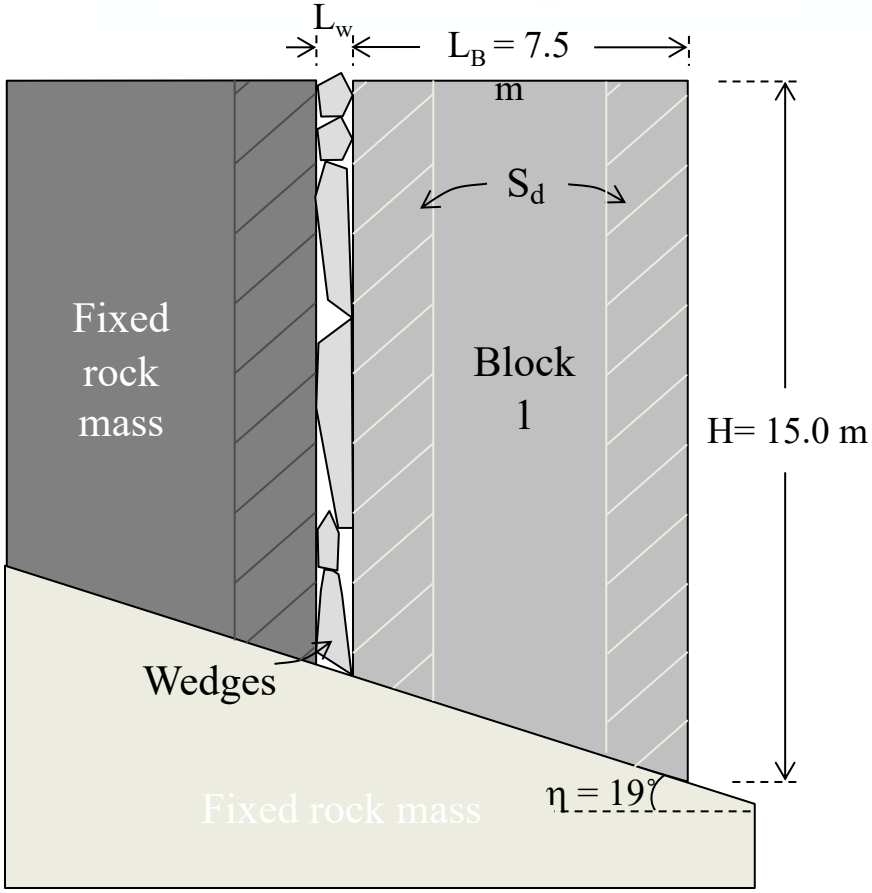

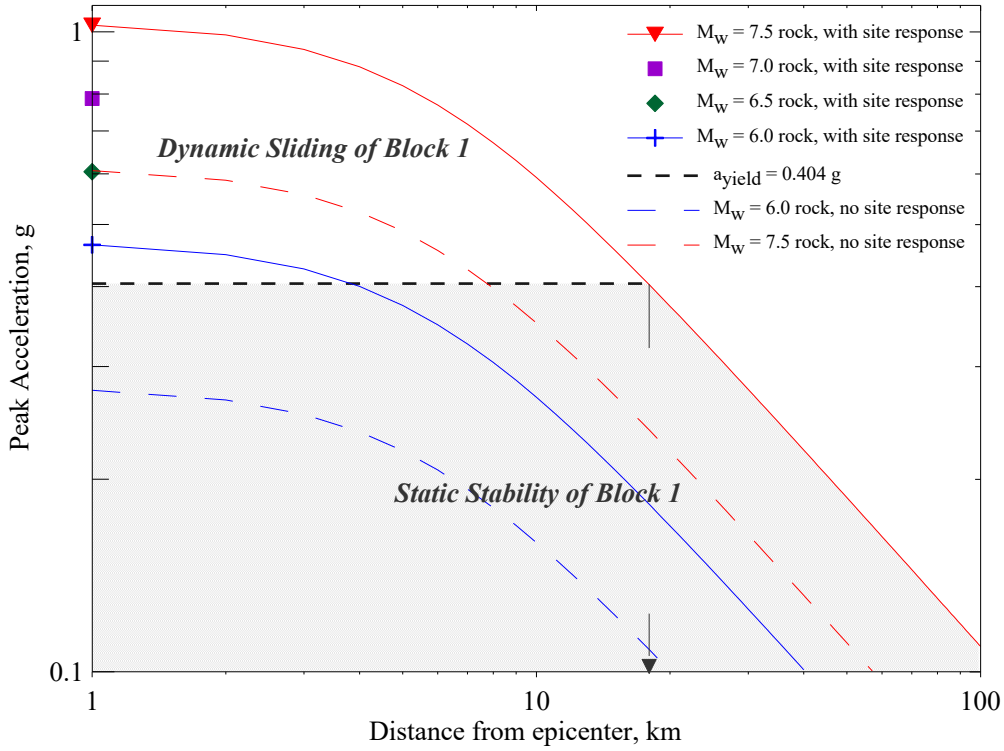

Assumed attenuation curves for Dead Sea Rift earthquakes (after *Boore et al., 1997*) (dashed lines) with amplification due to topographic site effect at Masada (solid lines and symbols). Shaded region delineates conditions at which seismically-induced sliding of Block 1 at Masada is not possible. The geometry for the block for which dynamic DDA is performed is shown on the left.

Total displacement of Block 1 in a single earthquake

DDA results for dynamic displacement of Block 1 when subjected to amplified Nuweiba records corresponding to earthquakes with moment magnitude between 6.0 to 7.5 and epicenter distance of 1 km from Masada. Mapped joint opening in the field is plotted (dashed) for reference.

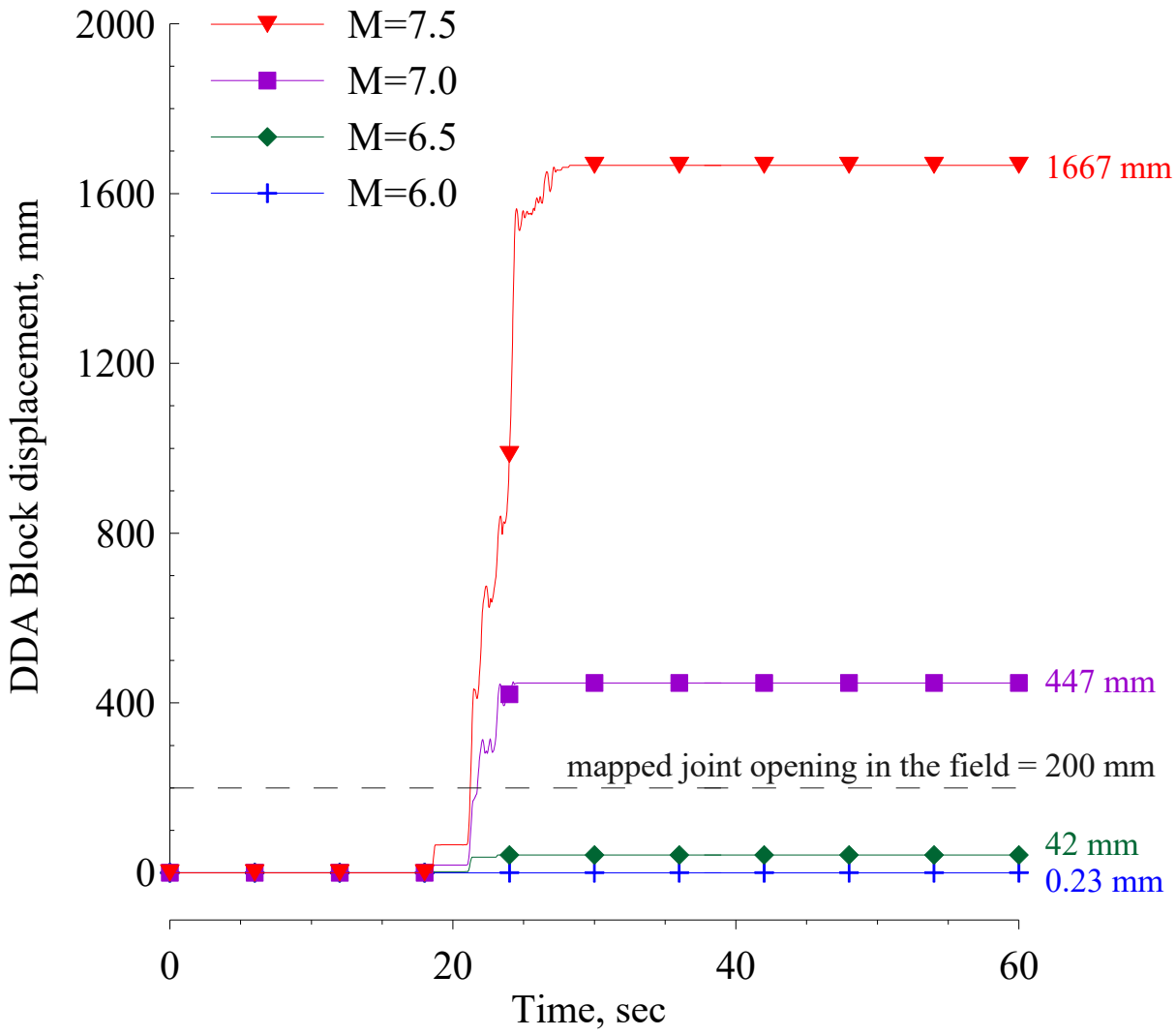

Thermally vs. seismic displacement rates

- Thermal displacement rate is calculated assuming β = 0.3 and 0.5.
- Seismic displacement rate is obtained by summation of earthquake magnitudes 6.0 to 7.0 with epicenter located 1 km from Masada based on the seismicity of the region.
- The seismic rates in the zoom-in box are for the long term seismicity (5000 years).

β is a coefficient accounting for non-uniform diffusive temperature distribution inside the sliding block and the rock mass ($0 < \beta < 1$). Note that β is introduced when the skin depth Sd is smaller than half length of the rock element.

Bakun-Mazor et al. (2013).

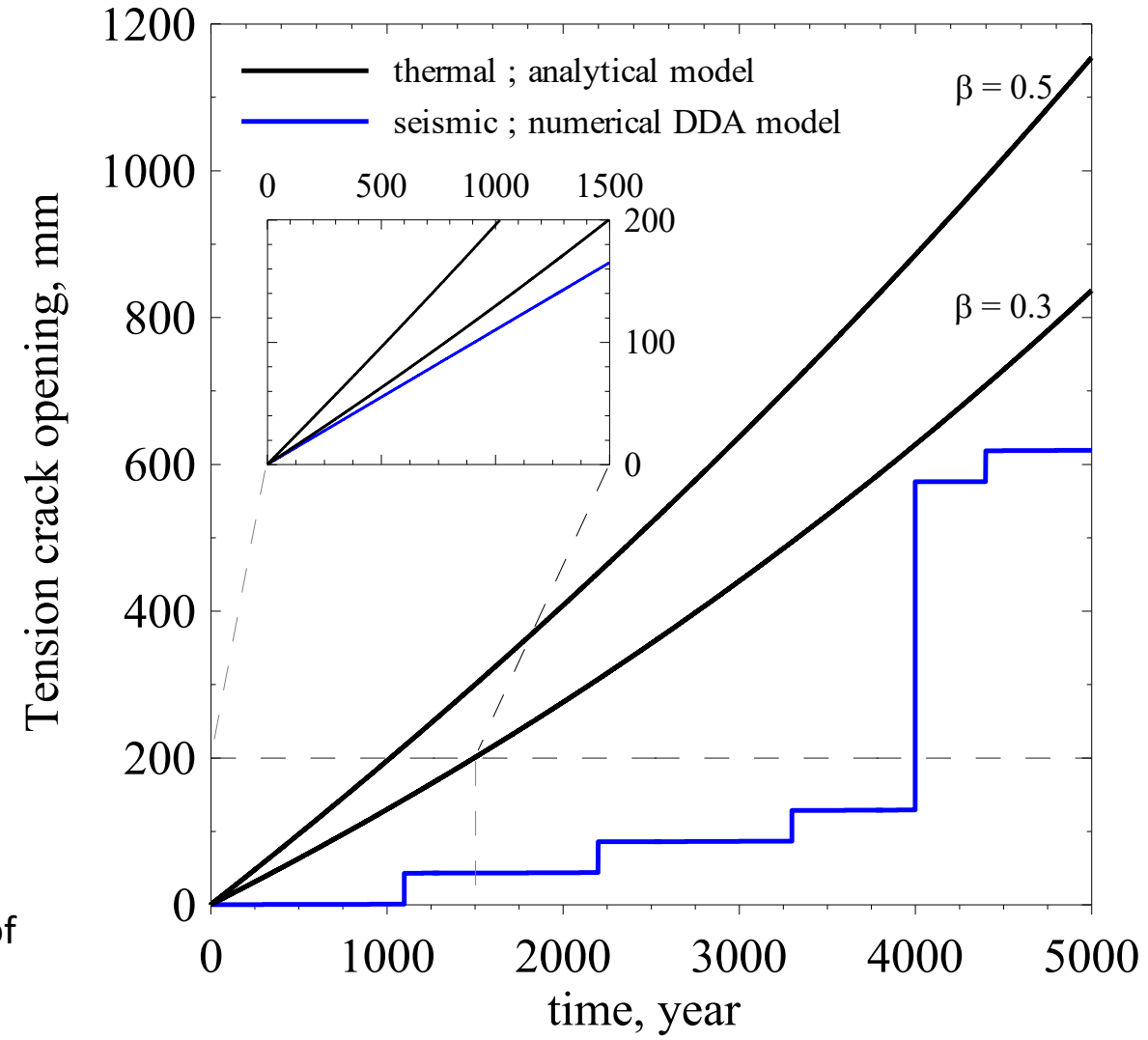

But, can this help us with safety of tunneling in high *in-situ* stress environments ☺ ?

Modeling Rock Bursts with DDA

Preliminary Results

Work in progress with Ben-Guo He and Ravit Zelig (BGU), and Xia-Ting Feng (CAS)

We assume pre-existing key blocks in a discontinuous rock-mass will be ejected as rock bursts *before* intact rock will be fractured

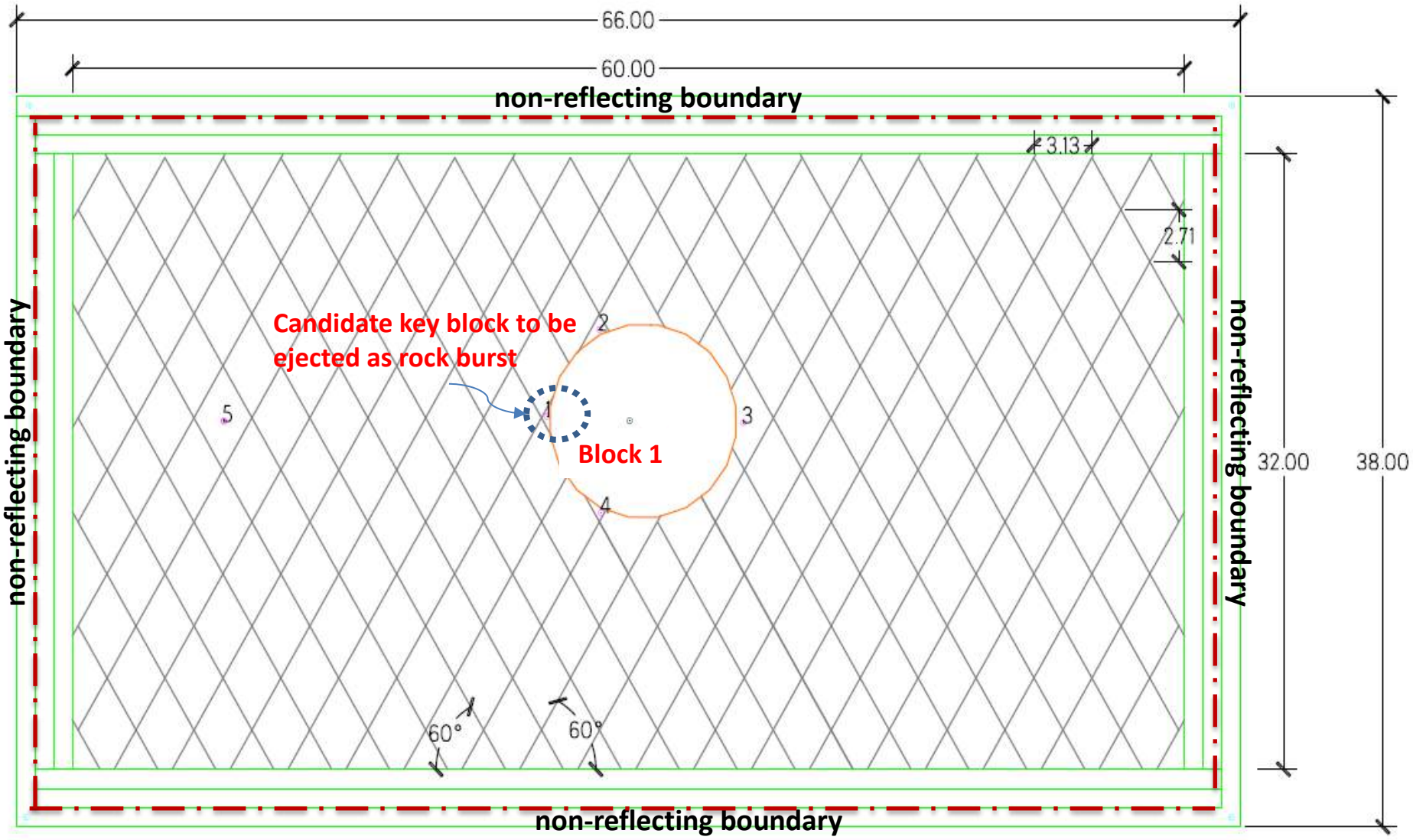

Stress redistribution after tunnel removal

Vertical stress component @ Pt. 5 - far away and @ Pt. 3 - right sidewall of tunnel

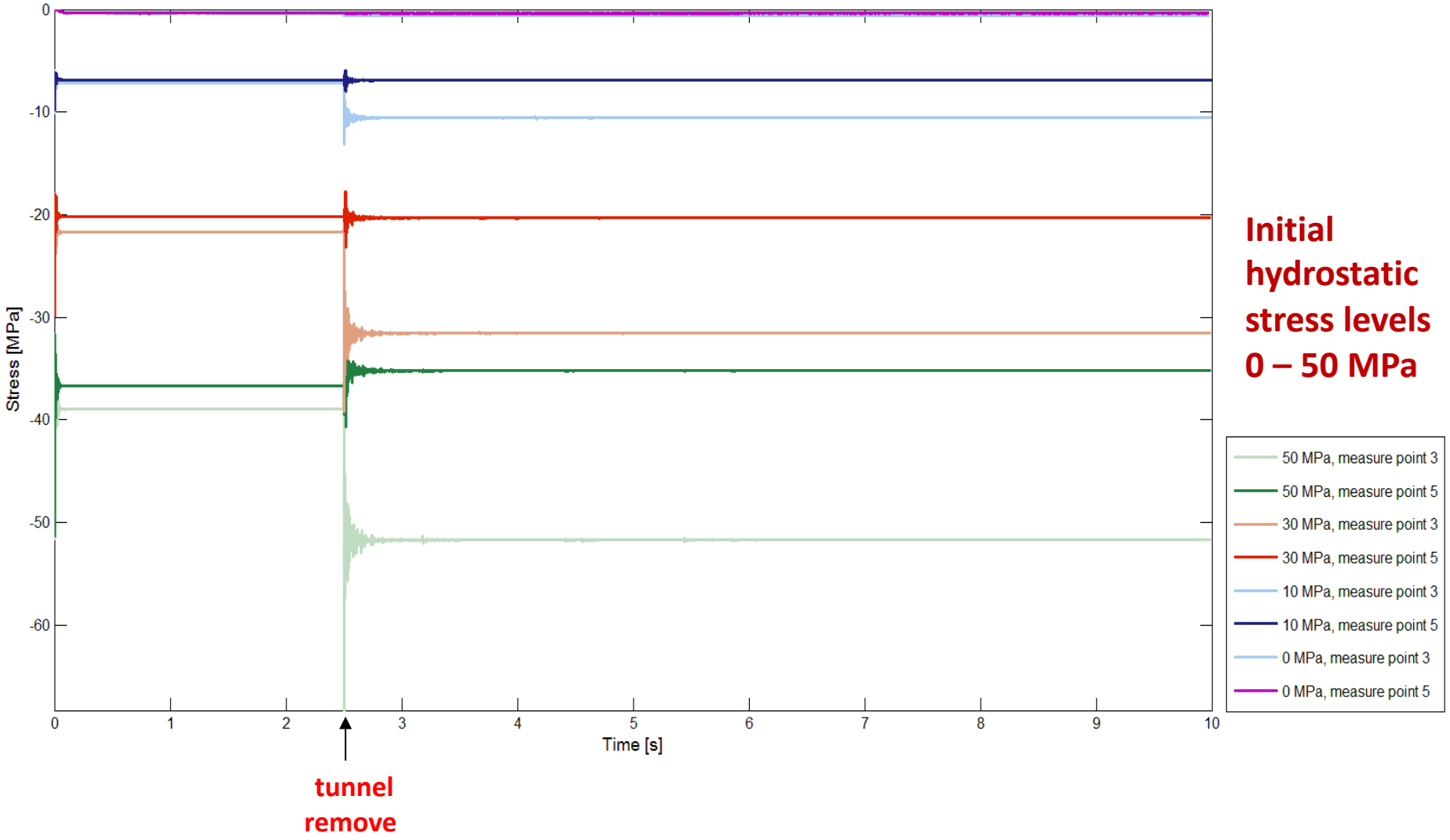

Initial hydrostatic stress levels 0 – 50 MPa

tunnel remove

Strain relaxation causes block ejection, the peak acceleration of which increases with increasing level of initial *in situ* stress

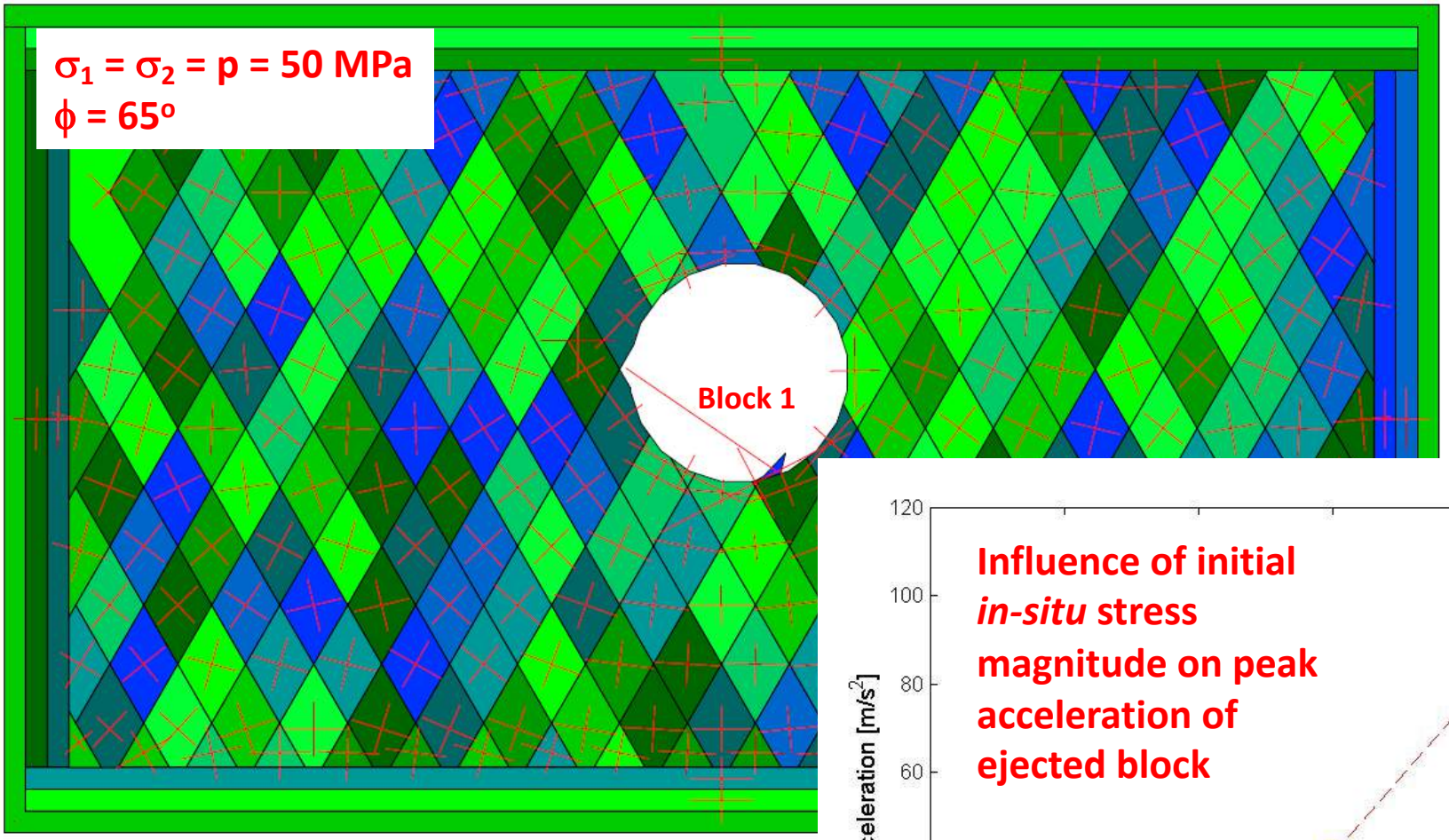

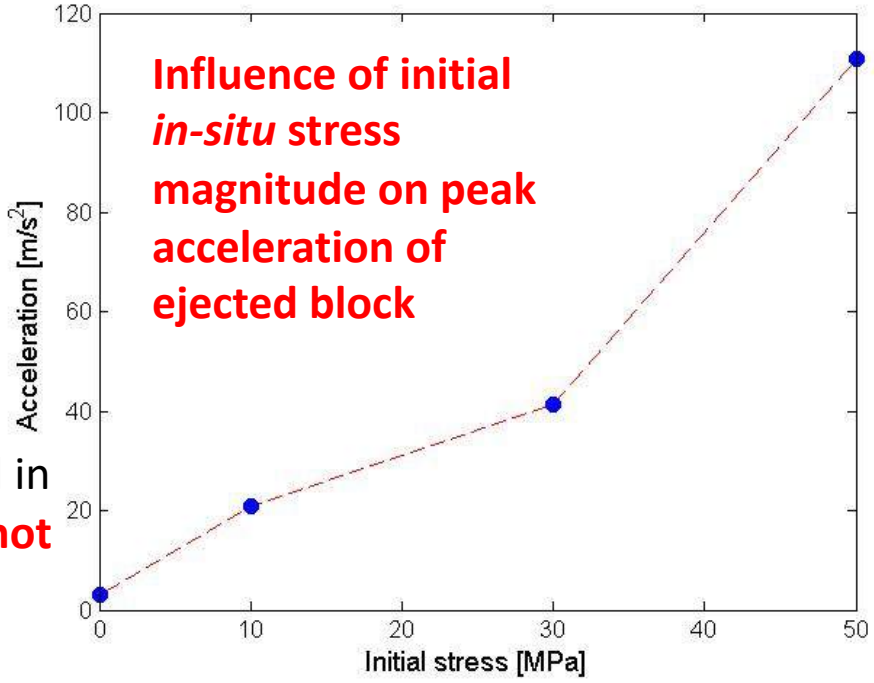

Tunnel removal prompts a block ejection from sidewall (block 1). All other blocks remain locked in place. **Note: Due to high friction the block was not supposed to move under static conditions.**

Energy considerations: starting with a continuous domain

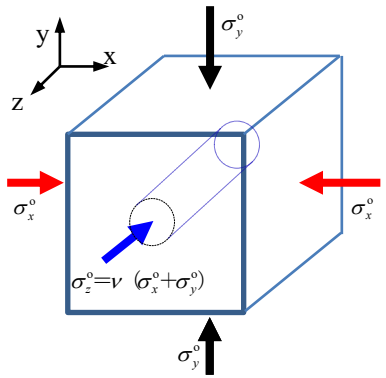

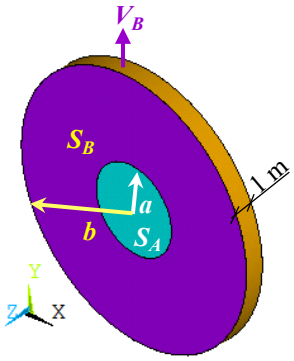

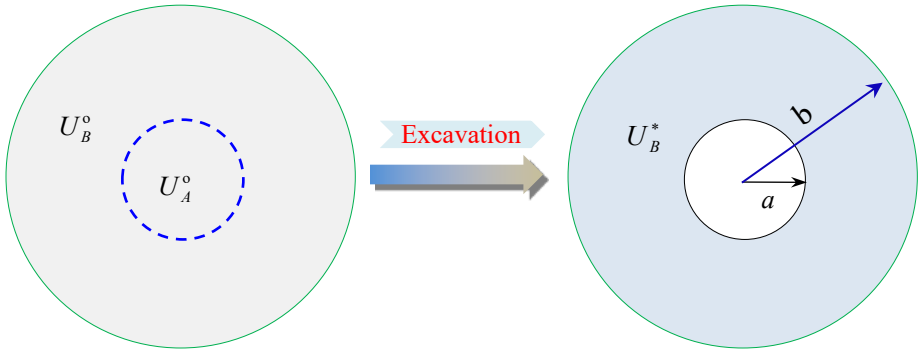

Initial Energy:

$$U_{A,B}^0 = \frac{1}{2E}\left[(1-\upsilon^2)(\sigma_x^0+\sigma_y^0)^2 - 2(\upsilon+1)\sigma_x^0\sigma_y^0\right]\times S_{A,B}$$

For complete derivation of analytical solution see He B. G. et al. (in preparation).

Energy after tunnel removal:

$$U_B^* = \frac{\pi}{E}\left\{(1-\upsilon^2)\int_a^b\left[(\sigma_x^o+\sigma_y^o)^2 r + 2(\sigma_x^o-\sigma_y^o)^2\frac{a^4}{r^3}\right]dr + \right.$$

$$\left. 2(1+\upsilon)\int_a^b\left[\frac{(\sigma_x^o+\sigma_y^o)^2}{4}\frac{a^4}{r^3} + \frac{(\sigma_x^o-\sigma_y^o)^2 a^4}{4}\left(\frac{2}{r^3}-\frac{12a^2}{r^5}+\frac{9a^4}{r^7}\right) - \sigma_x^o\sigma_y^o r\right]dr\right\} =$$

$$= \frac{\pi}{E}\left\{(1-\upsilon^2)\left[\frac{1}{2}(\sigma_x^o+\sigma_y^o)^2 r^2\Big|_a^b - (\sigma_x^o-\sigma_y^o)^2 a^4\frac{1}{r^2}\Big|_a^b\right] + \right.$$

$$\left. 2(1+\upsilon)\left[-\frac{(\sigma_x^o+\sigma_y^o)^2}{8}a^4\frac{1}{r^2}\Big|_a^b + \frac{(\sigma_x^o-\sigma_y^o)^2 a^4}{4}\left(-\frac{1}{r^2}\Big|_a^b + 3a^2\frac{1}{r^4}\Big|_a^b - \frac{3}{2}a^4\frac{1}{r^6}\Big|_a^b\right) - \frac{\sigma_x^o\sigma_y^o}{2}r^2\Big|_a^b\right]\right\}$$

Assumptions:

- CHILE material
- Plane strain
- Principal stresses
- No body forces

Relative energy increase in annulus around tunnel $\frac{U_B^* - U_B^o}{U_A^o} \times 100\%$

Case No.	Initial Principal Stress (MPa)			Excavation Radius	Analyzed Domain Radius *b* (m)				
	σ_1	σ_2	σ_1/σ_2	*a* (m)	0.75*D*	1*D*	1.5*D*	3*D*	100*D*
No. 1	60	30	2	4	95.47 %	131.11%	159.29 %	177.69%	184.10 %
No. 2	10	5	2	6					
No. 3	30	30	1	4	99.21 %	133.93 %	158.73 %	173.61 %	178.57 %

Energy increase:

- The principal stress ratio is more important than initial tunnel diameter
- At a distance of 3 tunnel diameters the energy increase ratio is ~ 1.7 .
- This result is independent of Young's modulus of the intact rock
- Thes same result is obtained regardless of excavation radius, initial principal stress ratio, and the magnitude of the initial principal stresses.

Energy concentrations:

- Most of the energy concentration is focused in an annulus between tunnel boundary (@ 0.5D from center) and 1.0D from center.

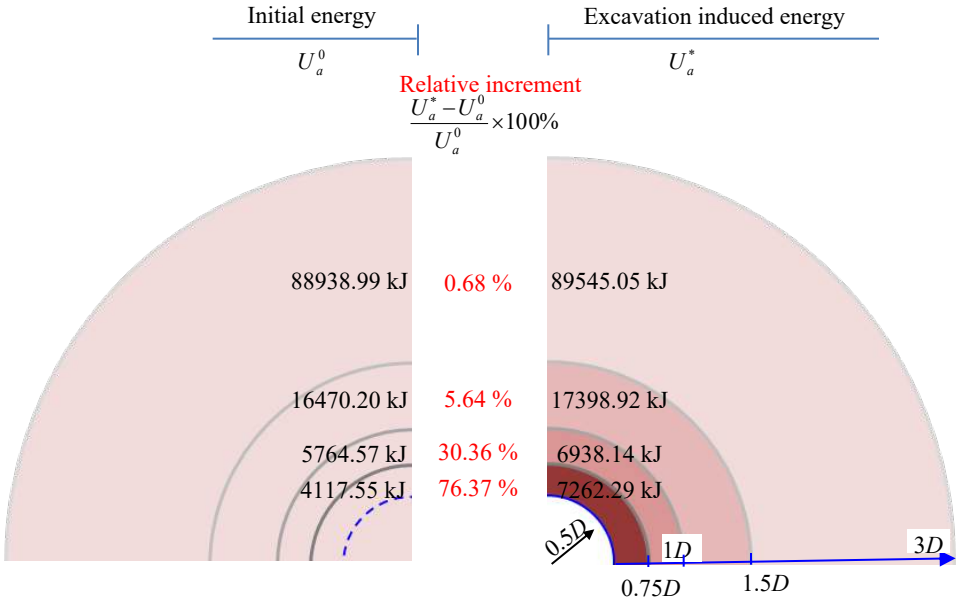

Influence of principal stress direction on local energy density concentration

Important observations:

- Maximum energy density parallel to major principal stress
- In the example shown here this is in the roof
- In hydrostatic conditions (k=1.0) a symmetric energy density concentration is obtained all around the tunnel
- Maximum energy density concentration is obtained between tunnel boundary and a distance of 0.75D from tunnel center
- At distance greater than 1.0D from tunnel center energy density increase is negligible.

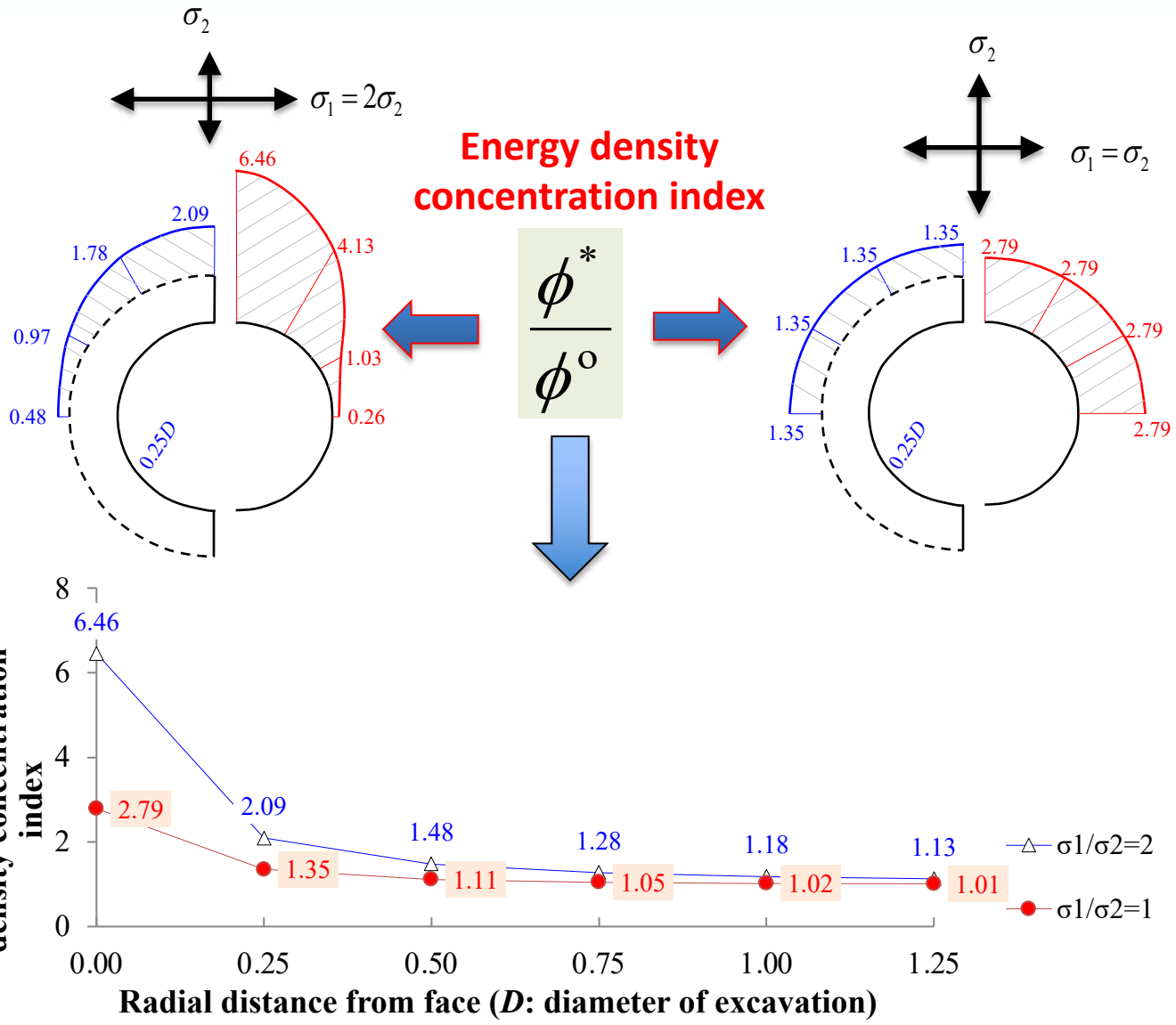

Energy balance in an initially discontinuous rock mass

We shall consider now the affected area due to tunneling in terms of energy increase which was found analytically to be concentrated in an annulus with boundary at a distance of 3D from the tunnel center.

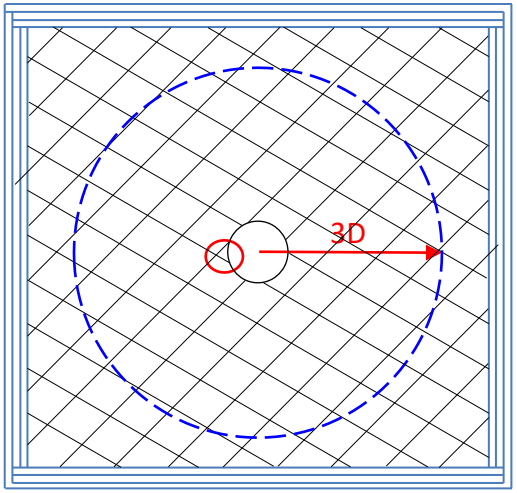

DDA Input

- 71 bocks within dashed line
- All blocks monitored
- E = 25.3 GPa ; ν = 0.22
- $\sigma_1 = \sigma_x = 60$ MPa
- $\sigma_2 = \sigma_y = 30$ MPa
- No gravity

The energy equilibrium equation after the excavation is created may be written as follows:

$$U_B^o + 1.7 \times U_A^o = U_{e,B}^* + U_{k,B}^* + U_{s,B}^*$$

Where:

U_e = strain energy

U_k = kinetic energy

U_s = dissipated energy due to frictional sliding

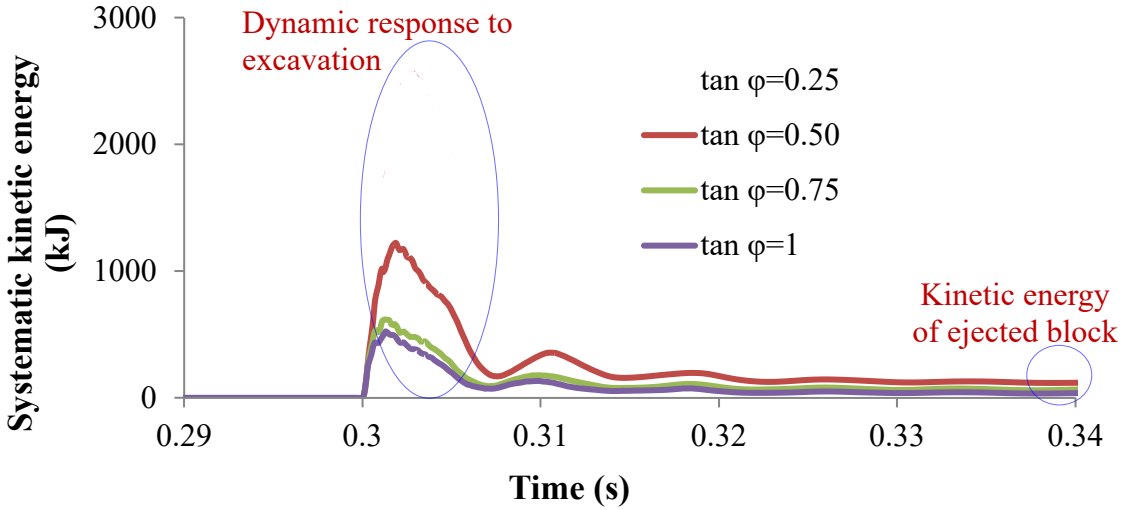

The kinetic energy of the analyzed domain as a function of friction angle and time as obtained with DDA. Note that at the end of the simulation 70 blocks have come to complete rest. Also note strong effect of friction angle on kinetic energy of the modeled block system.

Kinetic energy of rock burst as function of initial *in-situ* stress and joint friction

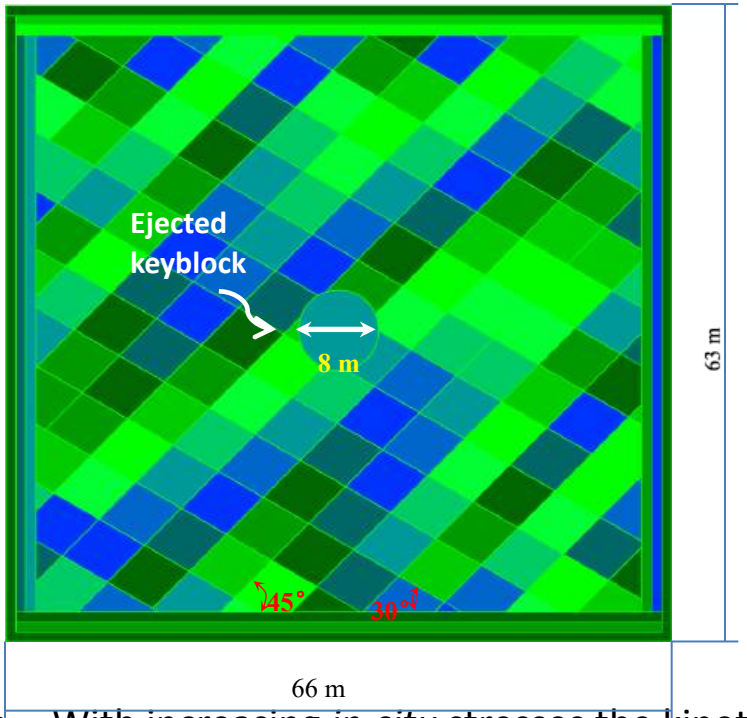

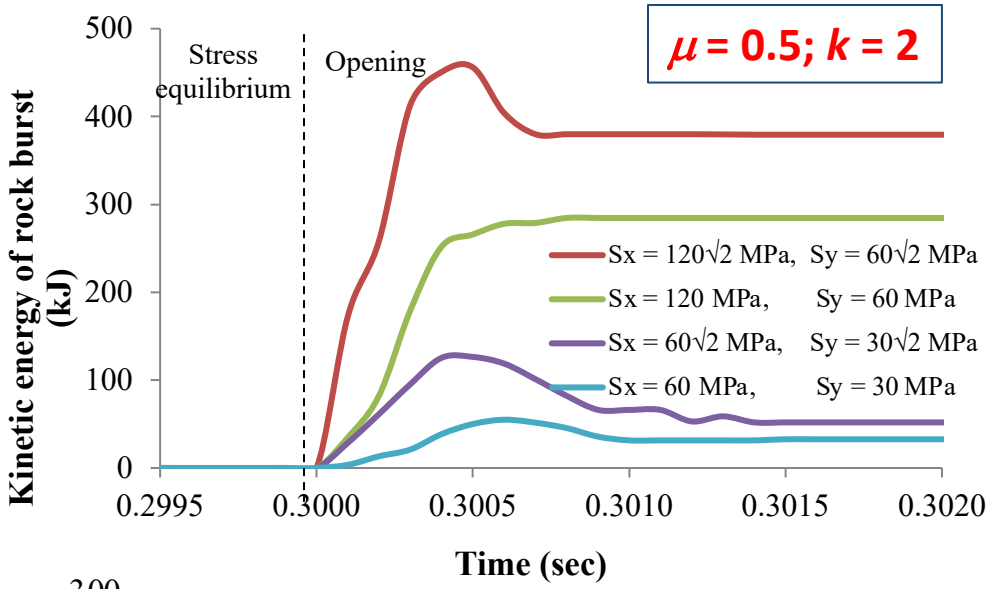

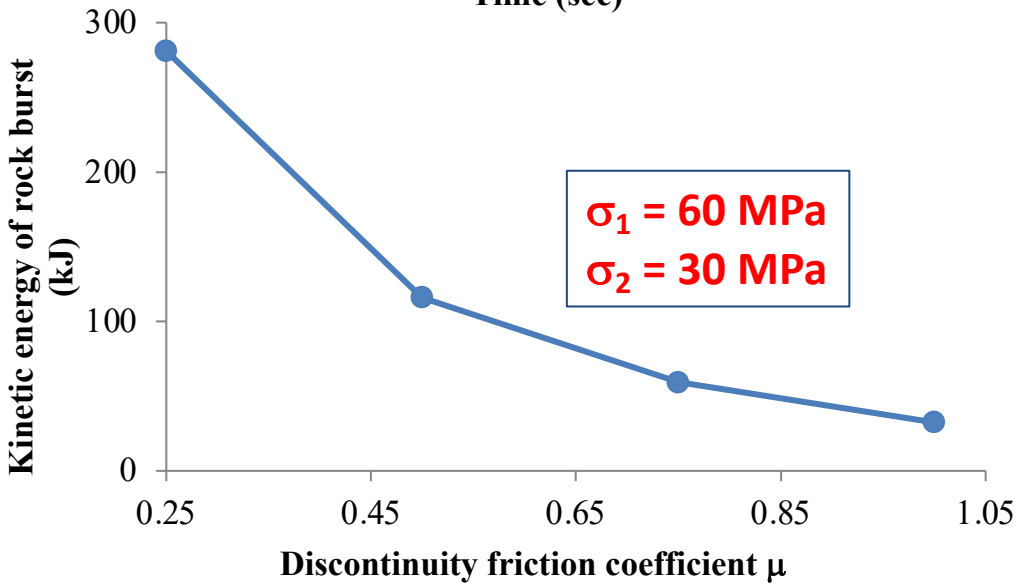

- With increasing *in-situ* stresses the kinetic energy of the rock burst increases.
- The kinetic energy of the rock burst is reduced with increasing joint friction
- **Therefore, the potential for violent energy release in the form of rock bursts increases with reduced frictional resistance and with increasing in situ stress.**

Summary

- DDA was invented by Dr. Gen-hua Shi in 1980's at U. C. Berkeley to provide an accurate and powerful method for modelling dynamic deformation in discontinuous rock masses
- Since then major improvements have been introduced by research groups all over the world including:
  - Block discretization and higher order displacement function
  - Improved contact algorithm
  - Viscous damping and non-reflective boundaries
  - Circular and elliptical elastic elements
  - Pore water pressure and fluid flow
  - Displacement/velocity dependent frictional resistance
- The method has been extensively verified using analytical solutions and validated using field tests and generally proved accurate and reliable provided that the numerical control parameters, particularly the penalty parameter, are properly conditioned
- Two rock mechanics applications have been reviewed, in both the dynamic capabilities of DDA were utilized.

Conclusions

- In the study of thermal vs. seismic effects on block stability in rock slopes that are exposed to high temperature changes it was found that thermal expansion of rock wedges in tension cracks may lead to greater plastic displacement than would periodic seismic activity in a region of moderate seismicity .
- In preliminary study of rock bursts it was shown that strain relaxation mechanism is capable of generating rock bursts in an initially discontinuous rock mass.
- The annulus around the opening most affected by strain relaxation extends to a distance of three diameters from the tunnel center.
- The kinetic energy of the block system once the tunnel is excavated increases with increasing magnitude of initial principal stresses and with decreasing frictional resistance of pre existing joints.
- The obtained kinetic energy of individual rock bursts may be used for effective reinforcement design, provided that reinforcement elements are installed in a timely manner.

Thank you!